UNIVERSITY of the
WESTERN CAPE

FACTORS INFLUENCING FUEL CELL LIFE AND A METHOD OF ASSESSMENT FOR STATE OF HEALTH

NOLUNTU DYANTYI

Dissertation in fulfilment of the degree of Doctor of Philosophy in Chemical Science

November 2018

HySA Systems
Hydrogen South Africa

SAIAMC
South African Institute for Advanced Materials Chemistry
MAKING RESEARCH WORK

DECLARATION

"I know the meaning of plagiarism and declare that all the work in this document, save for that which is properly acknowledged, is my own"

Noluntu Dyantyi

November 2018

ABSTRACT

Proton exchange membrane fuel cells (PEMFC) converts chemical energy from the electrochemical reaction of oxygen and hydrogen into electrical while emitting heat, oxygen depleted air (ODA) and water as by-products. The by-products have useful functions in aircrafts, such as heat that can be used for ice prevention, deoxygenated air for fire retardation and drinkable water for use on board. Consequently, the PEMFC is also studied to optimize recovery of the useful products. Despite the progress made, durability and reliability remain key challenges to the fuel cell technology. One of the reasons for this is the limited understanding of PEMFC behaviour in the aeronautic environment.

The aim of this thesis was to define a comprehensive non-intrusive diagnostic technique that provides real time diagnostics on the PEMFC State of Health (SoH). The framework of the study involved determining factors that have direct influence on fuel cell life in aeronautic environment through a literature survey, examining the effects of the factors by subjecting the PEMFC to simulated conditions, establishing measurable parameters reflective of the factors and defining the diagnostic tool based on literature review and this thesis finding.

The identified factors are cathode stoichiometry, operating temperature and load profile of an aircraft. The PEMFC was tested under the simulated load profile at 60 and 90°C supplied with fully humidified gases at atmospheric pressure and the stoichiometry was 1.8/2.5 anode/cathode. The cathode stoichiometry of 2.5 was selected based on literature review revealing that it is high enough to compensate for the low ambient pressure (0.7 bar at 2200 m) and low oxygen content (16.0% at 2200 m). The 60 and 90°C were employed as nominal and extreme respectively since PEMFC is likely to be exposed to these temperatures in aeronautic conditions.

The PEMFC successfully generated electrical power at all the flight stages at both temperatures, implying that it can withstand harsh aeronautic conditions. The higher

temperature yielded consistently lower power output for all the flight stages compared to the nominal. The PEMFC was further examined for its behaviour (performance and degradation) under the simulated conditions. The start-up and shutdown (SUSD) flight stage resulted in the most performance loss while the cruise mode (CH) caused the least. The observations were attributed to the harsh thermal cycling, high voltages encountered at the SUSD compared to the steady state of CH. The variable load demand (PC) and the idling (OCV) flight stages also caused significant performance, probably due to the high voltages. The polarization (IV) curves revealed that the losses were mostly caused by ohmic losses for the SUSD and the PC stages while the OCV was from a combination of ohmic and activation losses. The ex-situ results showed that loose Pt particles from collapsed carbon support were the major cause of degradation.

The measurable parameters associated with the factors were voltage, current, power, relative humidity and resistances (ohmic, charge and mass transfer). The parameters can be monitored by mapping water, cell voltage and reactants distribution within the fuel cell. The mapping can be carried out using the proposed nanosensor electrochemical scanner. The nanosensor electrochemical devise is a non-intrusive diagnostic tool that will provide real time mapping of the distributions without physically contacting the fuel cell. The nanosensor will take advantage of tiny nanomaterials and be developed as a small compact device equipped with sensors that can decode diagnostics.

ACKNOWLEDGEMENTS

To my supervisors Dr Sivakumar Pasupathi and Dr Piotr Bujlo, thank you for the technical input and professional guidance and for all the time and effort correcting what I feel were sometimes inexcusable mistakes! If this dissertation is even close to what you had in mind when you suggested this project, then I will be very happy.

This work is based on research supported by: Hydrogen and Fuel Cell Technologies RDI Programme (HySA), funded by the Department of Science and Technology in South Africa (Project KP3-S03). Any opinion, finding, conclusion or recommendation expressed in this material is that of the authors and the HySA does not accept any liability in this regard.

I would like to extend my gratitude to the following people:

- Adrian Parsons and Stanford Chidziva for your technical support in the laboratory at HySA Systems. Thank you for all the time and effort you have put in for me.
- Lucille Thomas, Denise Scheepers, Barbara Rodgers, David Abrahams and Yaseen Arend for all the help you have given me in sorting my administration.
- Natasha Peterson and colleagues in the Electron Microscope Unit at Physics Department at UWC for their assistance with HRTEM.
- Dr Remy Bucher and colleagues at iThemba Labs for their assistance with XRD analysis.
- Dr Elrika Harmzen-Pretorius and colleagues in the Geology Department for their assistance with HRSEM.

DEDICATION

I dedicate this thesis to my mother No-Amen Gertrude Dyantyi and my late father Mzolisi Thobisile Dyantyi. I am eternally grateful for all of the support. Thank you for loving me as you have and thank you for taking care of my son while I toiled away in pursuit of my studies. What you have done for me is nothing short of amazing. I hope to make you proud someday.

To my son, Bulumko Sixolise Dyantyi, I know that you cannot read this yet, but I hope that someday when you are old enough to understand, you will know that being away from you for many hours at a time was one of the hardest things I have ever had to do. I intend to spend the coming years making it up to you for all the time I spent away from you. Hopefully you will not get sick of seeing my face! ☺ Mommy loves you!

LIST OF PUBLICATIONS AND PRESENTATIONS

1. Dyantyi, N., Parsons, A., Sita, C. and Pasupathi, S. PEMFC for aeronautic applications: a behavioral study. 1st HySA Technical Meeting, 17-18 August 2015, Cape Town, South Africa.

2. Dyantyi, N., Parsons, A., Sita, C. and Pasupathi, S. Effects of operating conditions on PEMFC in aeronautical conditions. 6th European PEFC & H_2 Forum, 04-07 July 2017, Lucerne, Switzerland.

3. Dyantyi, N., Parsons, A., Sita, C. and Pasupathi, S. PEMFC for aeronautic applications: A review on the durability aspects, Open Engineering, 2017, 7, 287-302.

4. Dyantyi, N., Parsons, A., Bujlo, P. and Pasupathi, S. Behavioural study of PEMFC during start-up/shutdown cycling for aeronautic applications, Materials for Renewable and Sustainable Energy, 2019, 8:4, 1-8.

TABLE OF CONTENTS

LIST OF FIGURES

LIST OF TABLES

LIST OF ACRONYMS

ADR	Average Degradation Rate
AFC	Alkaline Fuel Cell
AST	Accelerated Stress Test
BoL	Beginning of Life
BSE	Back scattered electron
CH	Current hold/Cruise mode
CHP	Combined Heat and Power
CV	Cyclic Voltammetry
DST SA	South African Department of Science and Technology
ECM	Equivalent Circuit Model
ECS	Environmental Control System
ECSA	Electrochemically Active Surface Area
EDS	Energy Dispersive X-Ray Spectroscopy
EIS	Electrochemical Impedance Spectroscopy
EoL	End of Life
FDI	Fault Detection and Isolation
GDL	Gas Diffusion Layer
HOR	Hydrogen Oxidation Reaction
HRSEM	High Resolution Scanning Electron Microscopy
HRTEM	High Resolution Transmission Electron Microscopy
HySA	Hydrogen South Africa
IV curve	Polarization Curve
LSV	Linear Sweep Voltammetry
MCFC	Molten Carbon Fuel Cell
MEA	Membrane Electrode Assembly
MFC	Multifunctional Fuel Cell
OCV	Open Circuit Voltage/Idling
ODA	Oxygen Depleted Air

ORR	Oxygen Reduction Reaction
PAFC	Phosphoric Acid Fuel Cell
PC	Potential Cycling/Variable load demand
PEMFC	Polymer Electrolyte Membrane Fuel Cell
PFSA	Perfluorinated sulphonic acid
PHM	Prognostics and Health Management
PSD	Particle Size Distribution
RH	Relative Humidity
RUL	Remaining Useful Life
SOFC	Solid Oxide Fuel Cell
SUSD	Start-up and Shutdown
SoH	State of Health
US DOE	US Department of Energy
USEPA	US Environmental Protection Agency
XPS	X-Ray Photoelectron Spectroscopy
XRD	X-Ray Diffraction
WHO	World Health Organization

CHAPTER 1

INTRODUCTION

1.1 Background

Fuel cell is an electrochemical device that directly converts chemical energy into electrical energy. There are different types of fuel cells classified based on the nature of electrolyte. The fuel cells abbreviations in Figure 1 stand for Alkaline Fuel Cell (AFC), Molten Carbon Fuel Cell (MCFC),Solid Oxide Fuel Cell (SOFC) and Phosphoric Acid Fuel Cell (PAFC) while CHP is combined heat and power. Among the fuel cells shown in Figure 1, PEMFC is the most compatible and can be accustomed to any power output up to 1 MW depending on the end user requirements [1, 2]. PEMFC generates electrical energy from hydrogen and oxygen in the presence of a catalyst (commonly platinum catalyst) at relatively low temperature with only heat and water released as by-products. In addition to compatibility and zero in-situ pollutant emissions, PEMFC has high energy density, short recharging time, no moving parts and operates silently.

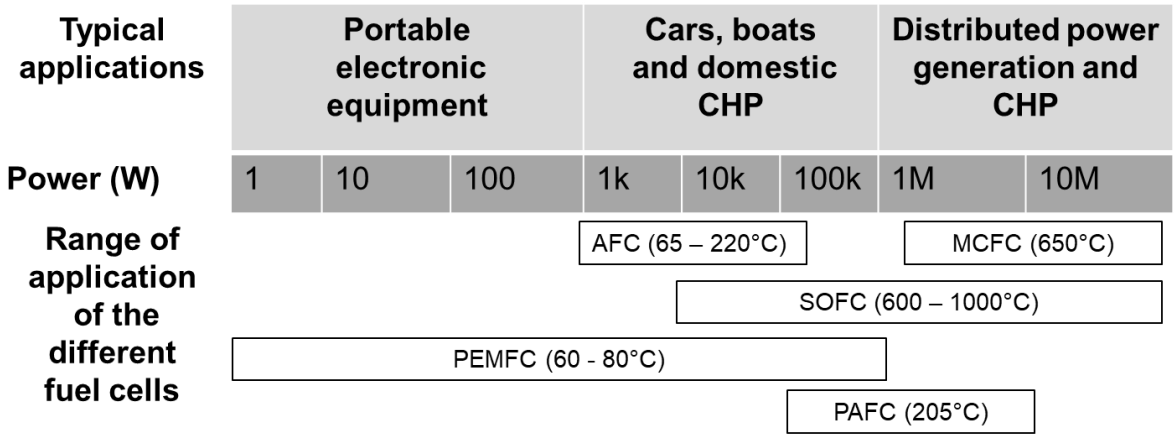

Figure 1: Summary of different types of fuel cells with different power capacities for various applications and operating temperature range in brackets [1].

South Africa contributes more than 75% to the world's platinum reserves and one-third of the fuel cell cost is attributed to platinum, main raw material to produce the catalyst. Hence South African Department of Science and Technology (DST SA) set up National Hydrogen and Fuel Cells Technologies Research, Development and Innovation strategy in 2008, commonly known as Hydrogen South Africa (HySA). The role of HySA is to establish hydrogen economy in South Africa by taking advantage of the local PGM's in order to reduce the cost of catalyst and subsequently the cost of fuel cells, more details on implementation and progress made by HySA can be found in [3]. HySA consists of three Centres of Competence: HySA Systems, HySA Infrastructure and HySA Catalysis. HySA Systems exhibits prototypes and demonstrators for both stationary and automotive applications (i.e. PEMFC-powered generator, FC-scooter, FC-forklift and FC-golf cart) as part of its System Integration and Validation program [3]. HySA Infrastructure work on hydrogen storage and distribution while Catalysis works on optimizing the platinum catalyst.

South African energy supply challenges include rural communities living without electricity, relying on one major power grid, global warming and depleting coal reserves. In addition to hydrogen economy that creates jobs, HySA supports the initiative to move from resource-based economy towards knowledge-based economy by training South Africans about the hydrogen and fuel cell technology. Consequently, there are fuel cell-powered prototypes and demonstrators which include University of the Western Cape's nature reserve and Naledi village powered by fuel cells using generators with power output of 2.5 kW and 15 kW respectively [4, 5]. PEMFC-powered forklift with stacks that each has 21 kW maximum power output was commissioned at Impala mines in Springs, South Africa [6, 7].

PEMFC was introduced by National Aeronautics and Space Administration (NASA) in the 1980's. Nowadays, the use of PEMFC is also appreciated by aircraft manufacturers, such as Airbus and Boeing [8-10]. Properties of PEMFC that add value to its application in aircrafts compared to internal combustion engines and batteries include silent operation, in-situ environmental benign emissions and fast recharging time. Furthermore, Figure 2 shows more benefits of employing PEMFC in aeronautics. For instance the PEMFC can generate electrical power for small loads (e.g. moving ailerons, cabin environmental control and pressurization), recharge batteries and emit useful by-products (i.e. water, deoxygenated air and heat) during operation in aircraft [9].

Discharged water and deoxygenated air can be used to cover water demands on board and fire retardation for jet fuel tank, respectively. Tibaquira *et al.* showed that water recovered from PEMFC complies with WHO and USEPA drinking water standards [11]. Heat generated can be used for hot water preparation and ice prevention on wings. The silent operation of fuel cell reduces noise in airports and alleviates hearing problems of airport personnel who are inadvertently exposed to high noise levels [12]. Hence, taking into account environmental and personnel health laws that restrict emission of

greenhouse gases and the interest to reduce noise in airports, PEMFC becomes a suitable alternative energy source.

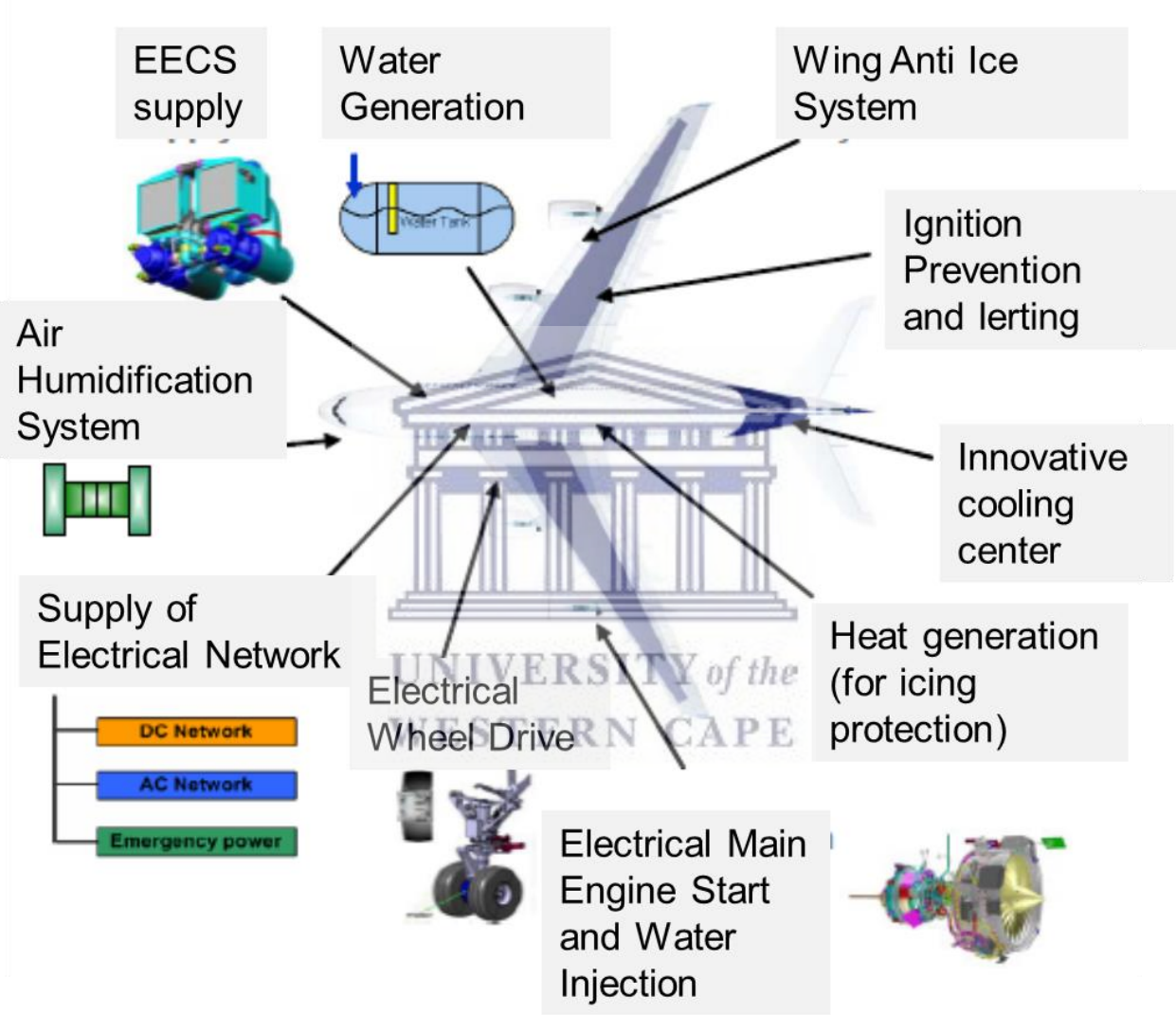

Figure 2: Additional functions of PEMFC in aircrafts [13].

Given the advantages of PEMFC, NASA proposed fuel cell-powered propulsion in attempts to discover "21st Century" aircrafts that are affordable, safe, environmentally compatible and silent [14]. In 2003, one of the major aircraft manufacturers, Boeing, bought into the idea of "more-electric" commercial aircraft [15]. Boeing further proposed change of the 7E7/787 pneumatically-powered environmental control system (ECS), and hydraulically-powered flight control and cargo doors system into electrically-powered as shown in Figure 3 [13]. Airbus also envisaged switching hydraulically-powered secondary flight control of A380 Advanced Testing and Research Aircraft (ATRA) to electro-mechanical actuators [13]. Airbus further collaborated with German Aerospace Center to establish a fuel cell-powered motorized glider (DLR Antares-H2) as a flying test laboratory [9]. Nowadays, research has shifted to testing the behaviour of PEMFC under field and simulated laboratory conditions [10, 16-19].

The number of commercial flight is projected to increase exponentially by 2050. Thus requires better management and decrease of emissions from the transport sector to minimize carbon footprint. The introduction of fuel cell technology in aviation is one of progressive initiatives that contribute towards embarking greenhouse gas emissions [20]. The goals set out by the European commission include emission-free taxiing of aircrafts, 65% noise reduction in aircrafts and 90% reduction in emission of NOx [20]. The PEMFC operates silently and does not emit any greenhouse gases, thus makes suitable alternative energy source in aeronautic applications.

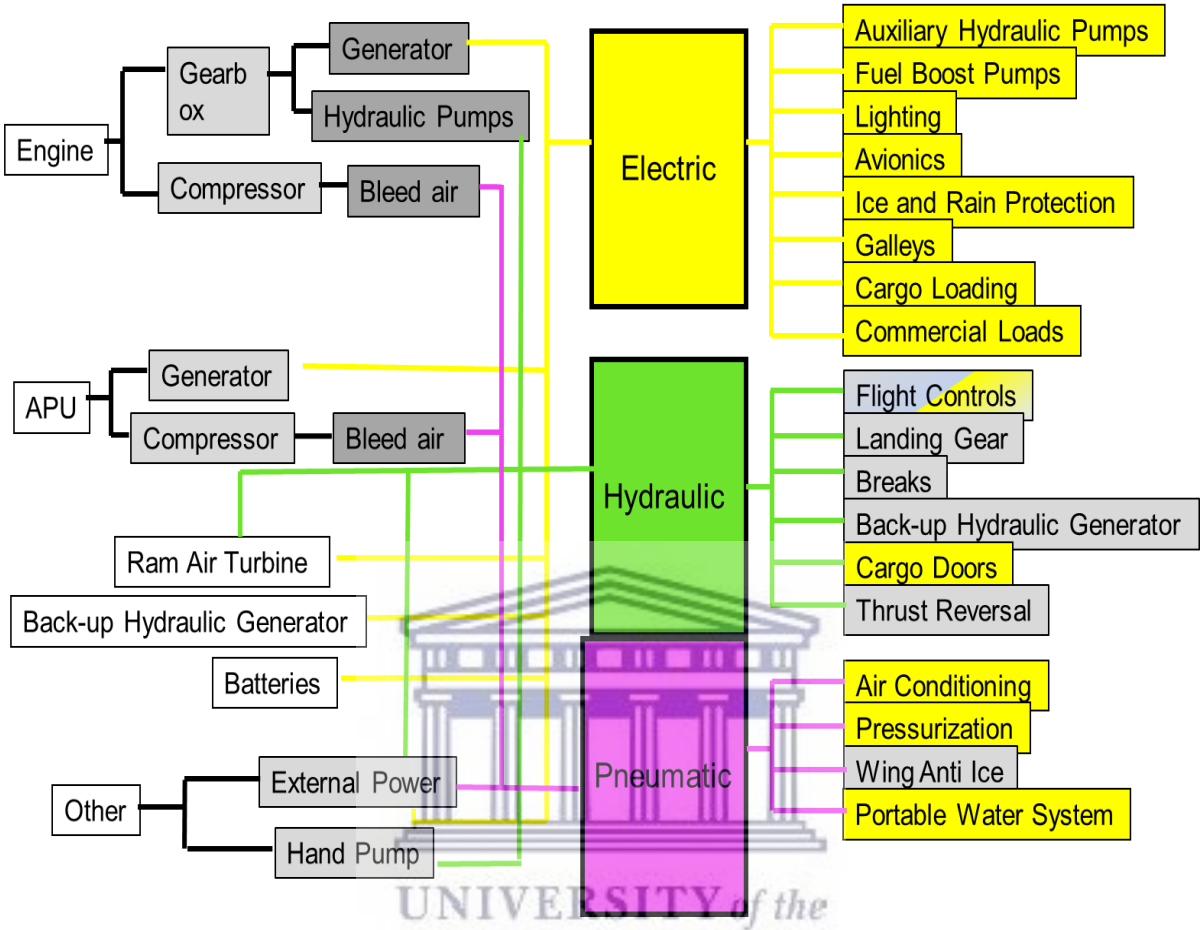

Figure 3: Energy supply (left) and consumers (right) for a more-electric aircraft proposed by Eelman *et al.* [13].

Specific targets set in 2004/05 for application of fuel cell in vehicles include a lifetime of 5000 hours (existing "standard" lifetime of internal combustion engine) and 60% electrical efficiency based on fuel's lower heating value [21]. Despite the progress made over a decade of research, only 2500 hours and 40% efficiency have been reported in literature [22, 23]. Major challenges experienced in operating and maintaining PEMFC that limit its industrialization are cost, efficiency, reliability and durability. The challenges stem from degradation of the fuel cell and its components resulting in shortened lifetime.

Potential solution to the challenges is to have a better understanding of PEMFC behaviour at various life stages in order to predict fuel cell SoH which allows scheduled maintenance to minimize degradation and ultimately prolong lifetime. Such information can be acquired by studying performance of PEMFC under conditions that have direct effect on its life.

The behaviour of fuel cells is studied by subjecting it to various operating conditions or surroundings and characterizing the properties either electrochemically in-situ or chemically/physically ex-situ. The in-situ electrochemical techniques provide information on overall performance, degradation rate and properties of individual components such as active catalyst area, membrane resistance, etc. Tested fuel cell components are further dissected for chemical/physical characterization to explore the extent and nature of degradation.

The methods available to evaluate parameters that reflect on fuel cell SoH and lifetime are mostly applicable to research purposes. For instance, the polarization curve provides information on overall electrical performance without specifying sources of voltage decay. The impedance spectroscopy is sensitive to operating conditions (i.e. fluctuating current in big stacks, unstable water levels in the MEA) and its data does not generate real-time diagnosis of fuel cell SoH. There are sensors developed that are still in research stages to test whether they are capable of providing real-time diagnosis [122-124]. There is limited information from literature regarding methods that are capable of providing real time diagnosis, portable and non-intrusive or disruptive to fuel cell performance, particularly for aeronautic applications. Consequently, research must be conducted to identify the factors and establish a method of assessment suitable for PEMFC in aeronautic conditions in order to optimize effectiveness, efficiency and lifetime.

1.2 Problem Statement

The Background highlighted limited research on studying behavior of fuel cells under aeronautic conditions and lack of comprehensive prediction technique for the SoH. Hence, differences and similarities between behaviors of parameters that influence fuel cell life on land applications compared to aeronautic applications are neither well-defined nor well-documented. Consequently, there is no clear understanding of factors that influence fuel cell life in aeronautic environment. Effective assessment of fuel cell SoH in aeronautic environment relies on identifying measurable parameters that are reflective of the factors and have prediction methods suitable for aeronautic conditions. Thus points out the necessity to study and document key parameters that are reflective of SoH on-board and devise prediction methods that provide real time information, non-intrusive and cost effective.

1.3 Research Scope

1.3.1 Overarching research objective

The broader objective of the work is to develop diagnostic tool that is capable of detecting degradations and sources of performance loss in fuel cells used under aeronautical conditions. One of the steps towards establishing the objective is to define and document key factors that directly influence PEMFC life. Hence, the aim of this PhD study is to better understand behavior of PEMFC under aeronautic conditions and define prediction methods. In order to achieve the aim, the study objectives to:

I. Investigate factors that influence fuel cell life under aeronautic environment.

II. Identify and document measurable parameters that have direct effect on fuel cell SoH.

III. Define non-intrusive test methods conducive for aeronautic environment to evaluate the fuel cell parameters that are directly linked to the factors.

1.3.2. Scope of the study

This thesis seeks to better understand effects of aeronautic environment on performance and degradation of low temperature PEMFC. The study entails subjecting the PEMFC to simulated aeronautic operating conditions, electrochemical characterization for performance of fuel cell components, physical/chemical characterization for components transformation and exploration of degradation mechanisms. The study is focused on laboratory testing of single cell operating with 25

cm^2 of electrode active area MEA using Greenlight G20 Fuel Cell Test Station and its built-in Emerald™ control and automation software. The simulated aeronautic operating conditions such as operating temperature and load profile were controlled by implementation of suitable testing procedure and by the use of the control software.

Electrochemical and physical/chemical characterizations were conducted using Polarization (IV) curves, High Resolution Transmission Electron Microscopy (HRTEM), High Resolution Scanning Electron Microscopy coupled with Energy Dispersive X-Ray Spectrometry (HRSEM/EDS) and X-Ray Diffraction (XRD). The data acquired from the study was used to examine effects of the operating conditions, nature and extent of degradation. The information generated is going to be documented and used to build database library on behaviour of PEMFC under aeronautic environment. Ultimately, a comprehensive prediction method for PEMFC SoH under aeronautic conditions is going to be defined.

1.4. Thesis structure

This thesis consists of six chapters: The Introduction in Chapter 1 provides a background to the study that outlines the problem statement, objectives and scope of the study. Chapter 2 provides a Literature Review which covers the use of PEMFC in aeronautic applications, value-added benefits of multifunctional use of PEMFCs and their limitations that delay industrialization. The identified factors affecting fuel cell life are discussed in details and available method of assessing PEMFC SoH prediction methods, highlighting their capabilities and shortfalls are proposed. The derivation of the hypotheses and key questions of the study based on the rationale to conduct this research are outlined in Chapter 3. Details of the test station setup, materials used and characterization techniques employed are outlined in Chapter 4. The gathered data and results from this study are presented and discussed in Chapter 5. Chapter 6 highlights

and summarizes the work by the Conclusions of the study and provides Recommendations for future work. An outline of the thesis is presented schematically in Figure 4. The thesis is an extension of Publication number 3 from the list of publication and as such, Chapter 2 overlaps with this publication.

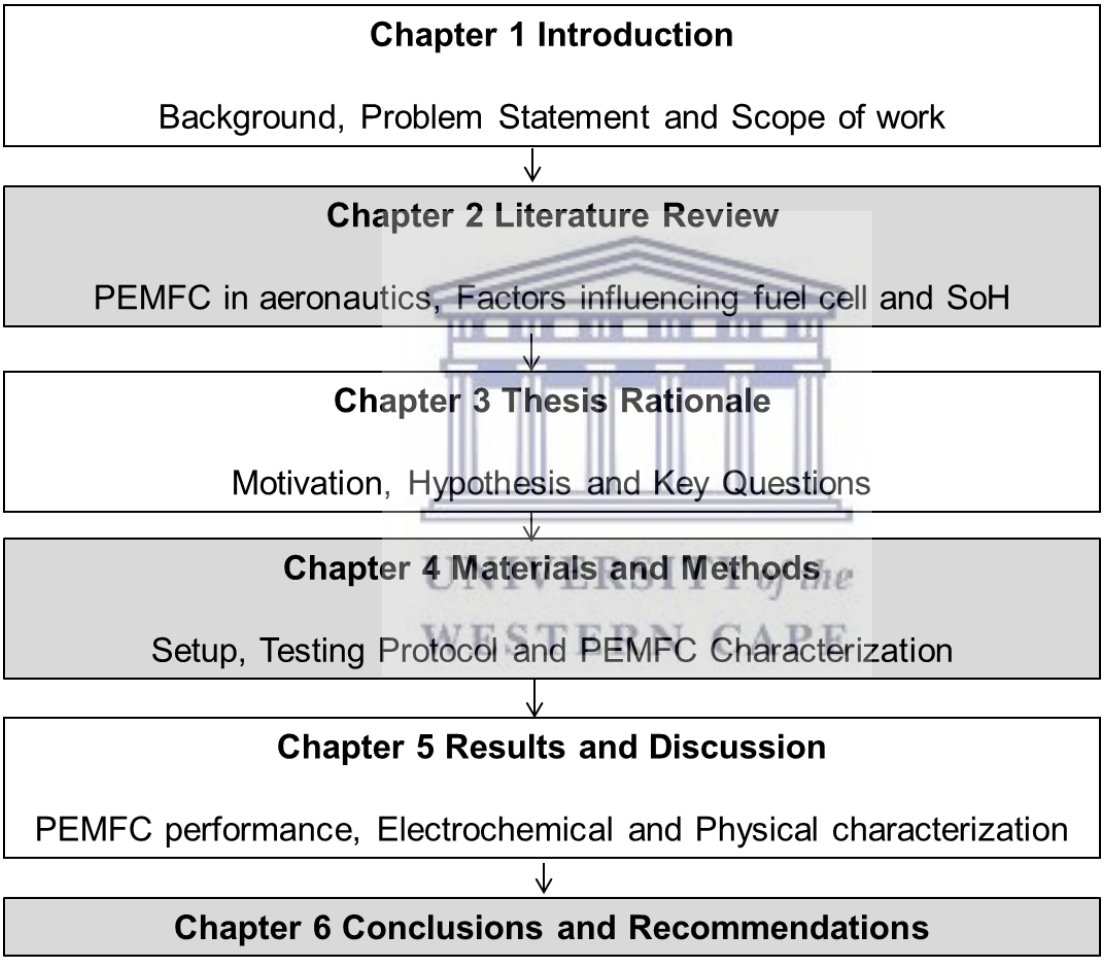

Figure 4: Schematic diagram of the thesis structure.

CHAPTER 2

LITERATURE REVIEW

2.1 PEMFC for aeronautics

PEMFC illustrated in Figure 5 is a device made up of bipolar plates, cathode and anode gas diffusion layers (GDL), cathode and anode electrodes and polymer membrane. The membrane together with electrodes and GDLs constitutes MEA which is the core of fuel cell where the electrochemical, catalyst-assisted reactions take place to generate electricity from a reaction of hydrogen and oxygen. The fuel (hydrogen gas in PEMFC) is oxidized at the anode side with the aid of present catalyst releasing electrons which are transferred to the cathode side via external electrical circuit. The electrons reduce oxidant species (oxygen) and the reduced oxygen reacts with the hydrogen ions (protons) to form, water, generate electrical energy and release heat and deoxygenated air (in cases of self-breathing fuel cell) [12].

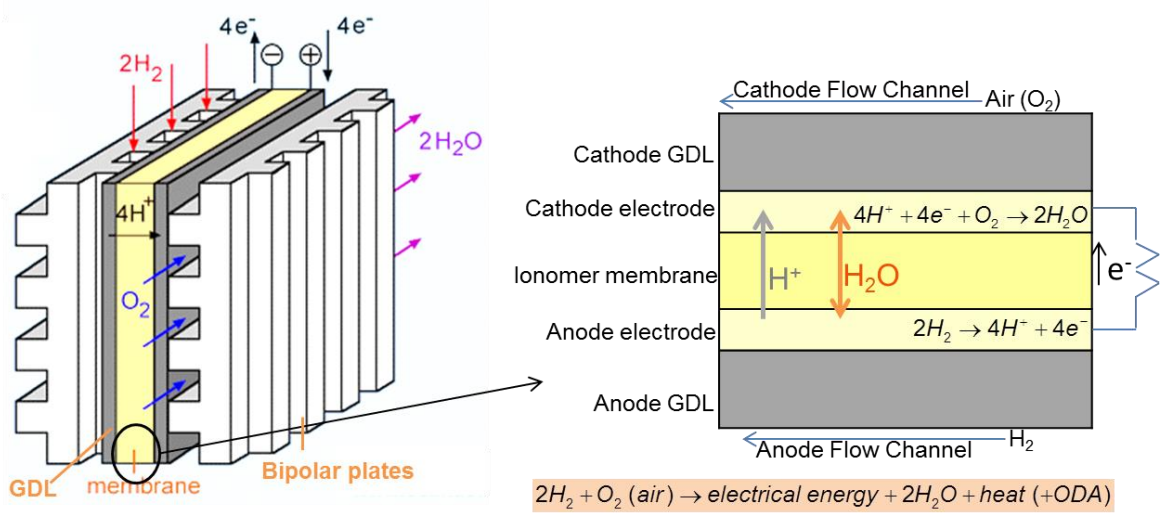

Figure 5: Schematic diagram of PEMFC illustrating chemical reactions taking place.

Each component of fuel cell has a function with varying levels of importance in terms of performance and effect on the quality of PEMFC as well as its life. MEA is the most expensive part of the fuel cell and equivalently most essential. Bipolar plates with gas flow patterns supply reactants to the places of electrochemical reactions as well as provide path for electrons to travel between cells, they serve as a barrier between anode and cathode, and provide structural integrity. GDL must be electrically conductive, hydrophobic and gas permeable to allow gas distribution to the catalyst layer and to provide pathway for water removal. Jouin *et al.* created components hierarchy by evaluating whether a component play a role in power output or its degradation results in power loss and/or complete stack death [24]. The components grouped into three classes, with A and C being the most and the least crucial respectively are:

1. Class A: Membrane and electrode
2. Class B: GDL and bipolar plates
3. Class C: Sealing gaskets

In line with the scope of this study, the following sections explore properties, functions and degradation mechanisms of only membrane, electrode and carbon support being the most crucial components of the PEMFC.

2.1.1 Membrane

Polymer electrolyte or proton exchange membrane facilitates selective movement of reactant gases (e.g. only allowing oxygen on cathode side) and formed water molecules in and out of the fuel cell. Therefore, the membrane (commonly used in PEMFC Nafion^{TM}) must be proton-conductive, highly selective to oxygen or hydrogen, gas impermeable, concurrently hydrophilic/hydrophobic, chemically and mechanically stable. Nafion^{TM} (Figure 6) is made up of perfluorinated sulphonate ionomer with the -SO_3H groups ionically bonded in such a way that the end of the chain has SO_3^- and H^+ ion in order to avoid clustering within the overall membrane structure [25]. The sulphonic acid at the end of side chain is hydrophilic to allow relative water accumulation since presence of water activates proton conductivity [26]. On the other hand, the backbone of the membrane is hydrophobic to avoid flooding and drive away excess water by means of electro-osmosis drag or back diffusion.

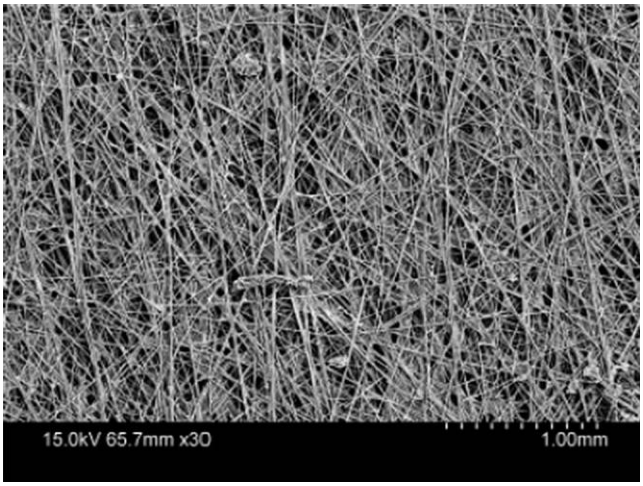

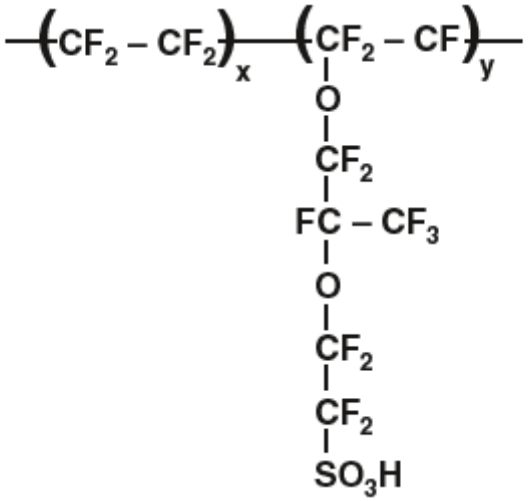

Figure 6: Micrograph and chemical structure of perfluorinated sulphonic acid membrane (Nafion^{TM}) [25].

The Nafion^{TM} membrane is however expensive and tends to lose conductivity at temperatures above 90°C. Proton conductivity strongly relies on water content within the membrane and it is difficult to maintain proper water balance within the membrane and fuel cell [27]. Desired water content is defined as enough water to facilitate transport of protons from anode to cathode without flooding the MEA, approximately 90 to 110% relative humidity (RH) at the outlet of cathode [1, 28].

Consequently, efficiency of the membrane is partly governed by operating temperature and RH since dehydration increases resistance while flooding hinders movement of reactant gases. Efforts to improve the membrane include reducing its thickness to fasten hydration by back diffusion from cathode to anode at high temperatures or low RH [29]. However, thinner membranes may not be mechanically strong enough and are prone to reactant crossover. Hence, US Department of Energy (DOE) proposed performance and technical standards for improved membranes. The targets are 0.1

Scm^{-1} proton conductivity, <20 $m\Omega cm^2$ area specific proton resistance at low RH, 1-10 $mAcm^{-2}$ hydrogen cross-over depending on type and thickness and <20 $\$m^{-2}$ cost [30].

One of research focus areas for membrane optimization is to study degradation mechanisms and mitigation methods with the aim of improving its performance, reliability and cost without compromising its durability. Membrane degrades in three forms: thermally, mechanically or chemically.

Thermal degradation only takes place at temperatures above 200°C and is therefore neglected for low temperature PEMFC.

Mechanical degradation is characterized by pinholes and cracks, attributed to high differential initial pressure, high temperature and RH cycling. Mechanical degradations cause direct mixing of reactant gases which is quantified as hydrogen crossover using Linear Sweep Voltammetry (LSV). Physical transformations on the membrane can be characterized for morphological changes and thickness using SEM. Lim *et al*. observed pinholes and 27% thickness loss on a membrane subjected to cyclic OCV at 75°C [31]. The study further showed loss of fluoride and reduction of side chain [31]. Shan *et al*. also visualised loss of membrane thickness due to exposure to high voltages under dynamic driving cycles using HRSEM as shown in Figure 7 [32]. The study by Banan *et al*. revealed that RH cycling causes membrane cracks while vibrations lead to delamination [33].

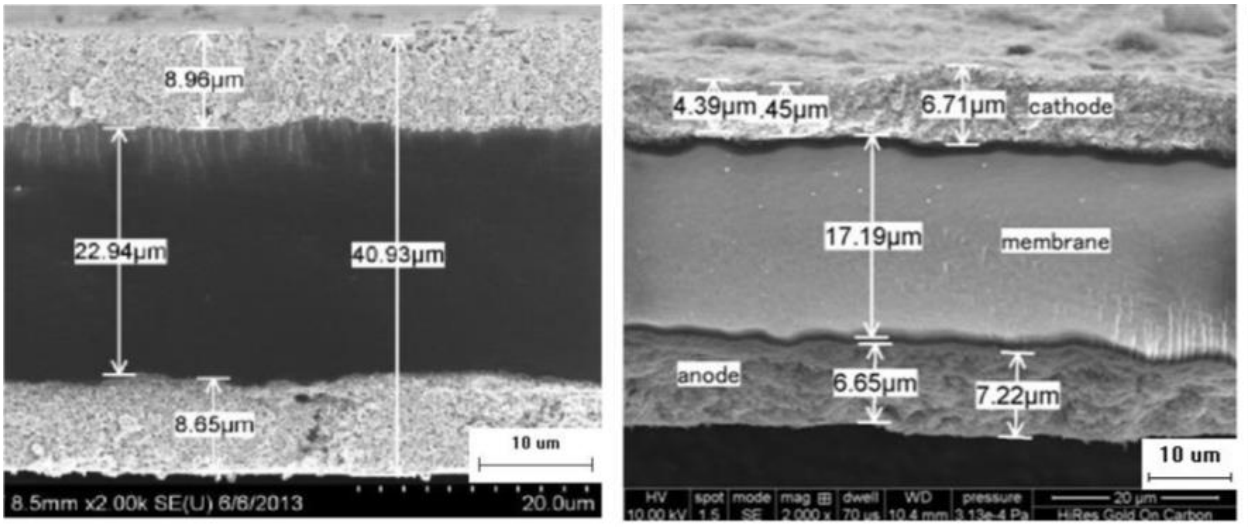

Figure 7 HRSEM cross-sections of new and tested MEA [32].

Chemical degradation refers to attack on polymer chains by hydroxyl or peroxyl radicals formed from decomposition of peroxide (Eq. 2-3), a by-product of oxidation reduction reaction (ORR) (Eq. 1) or product of H_2 and O_2 in the presence of Pt from electrode degradation [34, 35].

$$O_2 + 2H^+ + 2e^- \rightarrow H_2O_2 \qquad \textbf{Eq. 1}$$

$$M^{2+} + H_2O_2 \rightarrow M^{3+} + {}^{\bullet}OH + OH^- \qquad \textbf{Eq. 2}$$

$$M^{3+} + H_2O_2 \rightarrow M^{2+} + {}^{\bullet}OOH + OH^+ \qquad \textbf{Eq. 3}$$

Operating conditions favourable to radical attack are temperatures above 80°C, low RH, high gas pressure and high cell voltages [35, 36]. Mechanisms of polymer chain attacked by hydroxyl radical as observed by Curtin *et al* using XPS are outlined in Eq. 4-6, with overall reaction on Eq. 7 [37].

$$R_f - CF_2COOH + {}^{\bullet}OH \rightarrow R_f - CF_2^{\bullet} + CO_2 + H_2O \quad \textbf{Eq. 4}$$

$$R_f - CF_2^{\bullet} + {}^{\bullet}OH \rightarrow R_f - CF_zOH \rightarrow R_f - COF + HF \quad \textbf{Eq. 5}$$

$$R_f - COF + H_2O \rightarrow R_f - COOH + HF \quad \textbf{Eq. 6}$$

$$R_f - CF_2COOH + 2{}^{\bullet}OH \rightarrow R_f - COOH + 2HF + CO_2 \quad \textbf{Eq. 7}$$

The overall reaction (Eq. 7) shows that two fluoride molecules are released for each attack of the polymer. Healy *et al.* observed rate of fluoride release was 2 times more compared to a cell operated under mild conditions of 60°C and 100/100% anode/cathode RH [36]. In addition, the release rate of fluoride increased with decreasing membrane thickness [36]. The study also showed that pH can be used as indication of fluoride release rate.

2.1.2 Electrode

Typical PEMFC Pt/C electrodes consist of nanometre-sized Pt particles mixed with ionomer cast to form catalyst layer supported on high surface area carbon, as shown in Figure 8. Electrodes facilitate hydrogen oxidation reaction (HOR) and oxygen reduction reactions (ORR), hence they must be ion-conductive, porous for diffusion of reactant gases and have high electrochemically active surface area (ECSA) for optimal reaction

media. Electrodes are assembled as catalyst-coated ionomer membranes or catalyst coated substrates (GDLs) that have sufficient porosity and ion-conductivity to ensure high utilization of catalyst and low ionic resistance even when operated in dry conditions [38].

Pt is expensive and it subsequently increases the overall cost of fuel cells. As efforts to improve the fuel cell technology, the Pt loading is decreased by up to 80% but one-third of the cost of fuel cell is still due to platinum. In order to further cut the cost while ensuring good quality electrodes, US DOE set targets of 0.125 $mgPtcm^{-2}$ total Pt loading, rated 0.125 gkW^{-1} catalyst utilization and 0.44 Amg_{Pt}^{-1} mass activity by 2020 implying that the total amount of Pt needed for a fuel cell vehicle would be 8 g, which is similar to what internal combustion engines vehicles have today [30].

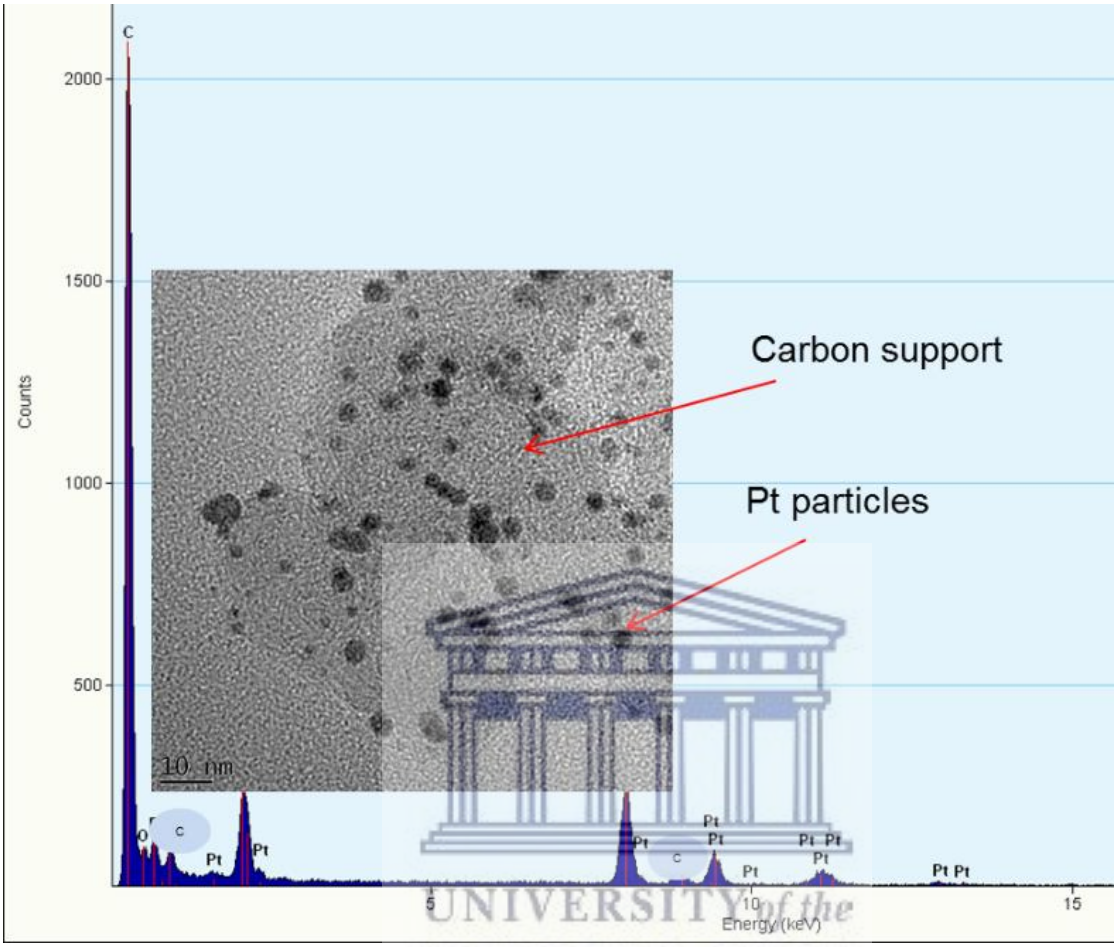

Figure 8: Backscatter electrons image and electron dispersive spectrum of Pt/C electrocatalyst studied in this thesis.

Electrode degradation is associated with hydrogen starvation at anode, OCV and load variation [39]. Symptoms of degraded electrode are loss of ECSA, Pt particle agglomeration and dissolution of Pt particles in the membrane phase. ECSA is calculated using CV to estimate catalyst utilization. For instance, Uribe *et al.* reported performance loss attributed to loss of ECSA after operating fuel cell at voltage greater than 0.8 V for an hour [40]. The two-thirds loss of ECSA at high voltage was believed to

be due to chemical oxidation of Pt into PtO by residual oxygen present in the cathode layer following mechanism on Eq. 8-9 [41]. The PtO covers the active surface area, medium of the energy conversion reaction, hence reducing available catalyst for the reactions. The PtO layer may also block pathways for reactant gases to the active sites.

$$Pt \leftrightarrow Pt^{2+} + 2e^{-} \quad \textbf{Eq. 8}$$

$$Pt^{2+} + H_2O \leftrightarrow PtO + 2H^{+} \quad \textbf{Eq. 9}$$

Starvation, which occurs when fuel cell is operated at sub-stoichiometric reaction conditions, results from sudden change in demand of reactant gases during load cycling, temporary blockage or water accumulation [42]. Starvation causes high cell potential which in turn facilitates cell reversal. Taniguchi *et al.* observed over 20% loss of ECSA and increase of Pt particle size distribution from an average of 2.64 to 4.95 nm after anode starvation due to platinum agglomeration caused by cell reversal [43].

In the case of cathode starvation, ECSA decreased by 40% while platinum particle size distribution increased from 2 to more than 4 nm after 120 minutes [44]. There were no notable changes observed on the anode side, suggesting that hydrogen oxidation is not affected by cathode starvation at low electrode potential [44]. On the other hand, the loss of ECSA caused by adsorption of OH^- on Pt-M surfaces can be reduced by pulsing voltage between 0.5 and 0.8 V. The voltage pulsing provides favourable conditions for PtO dissolution [45]. The Pt^{2+} ions are repeatedly oxidized/dissolved and reduced/redeposited into the membrane by diffusion of O_2 and H_2 as shown in Eq. 10-11 [46].

$$PtO + 2H^+ \rightarrow Pt^{2+} + H_2O \qquad \textbf{Eq. 10}$$

$$Pt^{2+} + H_2 \rightarrow 2H^+ + Pt \qquad \textbf{Eq. 11}$$

Loose Pt ions can easily be dissolved and redeposited at reverse current conditions created by start-up/shutdown cycling, likely to occur numerous times in aeronautic applications. Several studies have reported Pt particle growth caused by Pt ions redeposited on ionomer layer instead of on carbon support [47, 48]. The redeposition observed is due to higher equilibrium potential of dissolution of the Pt particles. Therefore, the Pt particles undergo Ostwald ripening in order to minimize specific surface energy. Rohendi's study of effect of OCV showed particle growth from 3.61 to 5.75 nm [49]. The 60% increase in particle size at cathode was attributed to dissolution of small Pt particles in the ionomer phase of MEA.

Similarly to Mamat *et al. and* Wang *et al.*, XRD data (Figure 9) further confirmed Pt migration to the ionomer through a reaction of Pt with the sulphonic group of the ionomer that formed PtS [49-51]. The effect of Pt on membrane degradation is an ongoing research. Some suggest that Pt coated membranes recorded higher degradation compared to pure membranes and the review by Rodgers discusses details of this behavior [46]. There is also a theory on Pt/C accelerating membrane degradation compared to pure Pt, implying that carbon also contributes to this effect [46]. Dubau *et al*. reported that membrane failure was directly linked to collapsed carbon layer [52].

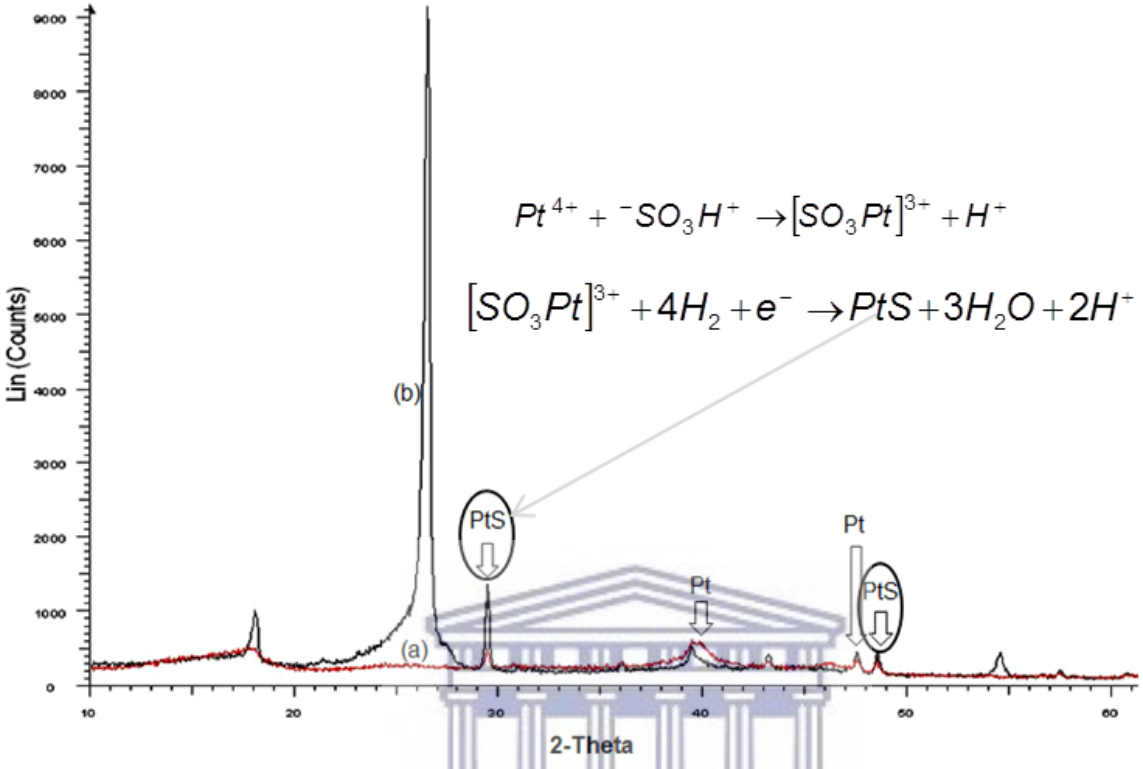

Figure 9: XRD diffractogram showing PtS peaks as observed by Rohendi *et al.* [49].

2.1.3 Carbon support

Catalyst is deposited on the carbon support and therefore it is equally important as the catalyst. The sizes of the carbon particles vary between 20 and 30 nm and they increase surface area of the catalyst. These particles also have a tendency to self-aggregate into agglomerates with a size in the range of 50-100 nm in diameter.

Degradations in catalyst aggravate degradations in carbon support and vice versa [53, 54]. Oxygen formed from water electrolysis reaction at the anode during hydrogen starvation can react with carbon to form carbon monoxide, a serious poison to the

platinum catalyst [55]. Carbon support degrades by corrosion as a result of carbon oxidation and water-gas shift reaction, as shown in Eq. 12-13 [53]. Similarly, carbon corrosion is caused by fuel starvation resulting from rapid change in potentials during cycling, start-stop, voltage greater than 0.8 V and high frequencies [45, 53, 54].

$$C + 2H_2O \rightarrow CO_2 + 4H^+ + 4e^- \qquad \textbf{Eq. 12}$$

$$C + H_2O \rightarrow CO + 2H^+ + 2e^- \qquad \textbf{Eq. 13}$$

HRSEM analysis of corroded cathodes has, in recent years, shown that the morphology of the electrode may undergo considerable changes upon carbon corrosion. The higher increase in particle size observed in cathode compared to anode is consistent with higher carbon corrosion at cathode as mapped by SEM [49]. Both Young *et al.* and Seo *et al.* only reported on the thickness of carbon support before and after potential cycling without including morphological changes [56, 57]. One reason to this is probably the difficulty to separate catalyst layer and carbon support, particularly for catalyst-coated membrane. Hence, carbon corrosion on catalyst-coated membranes is examined by monitoring carbon content through HRSEM/EDS.

2.2 PEMFC system testing under aeronautic conditions

Studies carried out since 2007 are mostly directed towards understanding behaviour of PEMFC at system level. Significant use of fuel cells in propulsion for manned aircraft has been mostly demonstrated by three projects: Boeing, Airbus with German

Aerospace Center (DLR) and Environmentally Friendly Inter City Aircraft powered by Fuel cell (ENFICA-FC) [10, 16, 18].

The first published work on PEMFC-powered manned aircraft flown by Boeing was in 2007 [10]. A 20 kW PEMFC in hybrid with Li-ion battery was used to power a 2-seater manned aircraft. PEMFC provided half of the 36 kW power demand for take-off and the full 15 kW required for cruise [10]. Airbus, DLR and Michelin in 2008 successfully used 25 kW PEMFC on a testbed A320 ATRA as emergency power system [8]. DLR in 2009 tested a piloted Antares DLR-H2 aircraft exclusively powered by approximately 33 kW PEMFC.

The flight test was a success reaching altitudes up to 2558 m without any significant PEMFC performance loss [16]. ENFICA-FC flew first European Commission-funded fuel cell-powered aircraft. The aircraft was powered by PEMFC/Li-ion batteries hybrid with fuel cell maximum power output of 20 kW [58]. In 2011, Airbus and DLR successfully demonstrated electric nose wheel of A320 ATRA powered by 25 kW PEMFC [59]. The success of the tests proved capability of PEMFC to perform in aeronautic conditions. Hence, the shift towards better understanding of PEMFC performance and durability at stack level under (simulated) aeronautic conditions.

2.3 PEMFC testing in aeronautics

Laboratory tests identified to explore environmental effects on PEMFC are orientation/inclination, high altitude/low pressure, vibrations, subfreezing and elevated temperatures. Feasibility studies of multifunctional fuel cell systems focus on produced water, heat and cathode exhaust gas management. For instance, tests carried out by Ross *et al*. to study mechanical behaviour of fuel cell on a vibrating platform simulating

aircraft conditions showed no significant damage on the fuel cell. The damage was estimated based on leak tests which showed no notable pressure changes [60]. The tests were conducted on a short stack which exhibited “elastic” properties. The “elastic” stack resembles non-linear multi-body behaviour that could decrease with increase in size of the stack [61]. Therefore, rigidity and balance-of-plant fittings could become an issue for larger stack.

Effect of subfreezing temperature on cell performance and its ability to self-start under different simulated operating scenarios representative for aircraft applications was studied by Bégot *et al*. using a climatic test chamber [62]. The scenarios were short reference tests (ambient temperature), low temperature tests (-34 to 15°C), ground survival tests (-40 to 20°C) and operating low temperature tests (-9 to -6°C). The key findings were that the PEMFC generated enough heat (stack operating temperature of 15°C) for self-heating at a surrounding temperature as low as -34°C in order to maintain required performance. However, the stack failed to self-start at operating temperature of -9°C due membrane perforation caused by insufficient drying prior to freezing [62]. It was further recommended that PEMFC must be properly dried prior to exposure to freezing conditions.

On the other hand, fuel cell operated at a low cathode stoichiometry of 1.6 showed voltage decrease at an angle of 30° during inclination tests while yielded better cathode exhaust gas (oxygen depleted by-product gas) quality with only 10% oxygen content [12]. High altitude/low pressure effects on fuel cell were studied in low pressure chambers or within a system of small manned aircrafts [63-65]. The altitude tests showed notable performance loss at 0.7 bar/2200 m altitude, which was later minimised by increasing stoichiometry [64-66].

Keim *et al.* and Werner *et al.* studied effect of temperature on oxygen content of cathode discharge gas (oxygen depleted air (ODA)), dryness of ODA and produced water [19, 67]. ODA must be dry with at most 2 $g_{(H2O)}kg^{-1}_{(ODA)}$ specific humidity and have

less than 12% oxygen content in order to avoid contaminating and effectively inert jet fuel, respectively [19, 67]. The study by Keim *et al*. showed that examined temperatures consume significant amount of energy, hence recommended further research. Werner *et al*. obtained the desired less than 12% oxygen content of ODA using twin fuel cell system at 2000 m, 60°C cell temperature and high cathode stoichiometry of 3.6. Again, stoichiometry above 2.5 may damage the stack. Both Hordé *et al.* and Werner *et al.* showed that cathode stoichiometry of 2.5 minimizes performance loss and improves quality of ODA at high altitude [19, 64].

2.4 Factors influencing PEMFC

Fuel cell life is influenced by operating conditions, material and configuration of components, impurities in the reactants, external environment and surrounding conditions within the system. "First fuel cell law" states that one cannot change one parameter in a fuel cell; change of one parameter causes a change in at least two other parameters, and at least one of them has an opposite effect of the one expected to be seen [25]. As a result, it is often difficult to single out the effect of one parameter as they occur either concurrently or simultaneously. Nevertheless studies are conducted to better understand factors that influence fuel cell life, predominantly for stationary and automotive applications rather than for aeronautics [19, 68-73]. Hence, factors discussed in this review are not necessarily representative of the aeronautic environment but taken as a reference in accordance with the purpose of this thesis.

2.4.1 Temperature and relative humidity

Nominal temperature operating range for low temperature PEMFC is within the range of 60 to 80°C [1]. PEMFC used for aeronautic applications is likely to be exposed to

environmental/surrounding temperatures that range from subzero to elevated temperatures up to 90°C [19, 62]. Theoretically, high temperature improves fuel cell performance by increasing reaction kinetics while lowering activation losses and mass transport limitations [1]. For example, Amirinejad *et al.* studied effect of operating temperature (50 to 80°C) on fuel cell performance on a humidified single cell (150 to 200% RH) [68].

Combination of high temperature and high current density yielded better performance while the opposite occurred at low current density regions. The reason for the improved performance was that high temperature increases diffusivity and conductivity while decreasing mass transport resistance. At high temperature and high current density, the fuel cell produced enough water at the cathode side to humidify anode side by back-diffusion mechanism. Amirinejad *et al.* also showed that fuel cell performance is mostly affected by anode humidification compared to cathode humidification [68].

Contrarily to improved performance at high temperature, temperatures above 80°C results in performance loss. Performance loss observed at high temperature is attributed to excessive membrane drying, particularly at low humidification. High temperature also creates conditions that exacerbate degradation of fuel cell components such as radical attack on membrane. The dryness of catalyst layer prohibits effective supply of reactants onto reactive sites and thus starvation.

2.4.2 Stoichiometry

Stoichiometry is the relationship between the relative quantities of substances taking part in a reaction or forming a compound. Stoichiometric ratio is a key in ensuring that sufficient reactant gases are supplied to fuel cell reactive sites in order to avoid detrimental effects caused by starvation. The demand for reactant gases varies with load [74]. As a result, several studies are conducted to better understand the effect of stoichiometric ratio on fuel cell performance [64, 70, 72, 75-77].

Wasterlain *et al.* observed that increasing anode stoichiometry has no significant effect at 60°C as it yielded better water drainage. On the other hand, minor performance losses revealed by the polarization curve with 20 mV loss in the high current region at 40°C were due to excessive drying. Contrarily, increased cathode stoichiometry resulted in better performance as long as there was sufficient humidification [70]. Figure 10 shows that cathode stoichiometry has no significant effect on ohmic and charge transfer resistances, except for mass transport [78].

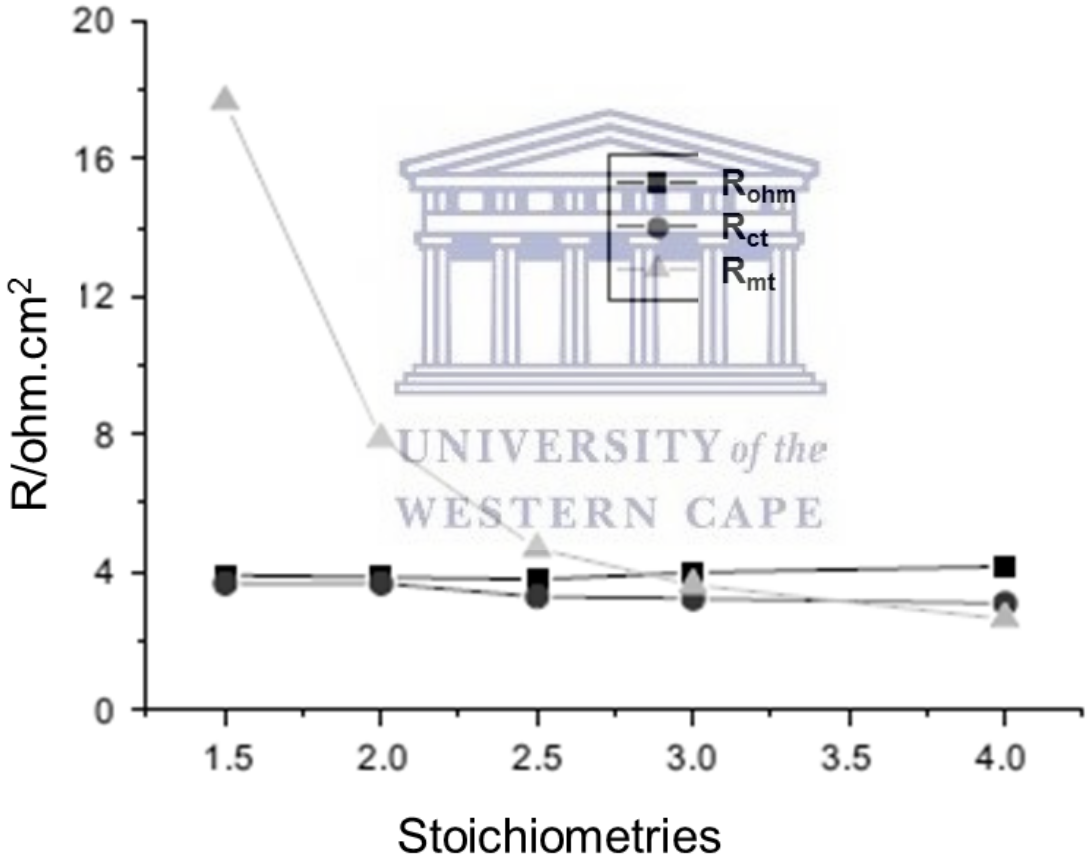

Figure 10: Effect of cathode stoichiometry on ohmic (R_{ohm}), charge transfer (R_{ct}) and mass transport (R_{mt}) resistances at 1.5 anode stoichiometry and 500 mAcm^{-2} current density as reported by Yan *et al.* [78].

The observation was attributed to the fact that only oxygen transport was affected since the membrane was hydrated at 80% RH for 1 hour. Furthermore, cathode stoichiometry has a positive effect on fuel cell performance unless it is below 1.6 [72]. Similarly to Harms *et al.,* Figure 11 shows that a significant voltage drop was observed at cathode stoichiometry of 1.5 [77].

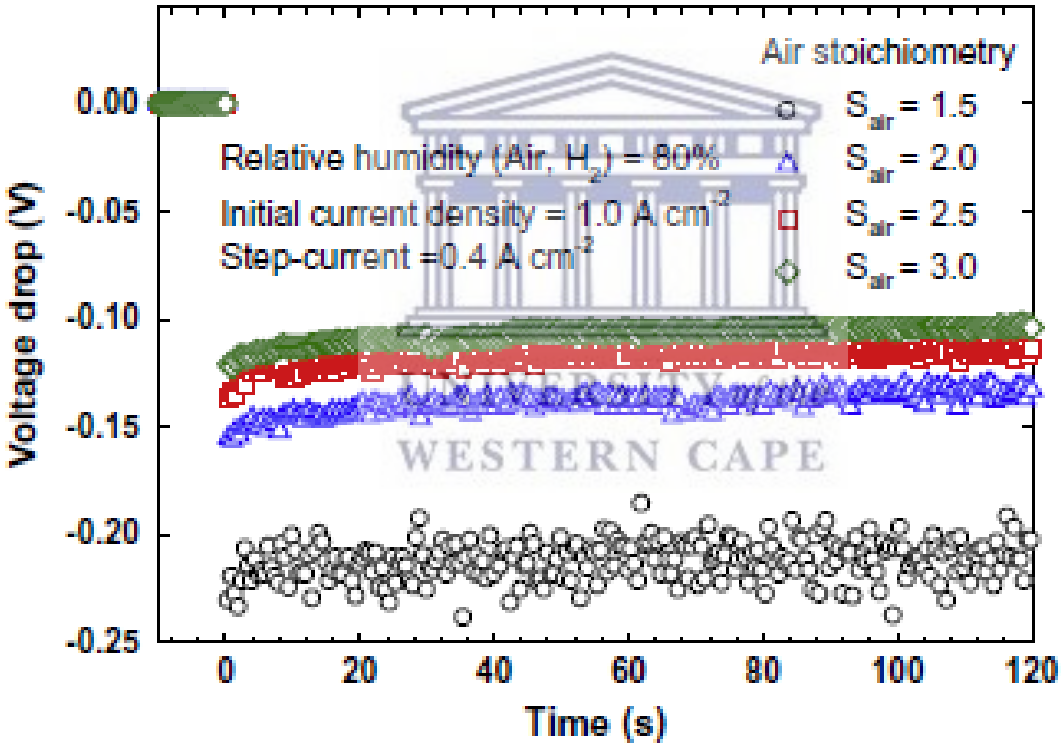

Figure 11: Transient response of cell voltage under load change at different cathode stoichiometries. Courtesy of Kim *et al.* [77].

Considering the effect of pressure/altitude in aeronautic applications, Hordé *et al.* evaluated the effect of cathode stoichiometry from 1.5 to 2.5. The desired performance was achieved at cathode stoichiometry of 1.75 and 2.5 for 1200 and 2200 m altitude respectively [64]. Cathode stoichiometry of 1.9 yielded the desired ODA with less than 12% oxygen content from single fuel cell system, although it was below the manufacturer's recommended operating conditions. Hence, authors recommended further research on cathode stoichiometry that can yield the desired oxygen content (less than 12%) within the recommendations in order to minimize damage to the stack.

2.4.3 Load

Typical operation of the aircraft that defines its load profile is as follows: ground taxi, take-off and climb, cruise, descend and landing and ground taxi [79]. Exploring effects of the load profile-related operating conditions on performance and degradation of PEMFC under aeronautics requires execution of lifetime and degradation testing. Lifetime studies under normal operating conditions are rarely conducted due to time and resources constraints. Hence, fuel cells are tested under conditions that accelerate performance loss and degradation rates using accelerated stress tests (AST) protocols. AST applies different accelerated stressors to determine and predict durability of particular component of fuel cells by examining known failure mechanisms and major precursors of failure.

Each of the AST protocols is designed to focus on specific fuel cell component. For instance, OCV, contamination and start-up/shutdown cycles facilitates chemical attack of the perfluorinated sulphonic acid (PSFA) membrane by peroxide radicals, poison platinum catalyst and corrosion of carbon support, respectively [34, 80-83]. Aircraft operating conditions can be classified as OCV (idling), start-up/shutdown cycling (start-ups and shutdowns), current hold (cruise) and potential cycling (take-off, variable load demand and landing) in comparison to laboratory testing.

2.5 Flight stages and associated AST

2.5.1 Idling

Idling encountered at ground taxiing draws no current and therefore creates high voltage conditions similar to the OCV conditions. The high voltage at OCV promotes formation of peroxide and hydroxyl radicals. The radicals attack the membrane and subsequently facilitate Pt particle migration from the catalyst layer and redeposition on either the catalyst layer or on the membrane [49]. Wu *et al*. and Kundu *et al*. observed overall degradation rates of 0.128 and 5.8 mVh^{-1} after 1200 and 900 hours of operation at OCV [84, 85]. High temperature, known to accelerate the radical-forming reaction, may be attributed to the higher degradation rate at 90°C from Kundu *et al*. compared to 70°C by Wu *et al*.

The study by Kundu *et al*. rather discovered that voltage decay goes through transient performance decay trend during the first 50 hours and that voltage decay is partially recovered after polarization curves are measured. The investigation of the potential cause of performance recovery was not undertaken, possibly due to research scope limits [84]. Similarly, Wu *et al*. observed partially recovery of voltage decay after in-situ characterization [85]. Wu *et al*., further reported presence of HF, H_2O_2 and CO_2 in the exhaust gas which implies membrane and carbon support degradations. Wu *et al*. substantiated the theory of MEA degradation exacerbated by high voltages at OCV.

Pei *et al*., Wu *et al*. and Jouin *et al*. suggested that 10% loss of voltage is equivalent to end of life (EoL) [42, 86]. However, the 10% is not applied as a measure of the length of the AST. Some tests are continued beyond 10% voltage loss. For instance Wu *et al*. declared EoL at 25% (0.128 mVh^{-1}) voltage loss after 1200 hours which was due to 43% loss of ECSA, CO_2 emission and increase of hydrogen crossover from 1.84 to

20.71 $mAcm^{-2}$ [85]. Zhao *et al*. reported up to 0.37 mVh^{-1} degradation rate due to 40% loss of ECSA and 55% Pt particle growth [48]. Up to 2 mVh^{-1} degradation rate after only 48 hours has been reported in literature, mostly caused by adsorption of anions (formed from membrane decomposition) by Pt particles which blocked active surface area of the catalyst [46, 87]. The loss of ECSA, emission of CO_2 and hydrogen crossover are indicators of catalyst, carbon support and membrane degradation which are components of MEA. OCV is therefore referred as AST method employed to specifically study MEA chemical stability since the test conditions favour membrane chemical degradation and electrode degradation.

2.5.2 Start-ups and shutdowns

PEMFC operated in aeronautic conditions is likely to experience several start-ups and shutdowns. The effect of start-ups and shutdowns is studied through the SUSD cycling. The SUSD methods involve applying controlled voltages either in square-wave or cycling manner to simulate the variation in load during SUSD. For instance, the study by Kim *et al*. simulated the SUSD cycling by alternating air supply, hydrogen supply and purging while applying a dummy load (labelled Load on and Load off in Figure 12) in between [88]. The dummy load was believed to reduce voltage decay. The fuel cell was also subjected to various RH to examine its effects on PEMFC performance.

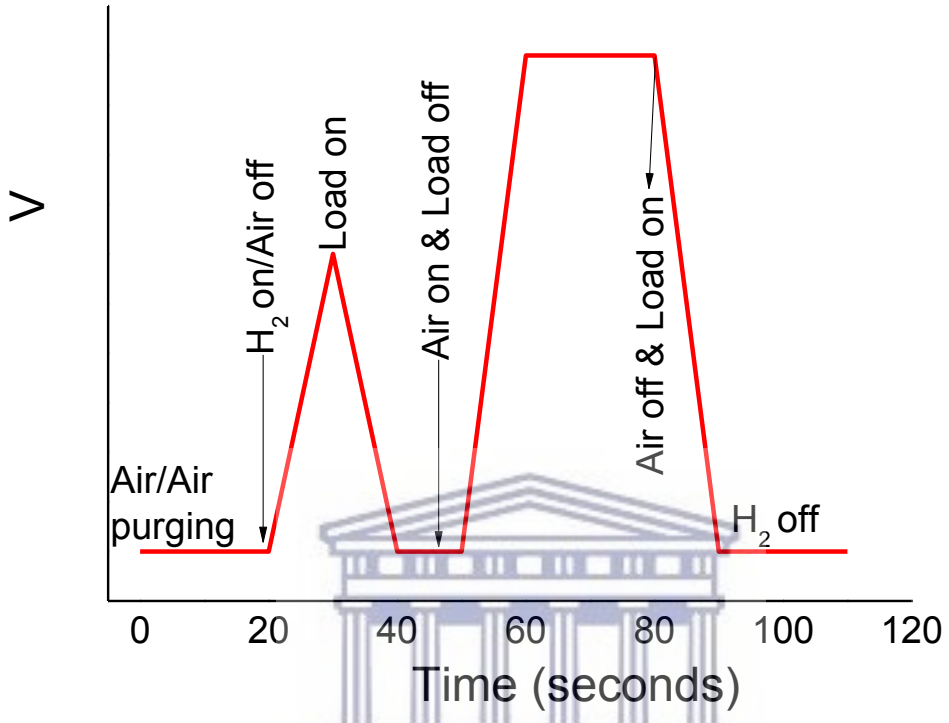

Figure 12: Experimental load profile of the start-up and shutdown operation of the PEMFC employed by Kim *et al*. [88].

The study reported higher performance loss at 100% RH associated with more than two-thirds ECSA loss. However, no significant changes in OCV and hydrogen crossover were observed for all tests. Hence, it was concluded that performance loss during SUSD cycling is due to catalyst degradation [88]. Jo *et al*. followed similar load profile applied by Kim *et al*. to study the effects of operating temperatures of up to 80°C during the SUSD cycling [47]. It was also concluded that performance decay was due to catalyst degradation rather than membrane since there was less than a percent of OCV lost while significant loss of ECSA and catalyst layer thickness were observed [47].

On the other hand, Lin *et al*. conducted SUSD cycling by operating the fuel cell between OCV and 100 $mAcm^{-2}$ at 30 and 10 s intervals respectively [89]. The applied cycling profile is shown in Figure 13.

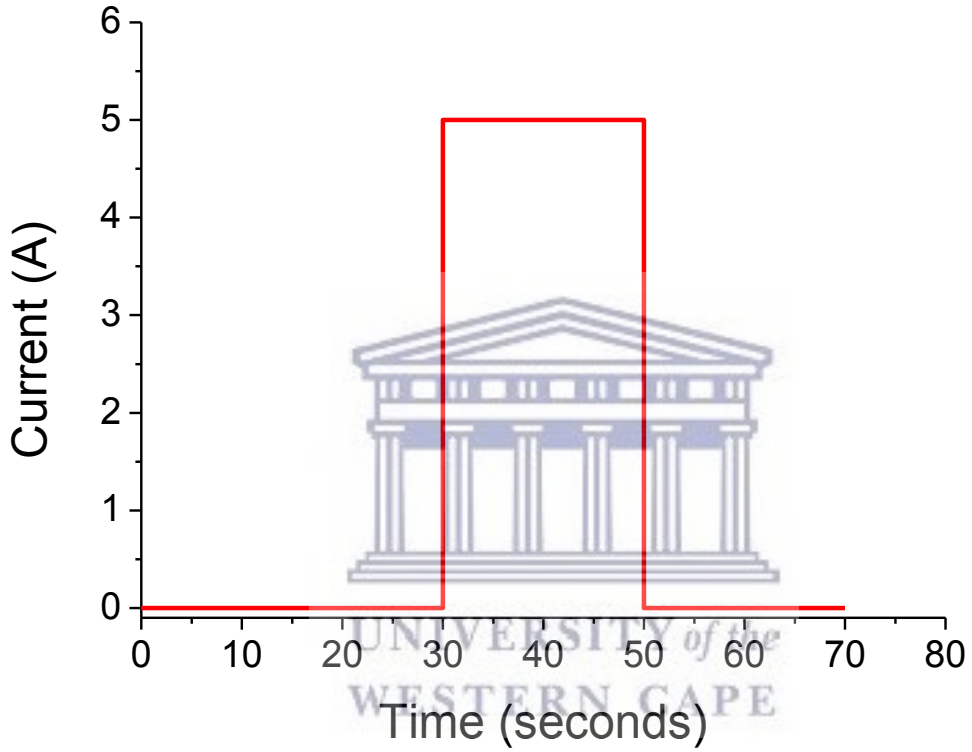

Figure 13: Current changes during one start-up and shut down cycle employed by Lin *et al.* [89].

The overall electrical performance was monitored by measuring IV curves. The average degradation rates (ADR) computed from the IV curves were faster at higher current densities with 0.061 and 0.021 $mVcycle^{-1}$ at 1400 and 500 $mAcm^{-2}$ respectively. The faster ADR at higher current densities were associated with mass transfer limitations. The study reported that degradation was due to cell reversal that caused severe carbon

corrosion, which was more apparent on cathode catalyst layer [89]. SEM cross-section images and CV measurements showed notable reduction in membrane thickness and ECSA respectively.

However, SUSD in real applications are much more complex than just voltage pulsing and use of dummy loads. Hence, the SUSD cycling carried out by Pei *et al*. involved start-up with operating conditions as 60°C, 1.2/2.5 anode and cathode stoichiometry, 100 A cell current, idling for 1 minute at 10 $mAcm^{-2}$, stop and purge with nitrogen until voltage was zero [42]. The degradation was attributed to high open circuit voltage. Even though there was a follow-up publication on post-analysis of the MEA, chemical and physical transformations of the fuel cell components caused by the degradation were not examined by the common techniques such as SEM, TEM or XRD [42].

2.5.3 Cruise mode

Aircraft draws more/less constant power when flying at cruise mode. Current hold refers to cruise mode at constant current encountered when an aircraft has stabilized at a given altitude. Available literature shows that current hold studies are conducted at different current densities that are classified as full load, overload or high power [32, 90].

For instance, the study by Franck-Lacaze *et al.* defined the current density of 540 $mAcm^{-2}$ as nominal load [91]. The study applied 120 and 20 $mAcm^{-2}$ to examine oxidative degradation caused by low current densities [91]. The lowest current density of 20 $mAcm^{-2}$ imposed most aggressive conditions that resulted in severe degradation of the catalyst layer and decomposition of the perfluorinated sulphonate polymer chain of the membrane layer [91]. The Pt PSD increased from 20-130 nm to 50-200 nm while fluoride concentration in recovered water was 3-5 times after the 20 $mAcm^{-2}$ test. The degradation was due to high voltages that promoted Pt dissolution.

Shan *et al*. defined nominal and overload as 900 and 1000 $mAcm^{-2}$ respectively [32]. Liu *et al*. also used 1060 $mAcm^{-2}$ as the highest current density and as control experiment against load cycling [90]. The overall driving cycles caused remarkably loss of catalyst activity due to Pt particles agglomeration and thinning of the membrane layer [32]. More than 50% loss of ECSA and 25% thinner membrane were reported. The degradation mechanisms were attributed to unstable water levels in the MEA that created favourable conditions for carbon corrosion. The humidification cycles caused fuel starvation that resulted in permanent catalyst damage.

As far as this literature survey extends, current hold is not yet standardized and is sometimes applied as lifetime study instead of AST. Thus motivates for establishing clear concise test specifications suitable for aeronautic conditions.

2.5.4 Take-off and landing

Potential cycling, reflective of variable electrical energy demand encountered during cruise mode (periodically), take-off and landing in aircrafts, is studied using various voltages ranging from 0.5 to 1.4 V. Just to clarify, the term potential cycling is sometimes used to emphasize that the test is conducted in potentiostatic mode. The load cycling represents the galvanostatic mode. However, the terms are used interchangeably in this thesis. Whether voltage is imposed or measured will be stated the necessity to differentiate arises in the text.

Load cycling affects the water content of fuel cells and the demand for reactant gases, which ultimately affect the performance and lifetime [74, 92, 93]. The 1.4 V is usually chosen as upper limit for studying carbon support corrosion since no oxygen evolution occurs and is the closest to cathode potential during cell reversal [94, 95]. The Pt surface starts to oxidize at voltages greater than 0.8 V [45]. Besides, voltages at real operations do not often reach 1.4 V. The US DOE also prescribed potential cycling voltage range to be between 0.7 and 0.9 V [30].

Effect of potential cycling is evident on individual cell components. For example, catalyst corrosion observed at voltages between 0.6 V and 0.9 V was caused by formation of platinum oxide which resulted in blocked catalyst surface [96, 97]. Fuel starvation attributed to load cycling caused permanent damage to the electrocatalyst in the form of carbon corrosion, reduced ECSA and platinum particles growth as revealed by respective analytical techniques [32, 93]. Furthermore, Bose *et al.* observed change in Pt and C concentration of MEA after 480 hours of load cycling [93]. The loss of C and Pt was taken as a reflection of carbon corrosion and subsequent loose catalyst particles.

The choice of voltage boundaries is dependent on the objective of the study. For instance, Shan *et al*. used 0.6 and 0.8 V [32]. It is worth noting that degradation was faster at low voltage with 1.7 $mAcm^{-2}cycle^{-1}$ and 0.21 $mAcm^{-2}cycle^{-1}$ at 0.6 V and 0.8 V respectively [32]. The observations are attributed to high current density at low voltage which results in higher reactant gases demand and water generation. Consequently, higher water content blocks the gas diffusion layer and catalyst layer and thereby limiting transport of gases to reactive sites [98]. Excess water accelerates carbon corrosion which in turn results in loss of ECSA, morphology changes and Pt migration/redeposition. Hence, potential cycling is classified by US DOE as AST suitable to study catalyst degradation.

2.6 PEMFC State of Health

PEMFC SoH is essential in determining durability, remaining useful life (RUL) of a fuel cell and reliability. The ability to monitor the SoH depends on how well the PEMFC behaviour under aeronautic conditions is understood. The first steps towards better understanding PEMFC behaviour are to identify factors that cause degradation, performance loss and shortened lifetime. In so doing, measurable parameters directly

linked to the factors can be identified. The identified measurable parameters can be used to establish prediction methods and techniques capable of providing real time information on PEMFC SoH without interrupting energy supply. Additionally, the data acquired on the factors and their respective measurable parameters can be used to develop benchmark-quality database for modelling purposes.

Several reviews have been published on fuel cell SoH that predominantly focus on terrestrial rather than aeronautic applications [39, 69, 74, 101, 119]. The reviews on diagnostic tools by Wu *et al*., Zheng *et al*. and Petrone *et al*. provide a general review of available techniques [106, 107, 111]. These reviews showed that there is no single technique capable of providing real-time diagnostic data, cost-effective, non-intrusive, compatible for aeronautic applications and insensitive to electrical network of the fuel cell. Hence, this section seeks to review available techniques for their capabilities and drawbacks in order to device ways to address the shortfalls and possibly recommend a method that is suitable for aeronautic applications.

2.6.1 Models

Complex reactions and occurrences taking place concurrently within a fuel cell (i.e. chemical, electrical, mechanical and thermal) make it difficult to single out causes of failure, performance loss or shortened lifetime. Despite the complexities, methods are developed to predict fuel cell SoH in terms of performance loss, degradation and, fault detection and isolation (FDI) [72, 74, 99-104]. Diagnostic methods available are model or non-model based [97, 105-119].

Model-based methods are further classified as white, grey or black box depending on the nature of input and output. The Black box model is most suitable for PEMFC since it is directly derived from experiments, requires little computational effort and, capable of on-line monitoring, detection and diagnostic applications [106]. In cases of very short transient periods, model-based methods such as statistics and knowledge of physical or

electrical phenomena become useful. Model-based methods can be used as a control strategy, although relevance and reliability of the methods depends on developments of dynamic ageing models [110].

On the other hand, non-model based methods are simple, flexible, capable of dealing with nonlinear problems and do not require system structure knowledge. Non-model based methods are further grouped as artificial intelligence, statistical method or signal processing [107]. An emerging area of science called Prognostics and Health Management (PHM) focuses on methods that assess SoH, predict RUL and decide mission achievement from mitigation actions [105, 110]. PHM can be classified as a signal processing method since it involves active data acquisition to identify and isolate faults (fault diagnosis) that accelerate ageing of a fuel cell. The fault diagnosis methods involve four steps: data pre-processing, feature extraction, feature reduction and fault classification.

One major drawback of the non-model based method is generating datasets for targeted fault conditions, which can be time-consuming in cases of multiple faults [107]. Dataset generation for data pre-processing includes acquiring data from different sensors and electrochemical characterization techniques such as IV curve, EIS, CV and LSV. A thorough review on the electrochemical techniques is published by [110]. CV and LSV are auxiliary techniques that provide useful information on catalyst activity and membrane health (crossover) respectively. Main drawbacks of CV and LSV are that current cannot be drawn during measurements and the quality of data is affected by non-uniform cell voltage distribution within large stacks [102, 112, 113].

2.6.2 Polarization curve

Polarization (IV) curve is a plot of voltage against current density measured under constant operating conditions. The IV curve is obtained by measuring voltage against current density or by measuring current density as a function of voltage. IV curve is the

most commonly used electrochemical method to characterise fuel cells. IV curve provide information on overall electrical performance and performance loss without differentiating between various sources of the loss. For instance, the polarization curves in Figure 14 showed no significant difference between dry and flooded cells and it is almost impossible to identify causes of voltage drop observed on the dry and the flooded cells [114]. Nyquist plot generated from the EIS technique differentiated between the drying and flooding [114]. Despite the limitation, polarization curve is useful in estimating overall voltage decay and average degradation rate [55, 115].

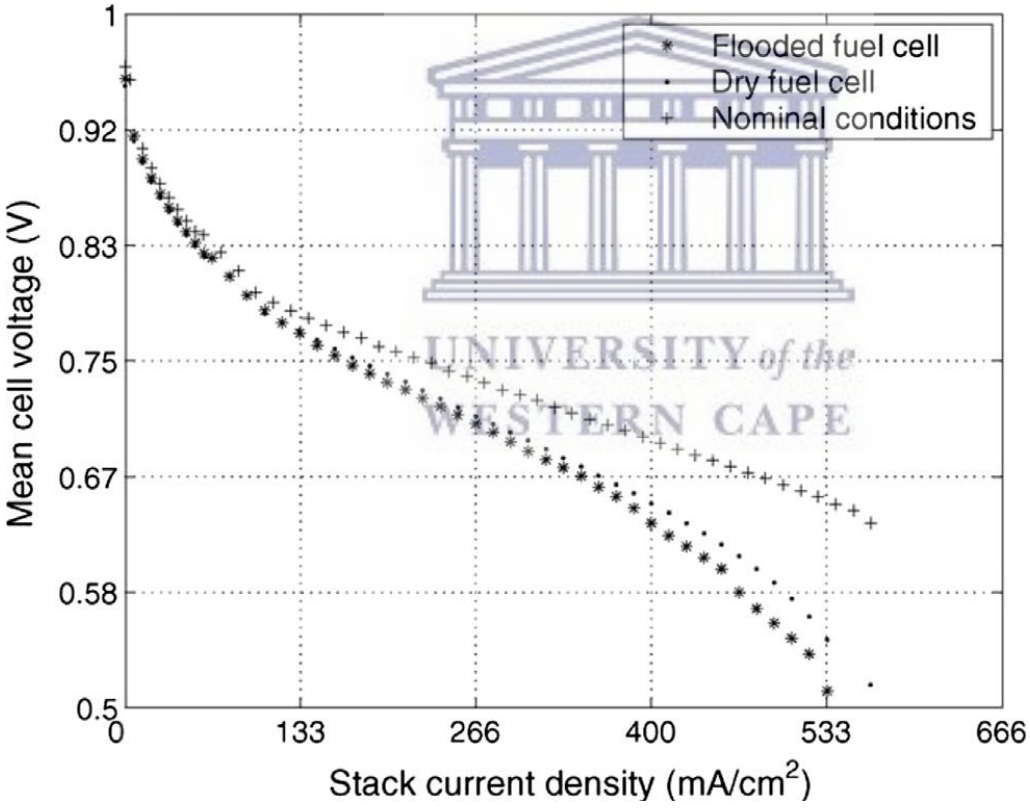

Figure 14: Measured polarization curve for a stack operating at normal, drying and flooding conditions by Fouquet *et al.* [114].

2.6.3 Electrochemical Impedance Spectroscopy

Electrochemical Impedance Spectroscopy (EIS) is measured by applying a small ac voltage or current signal of known amplitude and frequency to the fuel cell. The resultant amplitude and phase signals are measured as function of frequency, a measure of the cell's ability to impede flow of current. The EIS technique coupled with models compliments IV curve by differentiating the various losses [114, 116]. EIS data is presented as Nyquist plot with equivalent circuit models (ECM) to ease interpretation and estimate electrochemical parameters such as resistances, time constants and capacitance [117, 118]. The electrochemical parameters are reflective of SoH of fuel cell and state of its components such as drying/flooding of ionomer membrane and catalyst layer.

For instance, Fouquet *et al.* studied fuel cell SoH based on drying and flooding conditions using EIS and ECMs [114]. The study defined three subspaces related to nominal, drying and flooding conditions by measuring membrane and charge transfer resistances. Dry cell generates two semi-circled Nyquist plot whereas flooded cell tends to have higher low frequency resistance and a much wider single semi-circle.

Rubio *et al.* further proposed simplified ECM for the nominal, drying and flooding conditions within 1 Hz and 5 kHz frequency domain using an inexpensive and portable device [100]. However, the frequency domain is questionable as to whether it reflects all phenomena occurring within fuel cells.

Yuan *et al.* and Rezaei Niya *et al.* presented thorough review of applications of EIS and equivalent circuit models in characterizing PEMFC [119, 120]. Although EIS can effectively diagnose fuel cell state of health such as cathode flooding, membrane drying and catalyst ECSA, the technique is not ideal for on-board integration. Major drawback of the EIS technique in the context of aeronautics is compactness, sensitivity to electrical network stability and operating conditions, and complex data that does not yet

provide real-time diagnosis. The models can be used to develop database for instant fault detection and isolation however their capability is limited to testing of the operating conditions and available library [121].

2.6.4 Sensors

Performance loss due to voltage decay depends on the cause of the loss. Some decayed voltage can be recovered if detected timely. The nature of performance loss phenomena can happen in a matter of few seconds. For instance, water accumulation on the membrane can happen within seconds (Figure 15). The temporary performance loss can only be effectively detected by installing sensors that are capable of communicating any anomalies to users immediately.

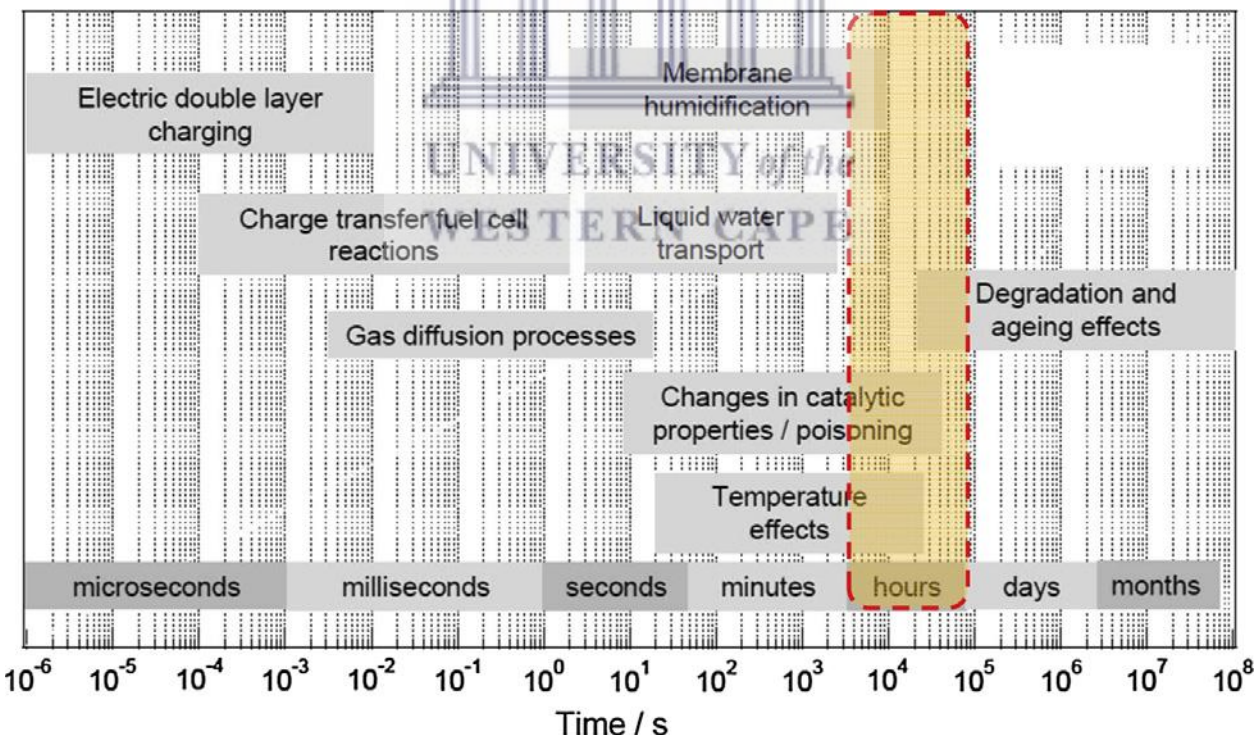

Figure 15: Time-scale of degradation mechanisms for PEMFC adapted from Jouin *et al.* [86].

Lee *et al*. developed 5-in-1 micro sensor (Figure 16) that monitors internal local temperature, voltage, pressure, flow rate and current density for high temperature PEMFC [122]. The in-situ diagnostic affects overall electrical performance by 1.3% due to reduced reaction area covered by the sensors and resistance of the sensors' material. As shown in Figure 17, the sensor's capability is limited by its contact to the fuel cell surface. A 10-cell stack requiring three sensors implies that a 20 kW 110-cell stack needs more than 30 sensors. Wiring from the sensors might compromise balance of plant and performance of PEMFC. Therefore, the micro sensor technology needs to be improved and customized for aeronautic applications.

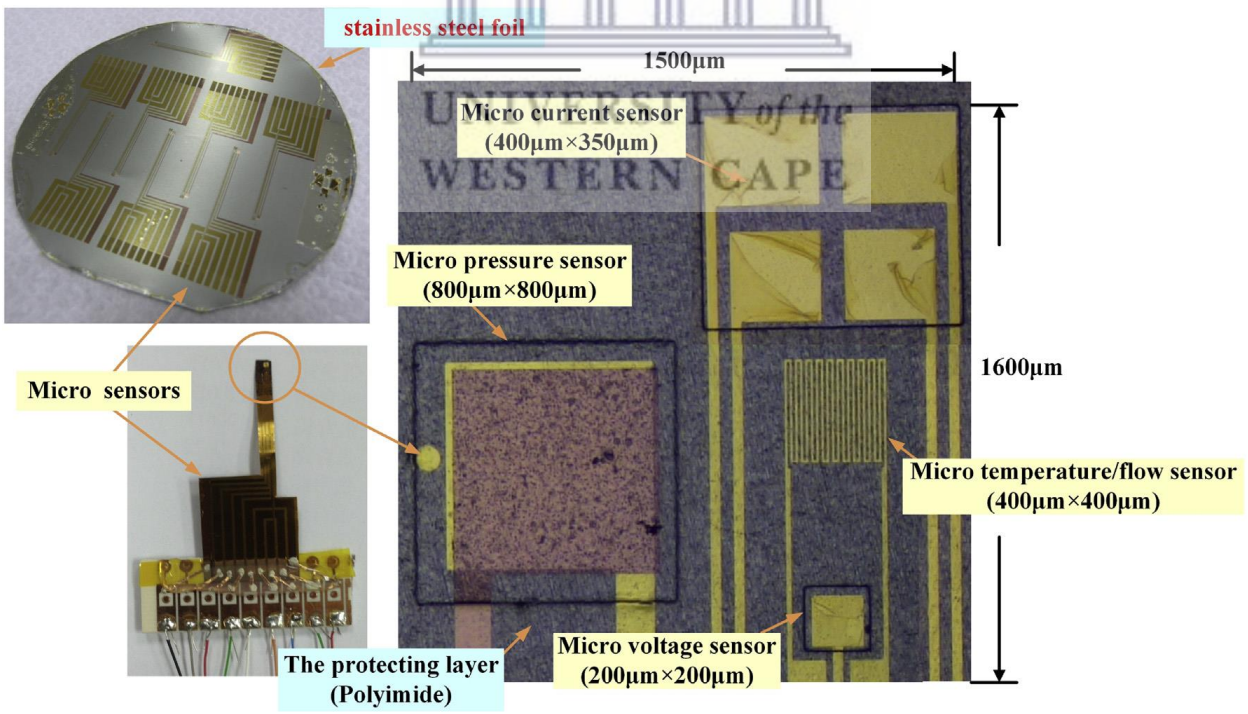

Figure 16: The five-in-one micro sensor devised by Lee *et al.* [122].

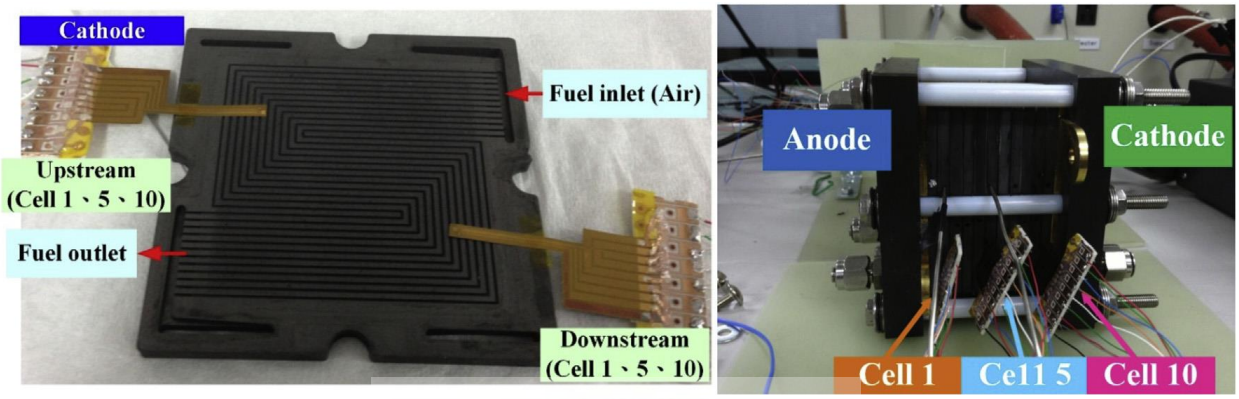

Figure 17: Illustration of the 5-in-1 sensor embedded on a cathode bipolar plate and on a stack [122]

One of the draw backs for the 5-in-1 micro sensor is that it only senses changes of the monitored parameters without providing comprehensive fault diagnosis information as to what caused the changes. The sensors proposed by Mao *et al*. intend to isolate features that will allow diagnosis of PEMFC state. The modelling results show that its library coupled with 10 sensors (5 on cathode and 5 on anode) can differentiate between normal, transitioning and flooding state based on voltage decay [123]. However, more than 10% voltage drop does not necessarily indicate flooding. The voltage drop may be from starvation or dehydration.

On the other hand, David *et al*. devised a fibre optic sensor that uses hygroscopic expansion and contraction of polyamide recoated Fibre Bragg grating to monitor RH [124]. The sensor is thin enough to be installed in the channels of bipolar plates and it showed negligible performance interruption. The response time off the sensor adequately short to resolve voltage decay attributed to transient RH changes that are due to osmotic drag and back diffusion [124].

2.7 Summary of the literature review

PEMFC directly convert chemical energy into electrical energy through the reaction of hydrogen and oxygen in the presence of Pt catalyst. PEMFC by-products (water, deoxygenated air and heat) have essential use in aircraft. PEMFC continually generates electrical power for as long as there is hydrogen and oxygen is supplied and it does not require recharging time like batteries. As a result, PEMFCs are not only considered as APUs but as MFC capable of producing drinkable water, generating useful heat, discharging oxygen-depleted air for inerting jet fuel, recharging batteries, replacing Ram Air Turbine and power small electrical systems on-board (i.e. flight control and landing gear). Consequently, PEMFCs were tested as main power source in small manned aircraft, as APU for commercial aircraft and as supplementary power source for aeronautic applications such as electric nose wheel.

The field testing has successfully shown that PEMFCs are capable of providing energy in case of emergency as well as power electric nose wheel in commercial aircraft. In addition to field testing, PEMFCs are also tested in laboratories under simulated aeronautic conditions such as vibrations, high altitude, subfreezing temperatures and inclination for effects of environmental conditions. Furthermore, PEMFC are examined under various operating conditions in efforts to optimize quality of the useful by-products. All the studies conducted revealed that fuel cell performance is affected by the aeronautic conditions.

The extent and nature of the effect of aeronautic environmental conditions on PEMFC behaviour is not yet quantified. Hence, it is crucial to conduct more research in order to establish differences/similarities between terrestrial and aerial effects on fuel cells. Establishing the effects of aeronautic conditions and MFC operating requirements is necessary to identify factors that influence fuel cell life and performance when used in

aircraft. Laboratory testing under simulated aeronautic environmental conditions showed that performance loss observed at high altitude associated with low pressure and lower concentration of oxygen in the air can be minimized by tuning operating conditions (e.g. operating temperature, cathode stoichiometry, relative humidity, etc.).

Thus, identified factors that have direct effect on PEMFC in aeronautic conditions are cathode stoichiometry, operating temperature and load profile. Increasing cathode stoichiometry to 2.5 compensates for the low pressure and content of oxygen at high altitudes. PEMFC operated in aeronautic conditions is likely to be exposed to temperatures ranging from 20 to 90°C whereas stacks are commonly designed for up to 80°C. Behaviour of PEMFC at 90°C under aeronautic environment is neither well-understood nor documented. Load profile of aircraft is different from vehicular and its effects on PEMFC SoH are also not well-understood.

Identified measurable parameters can be used to establish prediction methods and techniques capable of providing real time diagnosis on PEMFC SoH without interrupting the energy conversion reaction. Effects of the identified factors are quantified by monitoring overall performance by means of calculating average degradation rate from IV curves. Drawback of the IV curve data is that it is not capable of identifying source/cause of performance loss.

EIS coupled with physical models can differentiate between membrane and catalyst degradation. EIS however is not real-time and its capability is determined by available database of known degradation mechanisms caused by specific operating conditions. EIS is very sensitive to electrical network stability, which is great challenge for big stacks. Installing sensors or electrodes for each determinant (namely relative humidity, operating temperature, power output versus current drawn, etc.) would be impractical and difficult to manage.

On the other hand, techniques such as CV and SEM are either off-line or cannot be performed without interrupting electrical energy generation. Therefore, available techniques either do not provide comprehensive information on SoH, are invasive, sensitive to non-homogeneous current distribution observed in larger stacks or difficult to fit in aircraft (i.e. too large with complex balance of plant). There is no single technique capable of providing real-time diagnostic data, cost-effective, non-intrusive and insensitive to non-homogeneous electrical distribution in big stacks available yet.

CHAPTER 3

THESIS RATIONALE

3.1 Rationale and Motivation

The goal set by various ministries to reach cell lifetimes of 5, 000 h in vehicles, 20, 000 h in bus and 40, 000 h in stationary applications by 2015 has not been fully achieved. The main issue is degradation of fuel cell and its components. Fuel cell life can only be optimized by minimizing degradation, which can be effectively decreased by recognizing factors that cause degradation. Complex reactions and processes taking place within a cell and its surrounding system makes it difficult to clearly understand degradation mechanisms. Increasing use of PEMFC in aerial vehicles requires comprehensive knowledge of the technology. This study seeks to characterize PEMFC under simulated aeronautic conditions using electrochemical and chemical/physical techniques with the aim to identify factors that influence fuel cell life. In so doing, a method to assess fuel cell SOH will be designed. Information generated from the method will be used to determine potential defects and assist in scheduling necessary maintenance to avoid processes that lead to shortened cell lifetime.

3.2 Hypothesis

The key findings from the literature review highlighted the importance of understanding behaviour of PEMFC under aeronautic conditions as first step towards identifying factors that have direct effect on its SoH. The identified factors have measurable parameters but the techniques available are not comprehensive enough to provide real-time online diagnosis. The nature of effects of the factors on PEMFC performance and degradation under aeronautic conditions is not well-understood. Hence, hypotheses formulated based on the literature review of PEMFC behaviour in aeronautic environment are:

I. Start-ups and shutdowns cause more degradation that cruise mode.

II. Variable load demand (take-off and landing) and idling partially recovers temporary degradation.

III. Operating PEMFC at 90°C for a short period lowers performance but does not cause significant damage to fuel cell components.

3.3 Key Questions

Research questions to be addressed are as follows:

I. What are factors that influence fuel cell life in aeronautic environment?

   a. Which of the factors are influenced by aeronautic environment?

b. Which of the factors have reversible effects?

II. What are measurable parameters associated with the factors?

a. Is the signal/symptom dependent of time or operating conditions?

III. Which non-intrusive test methods are capable of evaluating the measurable parameters on-board?

IV. What does the information obtained tell about the fuel cell's SoH?

CHAPTER 4

MATERIALS AND METHODS

This chapter presents the experimental work undertaken in this study as outlined in Figure 18. The methodology of this project involves examining behaviour of MEAs under different operating conditions simulating aeronautic environment through monitoring electrochemical changes and evolution of fuel cell components as characterized for chemical/physical properties. Aeronautic environment is simulated by employing operating temperature, cathode stoichiometry and load profile likely to be encountered by PEMFC used in aircrafts. This chapter also provides details of the different test methods used to characterize the fuel cells and analyses performed on the single cell components sampled after the degradation tests.

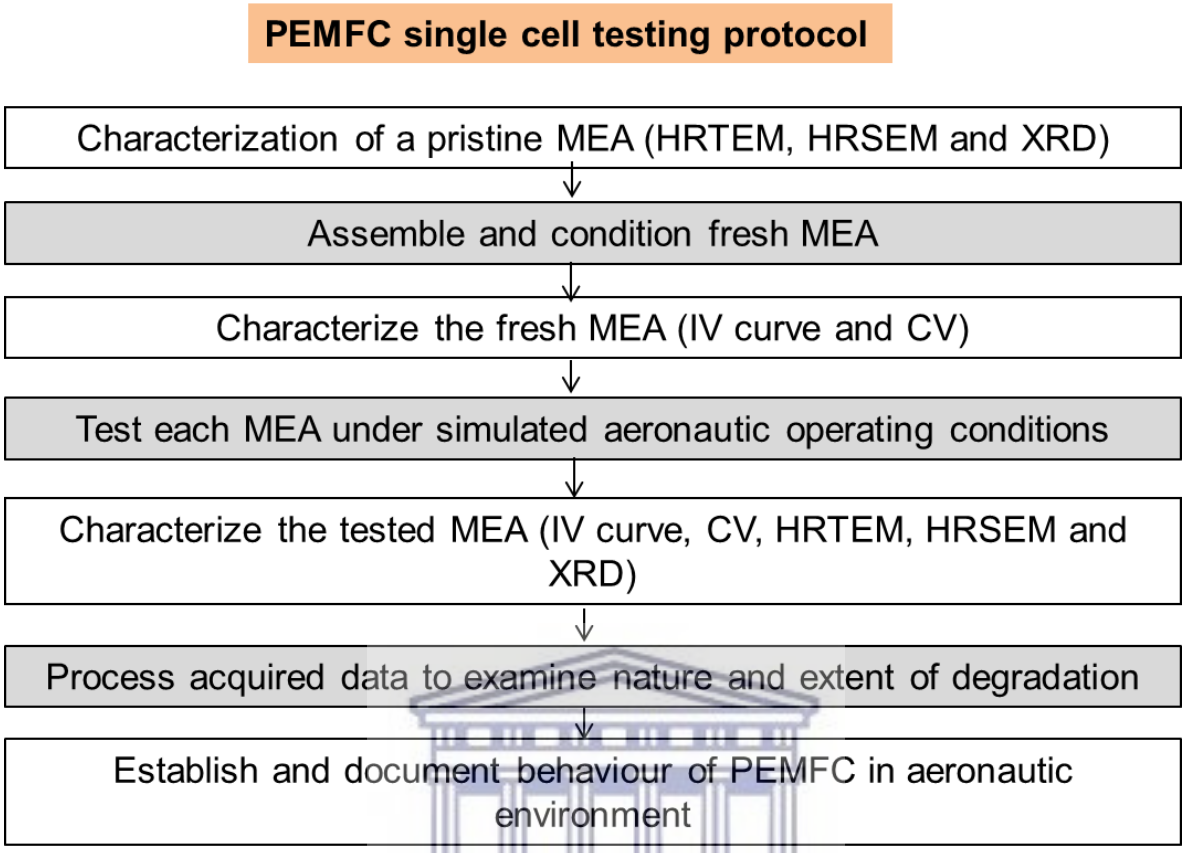

Figure 18: Schematic illustration of the experimental work carried out and the scope of this study.

4.1 Setup

The low-temperature PEMFC single cell (see Figure 19) used for testing consisted of a 25 cm^2 commercial MEA assembled in a commercial single cell fixture made of graphite bipolar plates with serpentine/parallel design of flow pattern and gold-plated current collectors. Both anode and cathode catalyst loadings were 1.0 $mgcm^{-2}$ Pt. The single cell was tested using Greenlight G20 Fuel Cell Test Station. The fuel cell was operated at atmospheric pressure with pure hydrogen and air supplied to anode and cathode, respectively. All the tests were carried out using fully humidified hydrogen and air supplied to anode and cathode respectively at atmospheric pressure. MEAs were used and subjected to the same activation method of operating the PEMFC at 0.7 V, supplied with fully humidified reactants at stoichiometry of 1.8/2.0 anode/cathode for 100 hours. Hence, IV curves measured at the beginning of each experiment confirmed repeatability of samples performance and quality. Additionally, obtaining similar IV curves after the activation stage was also an indication of functional and properly activated MEA. After the applied MEA activation, the MEAs were subjected to operation under simulated load profile related to flight stages. Fuel cell parameters such as operating temperature, dew point, stoichiometry/flow rates and load were controlled using Greenlight's Emerald™ control and automation software.

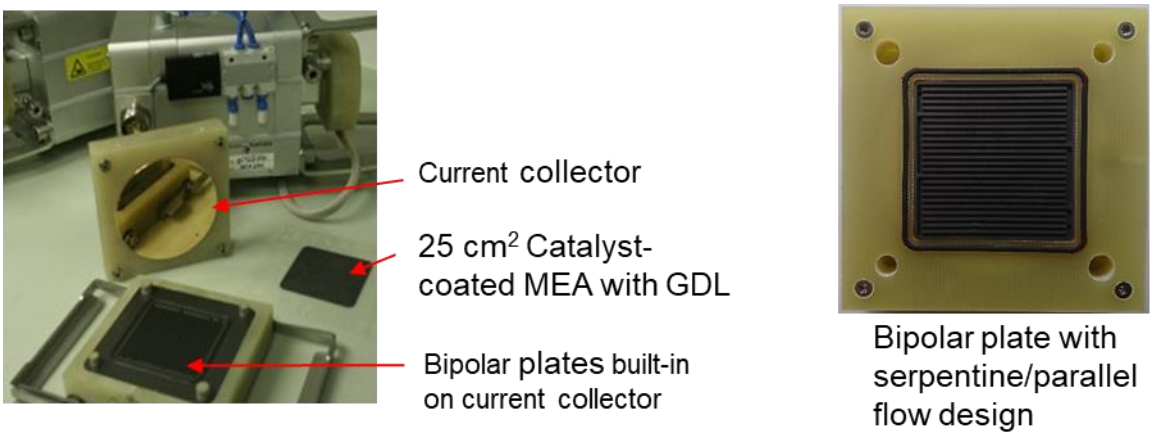

Figure 19: Components of the single cell used in this study.

4.2 Testing protocols

PEMFC performance and degradation are influenced by several factors ranging from operating conditions to environmental surrounding. However, only operating conditions were studied due to limits posed by scope of the thesis. The literature survey undertaken to investigate operating conditions that have effects on PEMFC operation under aeronautic environment revealed that the factors are cathode stoichiometry, operating temperature and load profile. Aeronautic environment at high altitude is characterised by low ambient pressure (0.7 atm at 2200 m) and low oxygen content (16.0% at 2200 m).

4.2.1 Cathode stoichiometry

Several studies were conducted to examine effect of cathode stoichiometry on PEMFC performance and to optimize MFC which collectively shown that increasing cathode stoichiometry minimizes performance loss at high altitudes (64, 67, 72). One of the

reasons for this observation is that low oxygen encountered at high altitude where air ambient pressure is low can be compensated by increasing air flow to the fuel cell through increasing cathode stoichiometry. On the other hand, anode stoichiometry showed no notable effects for as long as it was more than 1.5. Increasing anode stoichiometry any further than 2.0 is discouraged since it increases fuel consumption which reduces fuel cell efficiency [70]. The ultimate goal for all the studies conducted on PEMFC is exploring methods to improve efficiency while minimizing cost in order to accelerate industrialization of fuel cells. Therefore, identified techniques that improve efficiency must at least not compromise the cost of operation. Therefore, it is upon the literature findings that cathode stoichiometry of 2.5 was selected for all tests conducted in this study. The anode stoichiometry was kept constant at 1.8 for all the tests.

4.2.2 Operating temperature

Recommended operating temperature for low temperature fuel cell is between 60 and 70°C. Temperatures above 70°C tend to reduce fuel cell performance due to dryness induced by high temperatures. The extent of performance loss and effects of higher operating temperature on degradation of fuel cell components are not well-understood, particularly for aeronautical applications. Moreover, fuel cell employed in aircrafts is likely to be exposed to operating temperatures as high as 90°C. Hence operating temperature of 60 and 90°C were studied in this research. The 60°C was taken as reference (nominal) test while the 90°C represented extreme conditions in order to examine whether fuel cell can withstand such conditions.

4.2.3 Load

Load profile of an aircraft covers take off, idling and landing. Load is identified as one of key factors influencing fuel cell lifetime since changes in current drawn during flight affect operation of PEMFC. Load effects were studied by subjecting fuel cell to AST considered being representative of aircraft flight stages (79, 125). The flight stages based on AST test conditions are idling/OCV, cruise/CH, start-ups and shutdowns/SUSD and variable load demand/PC.

4.2.3.1 Idling mode

Idling represented as OCV, where there is no current drawn or power output required. The OCV mode was carried out by supplying the PEMFC with hydrogen and air with no load to draw current or impose voltage that resulted in initial voltage of 0.935 V (Figure 20). The nominal test (denoted as OCV1) at 60°C was carried out for 500 hours without interval characterization to omit the observed recovery effect. However, unforeseen circumstance rising from either reactant supply or technical fault resulted in forced shutdown. The tests at higher temperature (OCV2) was planned to be conducted for 500 hours. However, the cell degraded faster than anticipated at 90°C. Hence characterization at 100-hour interval was incorporated to explore whether the test can be extended through delaying degradation via recovering performance loss. The OCV2 test was terminated before reaching 500 hours.

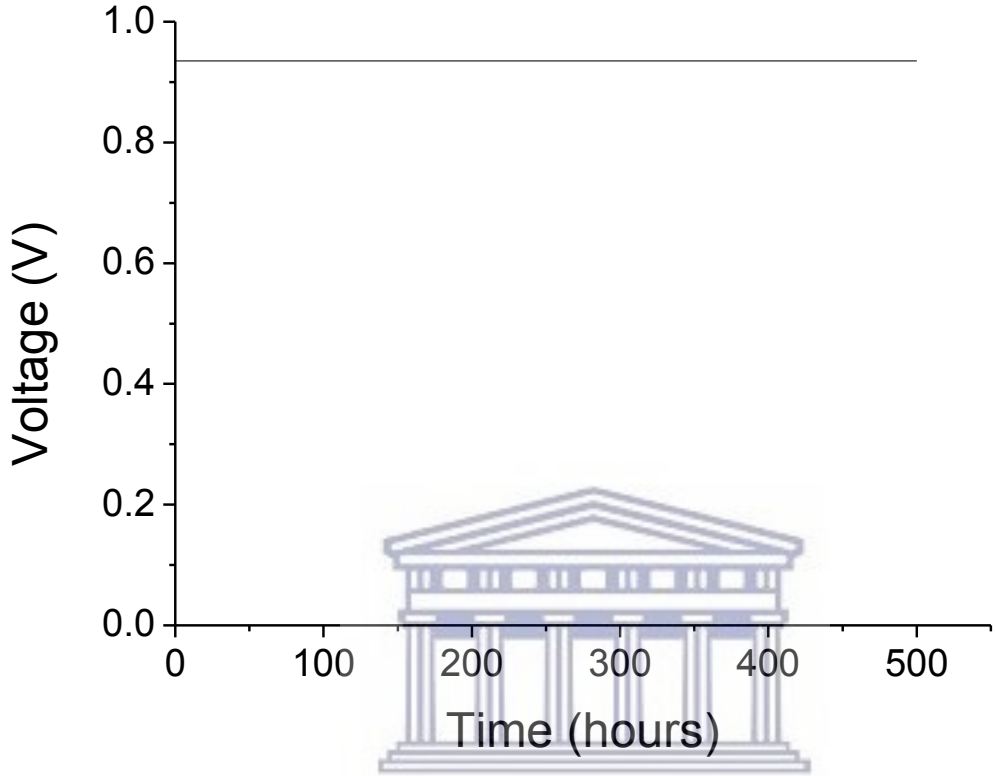

Figure 20: Ideal idling operating conditions with constant voltage at near-OCV.

4.2.3.2 Start-ups and Shutdowns

The PEMFC was subjected to simulated SUSD cycles that included heating and cooling in order to mimic aeronautic conditions as shown in Figure 21. The single cell was heated to 60°C at 0.7 V, 100% RH and 1.8/2.5 anode/cathode stoichiometry for the nominal test (SUSD1). When fuel cell reached 60°C, an IV curve was taken and the cell was cooled to room temperature followed by 5 minutes' rest prior to restart. A voltage of 0.7 V was imposed during the heating and cooling. While voltage was measured at imposed current when measuring IV curve and purging. The study by Oyarce *et al.* on

shutdown strategies revealed that purging is essential to minimize degradation caused by H_2/O_2 interface at anode [45]. However, purging until cell voltage reaches zero in real applications is impractical. Hence, the cells were purged for 5 minutes during shutdown. The temperature was heated up to 90°C for the SUSD2 test, following similar principle as for the SUSD1.

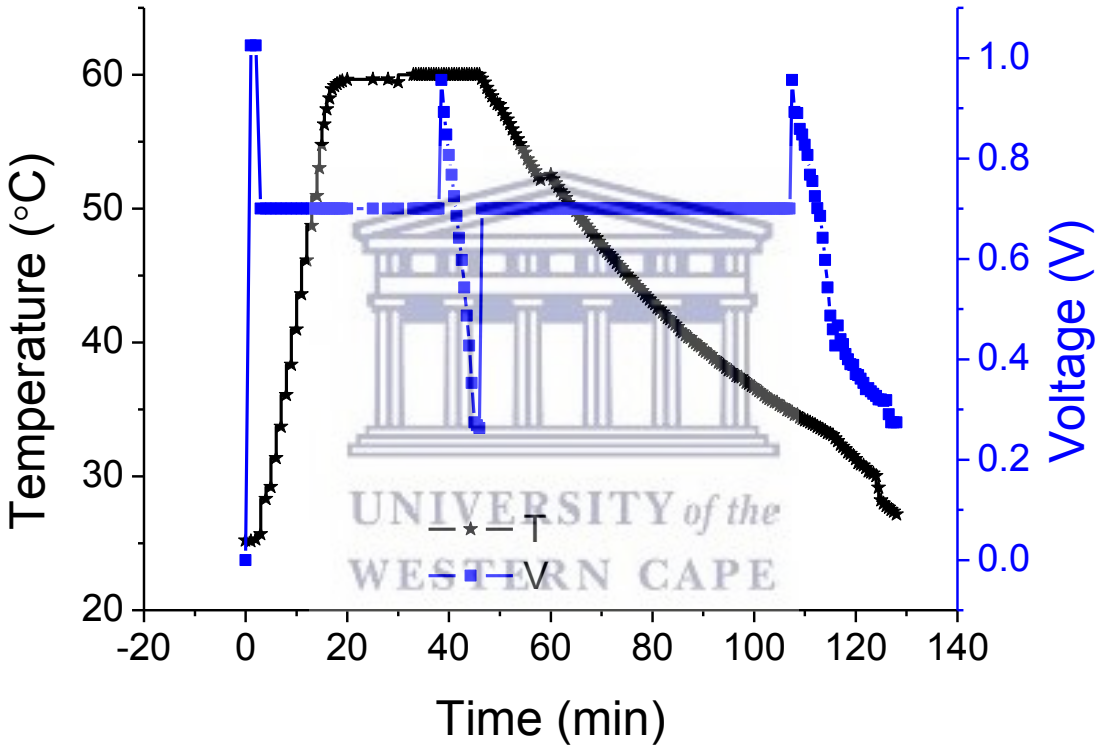

Figure 21: Schematic diagram of SU/SD cycle (heating up to 60°C and cooling down to room temperature) used during experimental part of the work.

4.2.3.3 Cruise mode

The cruise mode was studied by applying constant current density of 200 $mAcm^{-2}$ for a specific duration (Figure 22). The nominal test was conducted at 60°C (CH1) while the extreme test at 90°C (CH2) for 500 hours.

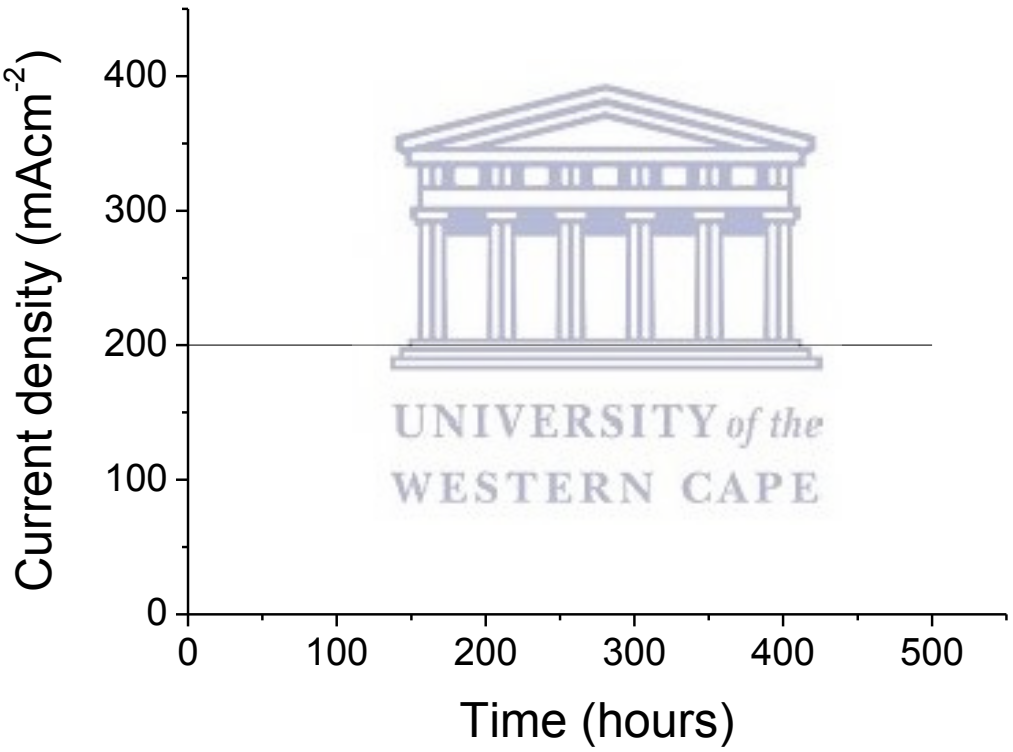

Figure 22: Ideal cruise mode operating conditions with constant average current density of 200 $mAcm^{-2}$.

4.2.3.4 Variable load demand

The variable load effects on PEMFC behavior was investigated by subjecting the fuel cell to potential cycling between 0.5 and 0.9 V at 3 minutes interval each as illustrated in Figure 23. The nominal test at 60°C (PC1) was carried for 5000 cycles while at 90°C (PC2) was terminated sooner due to faster degradation.

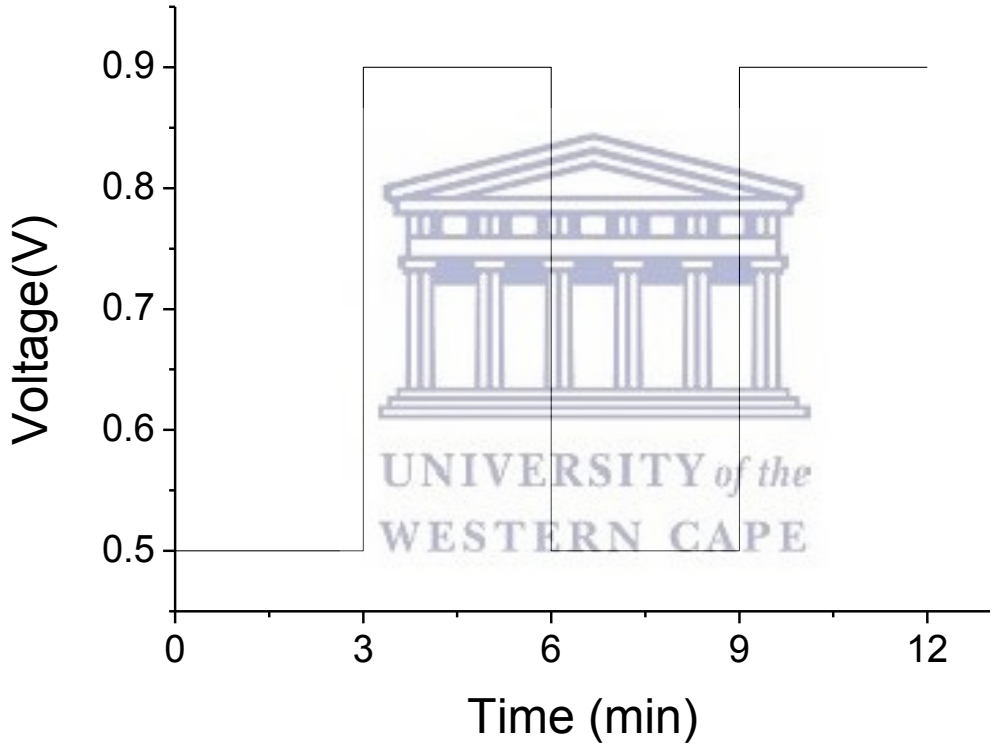

Figure 23: Potential cycling between 0.5 and 0.9 V at 3 minutes interval each.

4.3 PEMFC in-situ characterization

4.3.1 Polarization curve

The complex processes taking place within a fuel cell results in different degradation mechanisms. The performance loss cannot be linked to one isolated mechanism and the IV curve is not capable of differentiating between the causes of degradation. The IV curve provides rough estimation about contribution of known losses reflected by voltage decay at certain current densities. For instance, Figure 24 shows that rapid voltage decay at low current densities (0-0.2 Acm^{-2}) reflects activation losses whereas linear fast voltage loss at 0.4 Acm^{-2} region is associated with ohmic losses. The concentration losses are encountered at higher current densities, greater than 0.8 Acm^{-2}.

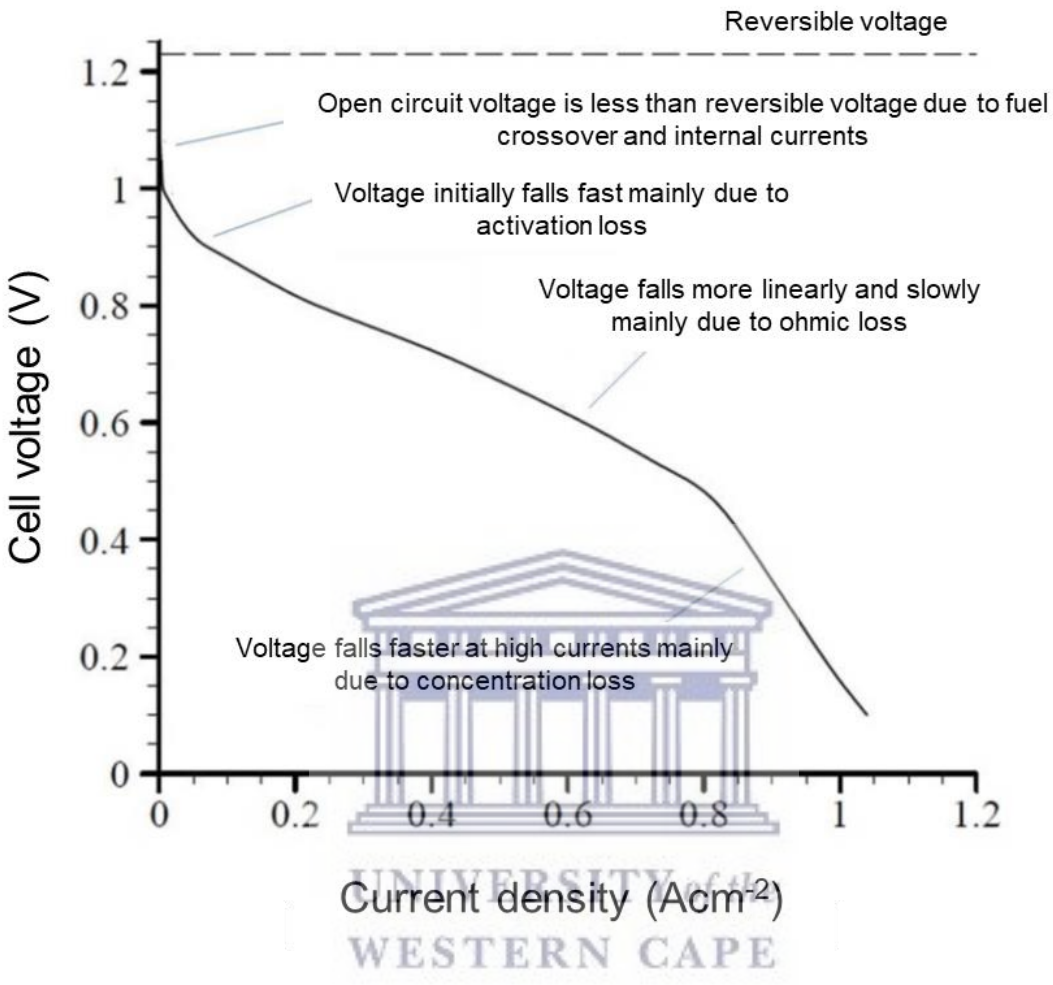

Figure 24: Schematic diagram of an ideal polarization curve demonstrating regions of losses [25].

Activation losses occur during the initial stage of electrochemical reactions whereby the voltages shift from equilibrium to create voltage gradient needed to trigger electrode kinetics. The majority of activation losses are due to sluggish kinetics of the ORR. Ohmic losses are caused by the resistance to flow of ions in the electrolyte and to the flow of electrons through the electrically conductive fuel cell components. Concentration losses result from concentration gradient created by rapid consumption of reactants at

the electrode by the electrochemical reactions. The concentration losses are mostly caused by transport limits of reactant gases through the GDL and the catalyst layer. The losses have been observed to take place categorically with respect to current density, as shown in Figure 24 [25].

The IV curve is measured using load that draws current at fixed operating conditions (namely cell temperature, RH and stoichiometry) to measure resulting voltage and power. The operating conditions must be carefully controlled to avoid starvation or uneven water distribution during the measurement. For instance, flow rate must change with increasing demand for reactants as current density increases. The resulting voltage is used as measure of its electrical performance. The IV curve provides information on overall fuel cell performance and is used to estimate ADR using voltage decay over time of the test (Eq. 14).

$$ADR = \frac{Initial\,voltage - Final\,voltage}{Test\,duration} \qquad \textbf{Eq. 14}$$

4.3.2 Cyclic Voltammetry

Cyclic voltammetry (CV) is a method used to examine the qualitative and quantitative properties of the electrocatalyst. The principle for PEMFC is based on the application of a cyclic potential to the anode electrodes of the fuel cell. The resulting current provides information on the ability of the Pt catalyst to adsorb hydrogen, as illustrated in Figure 25. Interferences are minimized by making the electrode of interest (anode for PEMFC) the working electrode and the second electrode (cathode) as both counter and reference electrode.

The fresh and tested MEAs were characterised for catalyst activity using the CV. The CV were taken using Autolab PGSTAT302N potentiostat with FRA2 module controlled by Nova software at 30°C, a voltage range of 0.015 to 1.00 V and a sweep rate of 30 mVs^{-1}. The gases supplied to the electrodes were hydrogen and nitrogen at anode and cathode respectively. The catalyst activity was quantified by calculating ECSA using Eq. 15. The charge is estimated from the hydrogen adsorption peak demonstrated in Figure 25.

$$ECSA = \frac{Charge}{210 \times 10^{-3} \times Pt\ loading} \qquad \textbf{Eq. 15}$$

Where ECSA (cm^2g^{-1}) is the catalyst active surface area, Charge ($mCcm^{-2}$) represents the charge associated to the hydrogen adsorption/desorption, 210×10^{-3} ($mCcm^{-2}$) is the hydrogen adsorption/desorption charge on a smooth Pt electrode and Pt loading (gcm^{-2}) is the loading of Pt at the studied electrode.

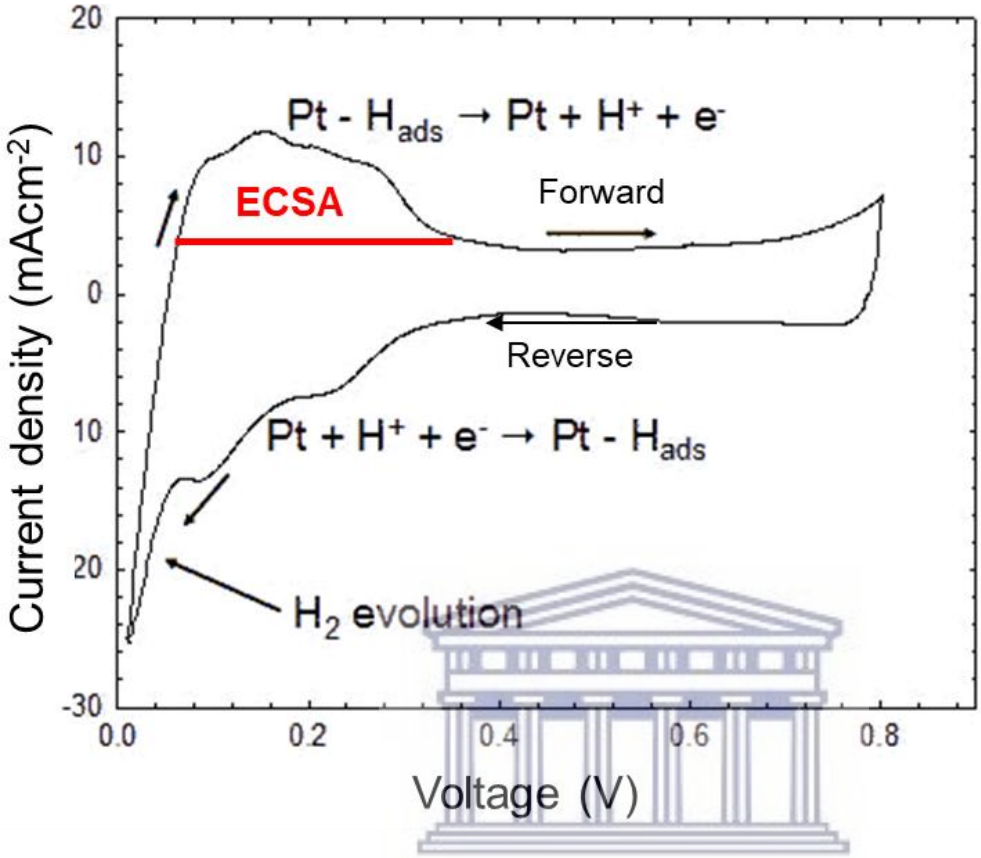

Figure 25: Schematic illustration of an ideal CV for PEMFC demonstrating the peak for hydrogen adsorption that is used to estimate ECSA

4.4 Chemical/physical analysis

4.4.1 X-Ray Diffraction

The crystal structure, phase purity and PSD of the Pt particles were examined by the Bruker D8 X-Ray Diffraction (XRD) with Vantec detector at the iThemba labs. Pieces from the pristine and tested MEAs were cut out into smaller sized suitable to be

mounted on the instrument. The crystal structure and phase purity of the elements were analyzed using Topas Rietveld refinement software. The PSD was analysed qualitatively through observing properties of the peaks from the diffractograms.

4.4.2 High Resolution Scanning Electron Microscopy

A ZEISS MERLIN High Resolution Scanning Electron Microscopy coupled with Energy Dispersive Spectroscopy (HRSEM/EDS) from the Geology Department at the University of Stellenbosch was used to characterize cross sections of the MEAs for chemical composition and particle migration/redeposition. Cross sections were cut out from the MEAs and mounted on copper tapes since carbon was one of the elements of interest. Powder samples scrapped from the cathode electrode were mounted on the copper tapes and analyzed for surface morphology and elemental composition. All micrographs were taken using a backscatter detector at 20 kV.

4.4.3 High Resolution Transmission Electron Microscopy

Scrapped from electrodes powder samples were also examined for changes in the structure of the catalyst layer by capturing transformation of Pt due to particle migration, particle growth from agglomeration and changes in the structure of the membrane surface using High Resolution Transmission Electron Microscopy (HRTEM). The HRTEM used was Hitachi H800 200 kV instrument fitted with digital image acquisition system from the Physics Department at the University of the Western Cape. The PSD was estimated by calculating the average particle diameter using ImageJ software. ImageJ software takes into account the known scale, resolution and magnification in which HRTEM images were recorded.

CHAPTER 5

RESULTS AND DISCUSSION

One of the objectives of this thesis is to identify factors that have direct influence on PEMFC SoH under aeronautic conditions. The identified factors were examined for their effects on performance and degradation of PEMFC operated in aeronautic environment. The observed effects are further studied to determine whether there are measurable parameters associated with the phenomena since the ultimate objective of this study is to devise prediction method for the SoH. Therefore, this chapter explores and discusses the effects of the identified factors (namely cathode stoichiometry, operating temperature and load) on PEMFC SoH and degradation mechanisms with respect to each effect.

5.1 PEMFC Performance

PEMFC performance in this thesis refers to electrical fuel cell performance and ADR monitored by recording IV curves and voltage evolution over test durations. This section explores performance of PEMFC under the simulated aircraft flight stages. The gathered data is further processed to assess whether voltage decay is recovered at the different operating conditions.

5.1.1 Electrical performance

The ability of PEMFC to generate power at a specific current is essential in determining its efficiency. The power output is governed by numerous factors such as cell temperature, RH and available reactants at the catalyst surface. The power output generated under the simulated aeronautic flight stages was monitored by recording IV curves. The power density was extracted from the IV curve data and plotted against the current density. This section explores thriving ability of PEMFC under extreme rapid changing operating conditions likely to be encountered in aeronautic environment.

The cruise mode was simulated by subjecting the PEMFC to constant current density for 500 hours. The imposed current density of 0.2 Acm^{-2} yielded power density of 0.12 Wcm^{-2} at 0.41 V for the PEMFC operated at 60°C, supplied with fully humidified reactants at atmospheric pressure at the beginning of life (BoL). The BoL is the first hour of operating the PEMFC under the simulated aeronautic flight stage.

Figure 26 presents the changes observed in power output during cruise mode at the nominal (CH1) and extreme (CH2) cell/operating temperatures. The power output declined slightly with less than 10% loss after the exposure to constant current from 0.13 to 0.12 Wcm^{-2} during CH1 at low current density of 0.2 Acm^{-2}. The power loss increased to more than 15% loss between 0.17 Wcm^{-2} (BoL) and 0.14 Wcm^{-2} (CH1) as the current density increases to middle region of 0.4 Acm^{-2}. The peak power output decreased (-24%) to 0.14 Wcm^{-2} after the CH1 test compared to 0.19 Wcm^{-2} obtained at BoL. The results presented in Figure 26 eloquently demonstrate that the electrical performance of PEMFC during cruise mode was affected by the current density. More performance losses were observed at higher current densities than at lower ones.

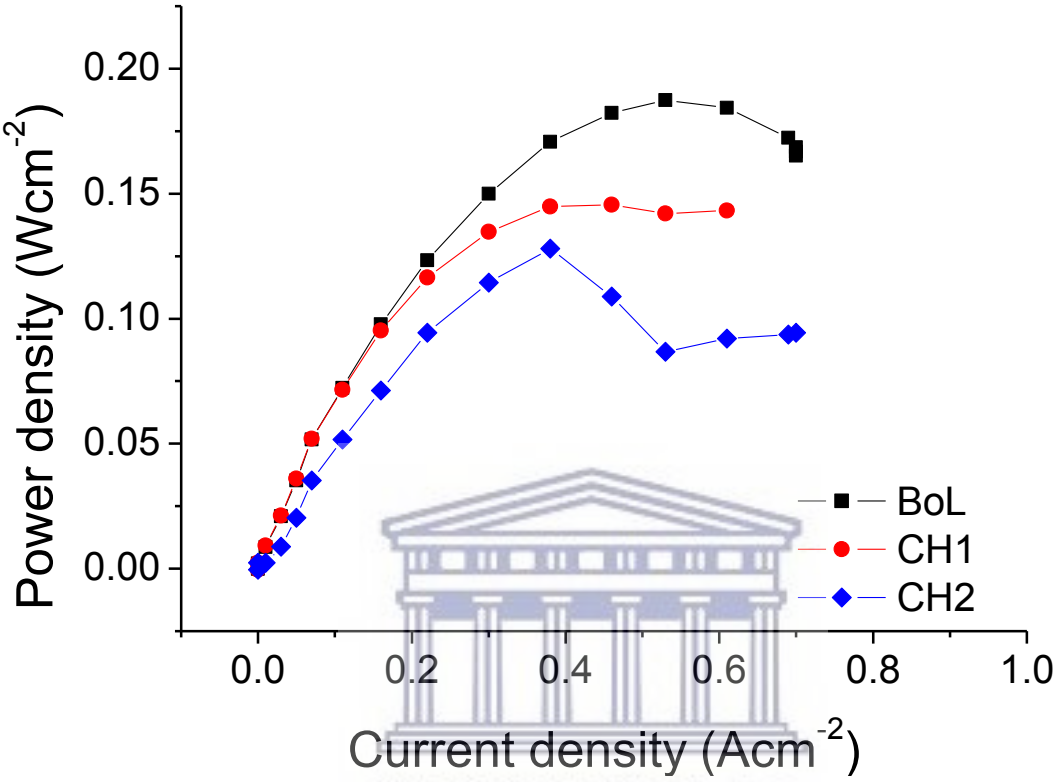

Figure 26: Power performance curves measured at beginning of the tests (BoL) and after cruise mode carried out at 60°C (CH1) and at 90°C (CH2). Measurement conditions: atmospheric pressure, cell temperature 60°C, reactants supplied at 65°C and 100 %RH, 1.8/2.5 anode/cathode stoichiometry.

The increase of operating temperature from 60 to 90°C resulted in decline on generated power. The power decreased by 25% from 0.12 and 0.14 Wcm^{-2} to 0.09 and 0.13 Wm^{-2} at low to middle current density after CH2. The peak power output after CH2 was very low at 0.13 Wcm^{-2} compared to the 0.19 Wcm^{-2} recorded at BoL, resulting in more than 30% performance decline. The power output at high current density (0.5 Acm^{-2}) decreased by 50% from 0.19 to 0.09 Wcm^{-2} after the CH2 test. The extreme

temperature exerts pressure on performance of PEMFC, thereby revealing that the 90°C is too high for PEMFC components.

The cruise mode is expected to be a milder flight stage due to the steady-state conditions created by the constant current drawn. The imposed 0.2 Acm^{-2} current density is within the low current density region where water generation rate through the ORR is much slower. Given that water content determines the conductivity of the membrane and ultimately the overall fuel cell performance [55]. This research seeks to discover whether the slow water generation compliments the fully humidified reactants water saturation. The aim is explored through comparing electrical performance observed under the flight stages. The aim can be further investigated by monitoring water distribution and its variations during the stages. However, resources constraints prevented realization of that. Thus point out the necessity to incorporate in-situ water monitoring system in fuel cell testing. For instance, the 5-in-1 sensor can be incorporated into the testing routine to monitor real-time local internal temperature and flow rate while the fibre Bragg grating sensors can be used to monitor RH [122, 124].

On the other hand, the idling mode examined by operating fuel cell at OCV where there was no load connected to draw current recorded an initial voltage 0.94 V after an hour of operation. The high voltage is associated with adverse effects on PEMFC components that lower the overall performance [21, 83]. The illustration of power evolution with respect to current density in Figure 27 shows that the performance drastically dropped after the OCV1 test.

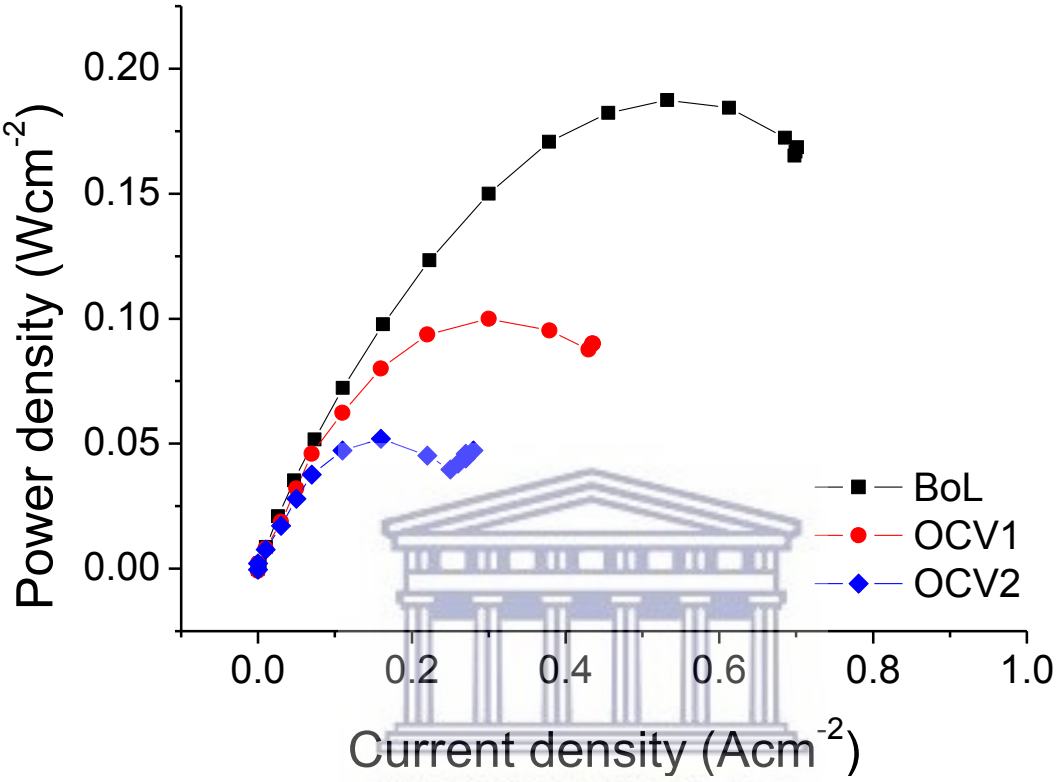

Figure 27: Power performance curves measured at beginning of the tests (BoL) and after idling mode carried out at 60°C (OCV1) and at 90°C (OCV2). Measurement conditions: atmospheric pressure, cell temperature 60°C, reactants supplied at 65°C and 100% RH, 1.8/2.5 anode/cathode stoichiometry.

The power output degeneration was more than 25% after the idling mode at nominal temperature from 0.13 to 0.12 Wcm^{-2} during OCV1 at the low current density. The performance declined worsened with more than 50% power output loss from 0.17 Wcm^{-2} (BoL) to 0.09 Wcm^{-2} (OCV1) at the middle current density. The OCV1 test did not generate any power at high current density. The maximum power output after the OCV1 test decreased to 0.10 Wcm^{-2} compared to 0.19 Wcm^{-2} yielded at BoL.

The OCV2 test recorded the least power output of 0.05 Wcm^{-2} at low current density. This was a 60% decline compared to the power recorded at the BoL. There was no power generated at middle to high current density. This power output of 0.05 Wcm^{-2} was the maximum power generated at 90°C during the idling stage. Figure 27 reveals that the high voltage and high temperature conditions at the OCV2 test caused a significant 70% performance loss.

The decline in power output after the OCV1 test can be attributed to the high voltage conditions known to accelerate fuel cell degradation and subsequent performance loss [40, 91]. The high temperature coupled with the high voltage caused much severe performance loss after the OCV2 test. In addition to the postulated changes in water content of the membrane (that were not monitored), sudden increase in reactants demand at high current density can also be the reason for the drastic performance loss.

This study aimed to better understanding behaviour of PEMFC during idling and cruise mode. The presented data thus far shows that the high voltages imposed during the idling stage deteriorate PEMFC performance while the cruise mode causes much less performance loss. Furthermore, operating the PEMFC at high temperature results in seriously reduced performance and that the PEMFC does not generate power at high current densities when voltage is also high.

The take-off, landing and periodically during cruise mode grouped as variable load was examined by subjecting the PEMFC to load cycling between 0.7 and 0.9 V. The variable load demand phase denoted as PC showed very low power output after the PC1 and the PC2 tests (Figure 28). The power output in Figure 28 shows that the difference between the BoL and the PC1 is almost 3 orders of magnitude. The PEMFC after the PC1 could not generate power beyond the low current density (0.3 Acm^{-2}). The same applies for the PC2 test.

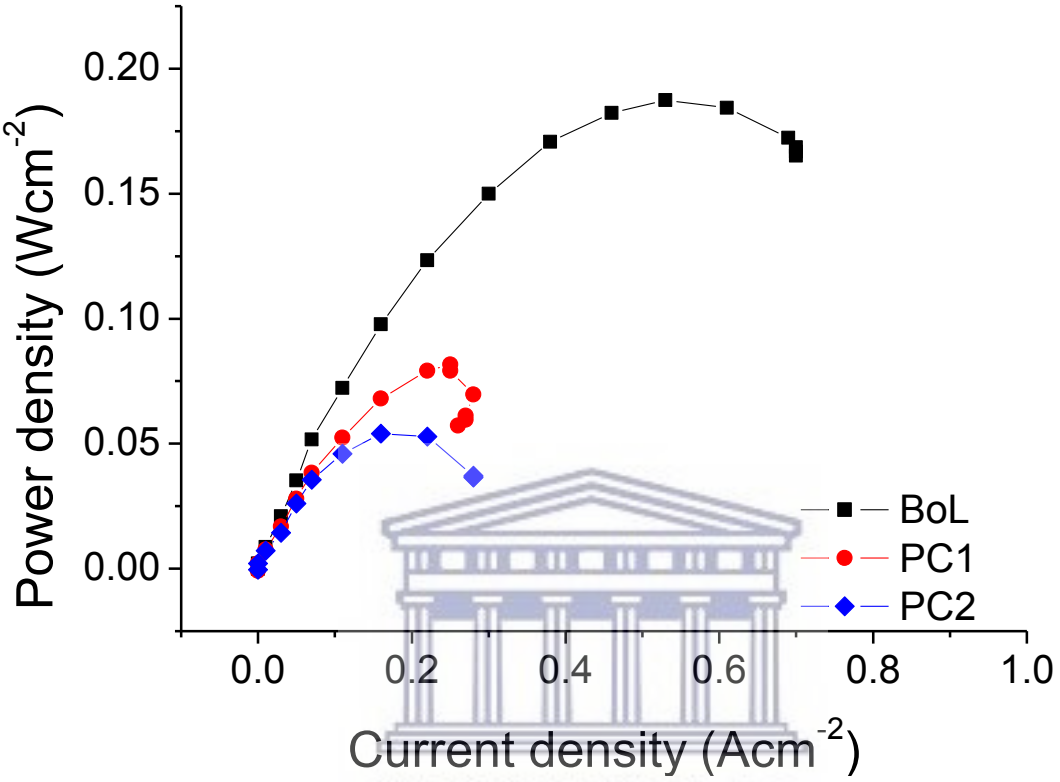

Figure 28: Power performance curves measured at beginning of the tests (BoL) and after variable load demand (take-off and landing) carried out at 60°C (PC1) and at 90°C (PC2). Measurement conditions: atmospheric pressure, cell temperature 60°C, reactants supplied at 65°C and 100% RH, 1.8/2.5 anode/cathode stoichiometry.

The maximum power recorded after the PC1 tests is 0.08 Wcm^{-2}, 36% less than 0.125 Wcm^{-2} at low current density for BoL. The maximum power of 0.19 Wcm^{-2} at the BoL is more than double the 0.08 Wcm^{-2} of the PC1 test. The variable load demand test conditions create rapid change of reactants demands and fluctuation of water levels in

the MEA that result in starvation [71, 126]. The starvation is caused by the lagged time response of reactants supplied to the demand during fast load changing rate [127].

The PC2 test only generated 0.05 Wcm^{-2} maximum power output. The very low performance at PC2 stage can be attributed to the high temperature. The results in Figure 28 attest the strenuous effect of variable load demand and high temperature to the PEMFC. Consequently, the study reveals that take-off and landing cause severe performance loss to the PEMFC. The extreme temperature operation needs to be refined prior to its application.

Lastly, the start-ups and shutdowns comprising of thermal cycling, high voltages and OCV test conditions recorded 0.34 and 0.94 V at 0.4 Acm^{-2} and at OCV respectively during the first hour of operation. The power output in Figure 29 is 47% less after the SUSD1 compared to at BoL at low current density. The difference widened at middle current density to 0.062 Wcm^{-2} after SUSD1 compared to 0.1708 Wcm^{-2} at BoL, implying more than 60% decline of power output. The highest recorded power output after the SUSD1 phase was 0.10 Wcm^{-2} for the entire flight stage. The combination of thermal cycling and the voltage conditions cause major performance loss irrespective of the nominal cell temperature imposed.

The SUSD2 test resulted in more power loss of 67% with 0.04 Wcm^{-2}. The SUSD2 phase generated power at middle current density, even though it was quite low at 0.02 Wcm^{-2}. The maximum power output yielded after the SUSD2 phase was 0.05 Wcm^{-2}, almost 70% less than at BoL. The SUSD flight phase caused highest power output loss compared to all the studied phases. The losses can be attributed to the high voltages coupled with thermal cycling.

The electrical performance results revealed that the cruise mode caused least power degeneration compared to the flight stages. The milder effect of the cruise mode is attributed to the steady-state nature of the operating conditions. However, the higher

operating temperature had adverse effect on the electrical behaviour of PEMFC during the cruise mode. The idling mode caused significant power loss, probably due to the high voltage conditions of the phase.

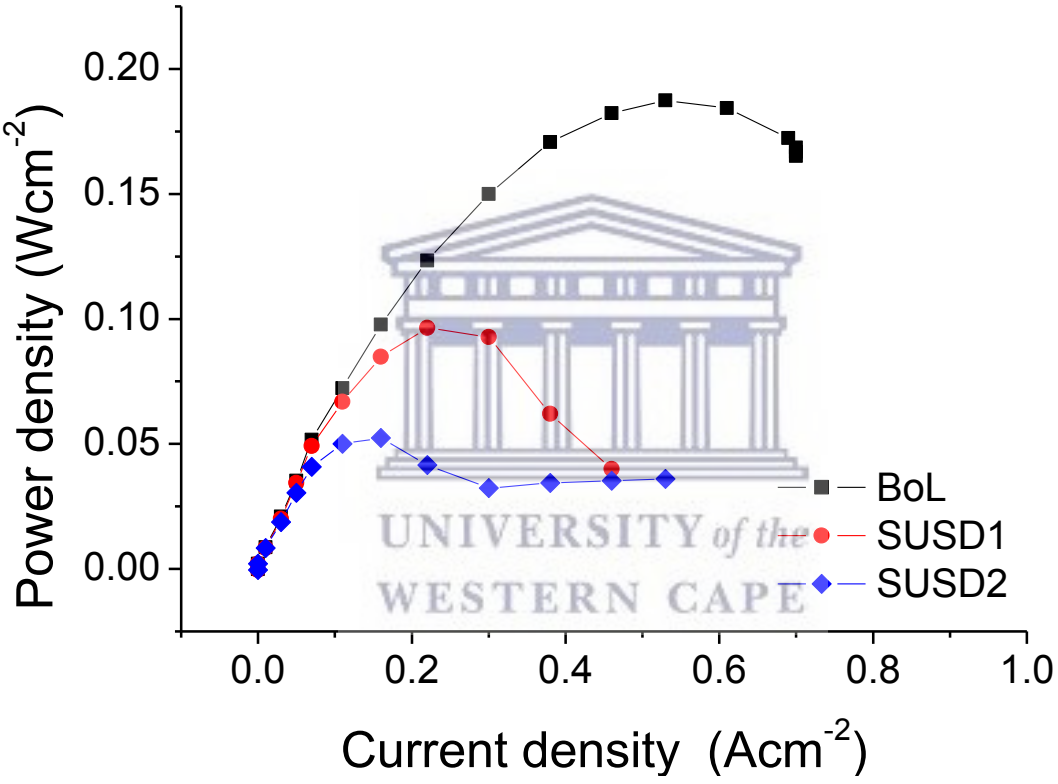

Figure 29: Power performance curves measured at beginning of the tests (BoL) and after several start-ups and shutdowns carried out at 60°C (SUSD1) and at 90°C (SUSD2). Measurement conditions: atmospheric pressure, cell temperature 60°C, reactants supplied at 65°C and 100 %RH, 1.8/2.5 anode/cathode stoichiometry.

The low power output during start-up/shutdowns, take-off and landing suggests that the operating conditions of fully humidified reactants supplied at atmospheric pressure and the cathode stoichiometry of 2.5 are not sufficient in ensuring good PEMFC performance. All the flight stages occur relatively on ground and are not expected to be mostly affected by the low ambient pressure and low oxygen content at high altitudes. The study also revealed that the supply of gases and water management during the flight stages needs to be improved.

5.1.2 Degradation rate

ADRs were tabled for all the tests classified according to operating temperatures in Table 1. The ADR after the SUSD and the PC were given for two current densities and voltages, respectively. Both the SUSD and the PC confirm that voltage/current decay was very little at low current densities of 0.0 and ~2.0 $mAcm^{-2}$ (0.9 V). The SUSD stage resulted in the highest ADR of 0.196 mVh^{-1} at 60°C followed by the OCV with 0.188 mVh^{-1} while the CH recorded the lowest with 0.086 mVh^{-1}. The ADR at 90°C was expectedly higher after the CH, PC and OCV stages compared to 60°C.

The CH initial voltage (measured after an hour of operation) was 0.4086 V at 90°C (CH2) compared to 0.5804 V at 60°C (CH1) even though ADR was lower at 90°C. The SUSD reached lower voltages at 90°C from the beginning and the test was terminated quicker than at 60°C. Both phenomena at the CH and the SUSD reveal that higher temperature yielded lower voltage output but degraded slower than at nominal temperature. Contrarily, the OCV showed notable increase of ADR at higher temperature (OCV2). The ADR increased with increasing operating temperature at both voltages during the PC stages. The high ADR at OCV2 may be due to the extreme temperature that promotes degradation of fuel cell components [46, 69, 128].

Table 1: ADR of PEMFC MEAs under the test conditions imposed by the respective AST at 60 and 90°C.

Flight phase	ADR at 60°C (mVh^{-1})	ADR at 90°C (mVh^{-1})
CH	0.086	0.071
OCV	0.188	0.417
SUSD	0.196 at 400 $mAcm^{-2}$	0.024 at 400 $mAcm^{-2}$
	0.015 at 0.0 $mAcm^{-2}$	0.0082 at 0.0 mAm^{-2}
PC	3.12 mAh^{-1} at 0.5 V	58 mAh^{-1} at 0.5 V
	0.013 mAh^{-1} at 0.9 V	2.07 mAh^{-1} at 0.9 V

Worth noting is that the ADR were consistently lower at higher voltages/lower current densities for the SUSD and the PC. The observation is consistent with result from Franc-Lacaze *et al*. and Shan *et al*. who reported lower degradation at higher voltages [32, 91]. Shan *et al.* reported that lower ADR at higher voltage was attributed to increased demand for reactants at lower voltage/higher current density [32]. Additionally, more water is generated at higher current densities that saturated GDL and catalyst layer [32, 53, 129]. The blocked GDL and catalyst prohibits reactants from reaching reactive sites. Excess water also promotes degradation of electrode and carbon support.

On the other hand, operating PEMFC at high temperature and low pressure produces low RH due to increased water absorbing capacity of air whereas exothermic hydrogen combustion exacerbates formation of hotspots and cracks on MEA at higher temperatures, particularly when humidification is insufficient [19, 43, 116]. Ensuring fully

humidification of reactant gases at 90°C becomes tricky due to increased rates of evaporation which could dry the gases prior to reaching the fuel cell's reaction medium. Increasing dew point temperature to 95°C to minimize condensation poses another risk of damaging fuel cell components.

Water content in the membrane determines electrical conductivity and efficiency of fuel cell to generate power. High temperature tends to decrease humidification and subsequently cause membrane to be less conductive. Water moves between anode and cathode through infiltration and reactions. The water lost on anode side through osmosis drag can be replenished by increasing air flow rate (cathode stoichiometry). However, the replenishing of water competes with supplementing the low ambient air pressure in aeronautic environment.

Full humidification of anode and cathode sides can be a disadvantage in some cases. For instance, Yan *et al*. discovered that high RH on cathode decreases partial pressure of oxygen in the air, which in turn decreases fuel cell performance due to decreased access of oxygen to the reactive sites [130]. Cathode is the naturally water generating electrode through ORR and electro-osmosis drag. Excess water from the cathode is removed with exhaust gases and by back diffusion to the anode. In cases where the anode is fully humidified, back diffusion becomes inefficient. Water accumulation on cathode or anode results in mass transfer challenges that cause local reactant starvations and ultimately degradation and performance loss. Anode starvation can be so severe to the extent of causing permanent electrocatalyst damage [32, 43, 70]. Another shortfall is that local starvation pertaining from uneven water distribution on MEA is not easily detected compared to overall starvation arising from low stoichiometry.

The sensitivity tests conducted by Harms *et al*. showed that fuel cell can only be stable at temperatures up to 85°C [72]. Instability and complex water management can be attributed to the reduced performance witnessed at 90°C. According to results in 5.1.1,

variable load demand and start-up/shutdowns are major causes of degradation in aeronautic environment. Pei *et al.* also reported that load changing and start-up/shutdown are major causes of degradation in vehicular applications [74]. Water management in low temperature PEMFC is known as the main parameter affecting fuel cell performance due to its complexity. The root of the degradation during the PC and the SUSD is the rapid change of load which changes demand of reactants and causes unstable water levels in MEA [42, 93, 98]. The same phenomena are encountered under simulated aeronautic environment. Thus reveals that effects of load profile operating conditions on PEMFC degradation are relatively similar for terrestrial and aeronautic applications.

5.1.3 Voltage recovery phenomena

Jouin *et al.* defined degradation in order to clear confusion on reversibility as part of degradation analysis studies [24]. Degradation is defined as an irreversible process of wearing or weakening in one or more characteristics of an item with time, use or external cause. However, the term reversible and irreversible degradation are used loosely in the fuel cell community. Therefore, the term reversible degradation is contradictory given that degradation is irreversible. Hence reversible losses are referred to as voltage recovery phenomena in this thesis.

The voltage and current values logged over the test duration demonstrate PEMFC operation during each flight phase. PEMFC sometimes recover voltage loss during rest periods when purging, accidentally stopping a test or performing measurements such as the IV curve. For instance, the CH in Figure 30 showed consistent low voltage decrease throughout the test duration with no visible voltage recoveries whereas the operation at OCV showed slight recovery between the rest periods, even though the recovery was temporary. The PEMFC voltage continued to drop despite the recovery. The PEMFC experienced slight current fluctuations at lower voltage during the PC (0.5 V) and the

SUSD (~0.3 V). The variable load demand encountered during the PC and the SUSD stages seem to be affecting fuel cell stability at lower voltages than when little or no current is drawn.

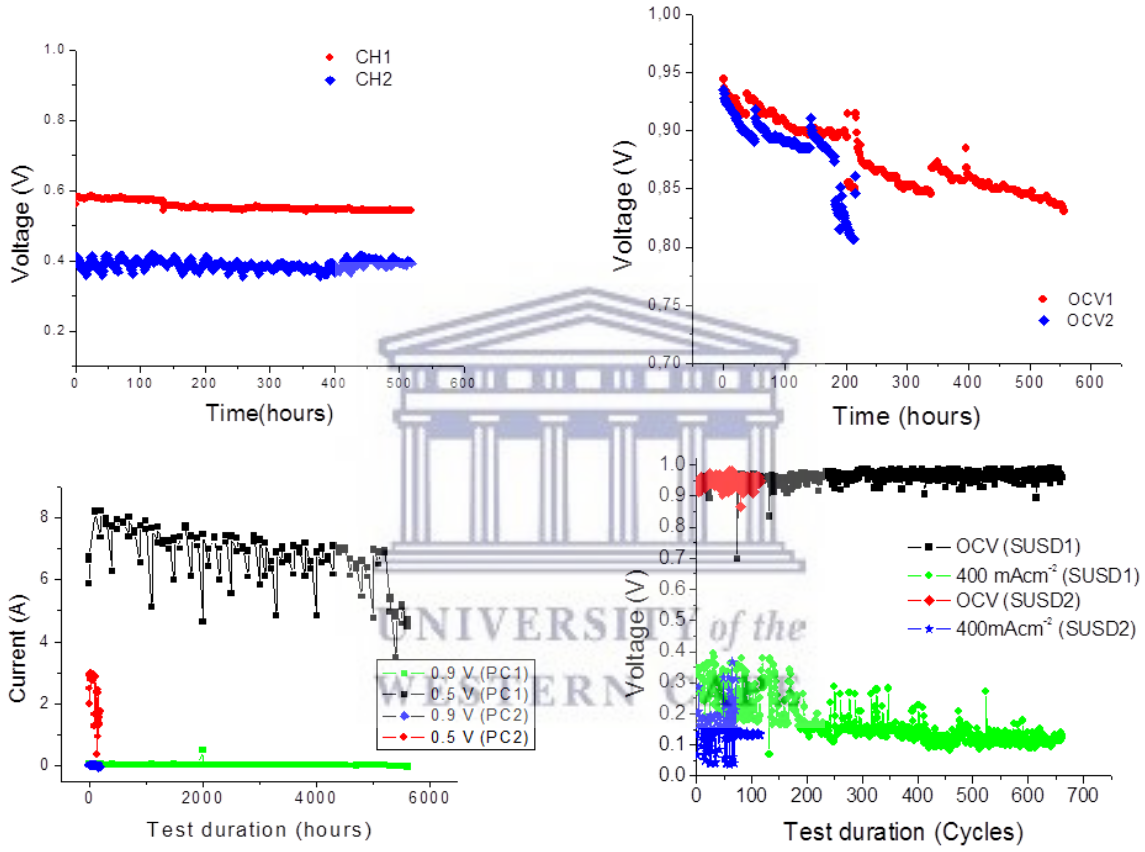

Figure 30: Voltage/current evolution during Polarization curves measured during the cruise mode (CH1 and CH2), variable load demand (PC1 and PC2), idling (OCV1 and OCV2) and start-up/shutdowns (SUSD1 and SUSD2) tests carried out at cell temperatures of 60 and 90°C. Measurement conditions: atmospheric pressure, reactants supplied at 100% RH, 1.8/2.5 anode/cathode stoichiometry.

The voltage recovery phenomena were only recorded to explore which flight phase recovers performance with no attempts to examine causes of the recovery due to scope

limitations. Kundu *et al*. and Zhang *et al*. also reported voltage recovery after interruptions during OCV tests [83, 131]. Kundu *et al*. did not investigate the cause of the voltage recovery but noted that temperature changes that affect MEA water content may contribute to the reversible voltage decay [131]. Zhang *et al*. reported that voltage lost due to temporary flooding that triggered platinum oxidation or catalyst contamination was recovered after nitrogen purge [83]. The nitrogen purging improved reactants transport by removing excess water that accumulated in the gas channels and in the GDL.

Swapping the voltage (between 0.3 and 0.6 V) partially recovered performance loss from operating PEMFC at high voltages [40]. Le Canut *et al*. reported that performance loss due to dehydration can be regained if detected timely [132]. Flooding caused by excess water produced at high current density prompts temporary performance loss that can be recovered when the rate of water generation decelerates at low current density [54]. Changes in water content due to varying load demand during the PC and the SUSD stages when transitioning from high to low current density may be the cause for the slight fluctuations. Therefore, temperature changes and load cycling that result in varying water levels on the gas channels, GDL and the catalyst layer could be the reasons for the recoverable voltage decay. The consistent observations highlight the need to investigate specific nature of the physical/chemical process taking place in the MEA.

5.2 Effects of temperature

All the IV curves recorded at 60°C were plotted in Figure 31 to examine the effects of each simulated flight stage on PEMFC performance. The different slopes on all of the IV curves in Figure 31 show that each flight phase operating conditions resulted in notable degradation and as a result the performance loss. Voltage after the OCV1 and the SUSD1 stages dropped linearly from low current densities until the end of the IV test whereas the PC1 dropped and plateaued at the middle current density region from 0.2 Acm^{-2}. The CH1 IV curve resembles the IV curve of fresh MEA but slightly steeper.

The activation losses were minimal for all the flight stages at the nominal temperature, except for the OCV1 phase. The activation losses at the low current density region of the IV curve (0-0.2 Acm^{-2}) are associated with voltage lost to create potential gradient necessary to trigger the ORR. The activation losses are also indicative of membrane SoH, particularly pinholes and hydrogen crossover/thinning [47, 48, 83]. Therefore, the IV curves suggest that the flight stages at 60°C caused notable membrane-associated performance loss except for the OCV1.

The middle current density region between 0.2 and 0.4 Acm^{-2} represents ohmic losses. The ohmic losses are associated with catalyst activity and charge transfer resistances. The PC1 showed highest ohmic losses followed by the SUSD1 phase. The CH1 recorded the least ohmic losses. The IV curves reveal that each flight stage had varying effects on the movement of reactants from the GDL to the reactive catalyst surface. Subsequently, the catalyst activity was influenced by the content of available reactants. As mentioned earlier, the rate of reactants supplies fails to match the rapid change for reactants demand caused by changes in current density or load. Only the CH1 stage had minimal losses associated with concentration at high current density. The

concentration losses are propelled by the ohmic losses. Hence, the other phases that experienced significant ohmic losses failed to perform at higher current density.

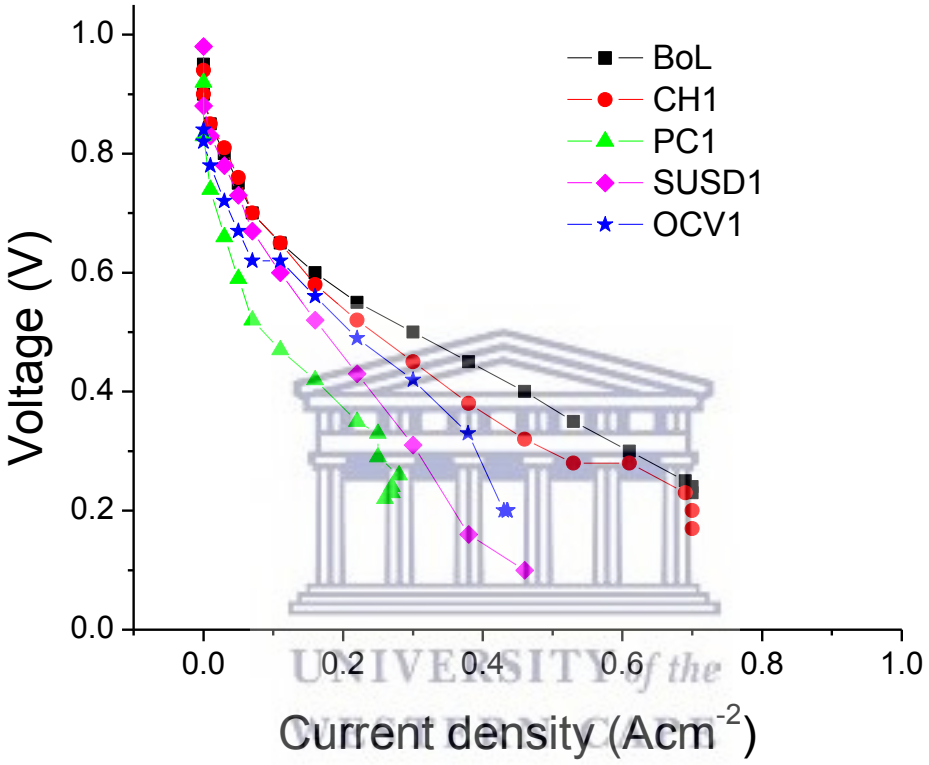

Figure 31: Polarization curves measured at beginning of the tests (BoL) and after cruise mode (CH1), variable load demand (PC1), idling (OCV1) and 600 start-up/shutdowns (SUSD1) tests carried out at 60°C. Measurement conditions: atmospheric pressure, cell temperature 60°C, reactants supplied at 65°C and 100% RH, 1.8/2.5 anode/cathode stoichiometry.

The IV curves at 90°C for all the stages plotted in Figure 32 simplifies evaluating influence of the higher temperature on each method and to establish whether the effects

are temperature dependent. The PC2, OCV2 and SUSD2 IV curves almost overlap at 90°C. The CH2 seems to follow similar behaviour at both temperatures. This suggests that higher temperature has impact on operation of PEMFC irrespective of operating load conditions.

The CH2 and the SUSD2 flight stages still showed no noticeable activation losses after operation at higher temperature. The PC2 showed slight activation losses compared to the one-third loss from the OCV2 phase. The operating conditions of high temperature and high voltages during the PC2 and the OCV2 stages adversely affected membrane SoH and the overall performance. The ohmic losses overlap for the PC2, OCV2 and the SUSD2 phases. The observation reveals that the behaviour of PEMFC at high temperatures is relatively similar during the flight stages. The CH2 experienced least ohmic losses compared to other phases.

It can be speculated that membrane water content, known to be a function of operating temperature, contributed to the performance losses. In other words, PEMFC behaviour changes differently for each test condition at the operating temperatures. Hence, the IV curves were plotted separately for each test in Figure 33 to better visualize the effects of temperature on each aeronautical flight operating stage.

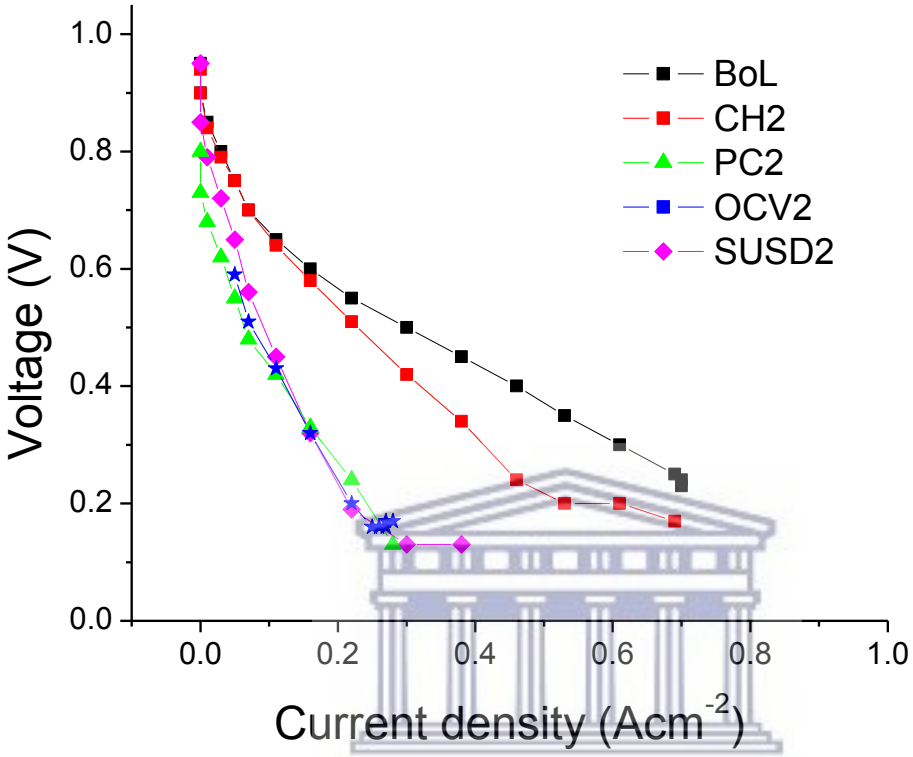

Figure 32: Polarization curves measured at beginning of the tests (BoL) and at the end of cruise mode (CH2), variable load demand (PC2), idling (OCV2) and start-up/shutdowns (SUSD2) tests carried out at 90°C. Measurement conditions: atmospheric pressure, cell temperature 60°C, reactants supplied at 65°C and 100% RH, 1.8/2.5 anode/cathode stoichiometry.

All the IV curves in Figure 33 show that increasing temperature to 90°C caused more performance loss than operating at 60°C. The effect of temperature on performance of the PEMFC during the cruise mode (CH1 and CH2) was relatively similar at nominal and high temperature. Both the CH1 and the CH2 resulted in minimal activation losses. The polarization losses became apparent at the concentration region. This reveals that the steady-state operating conditions

encountered during the cruise mode do not cause major damages to the PEMFC SoH.

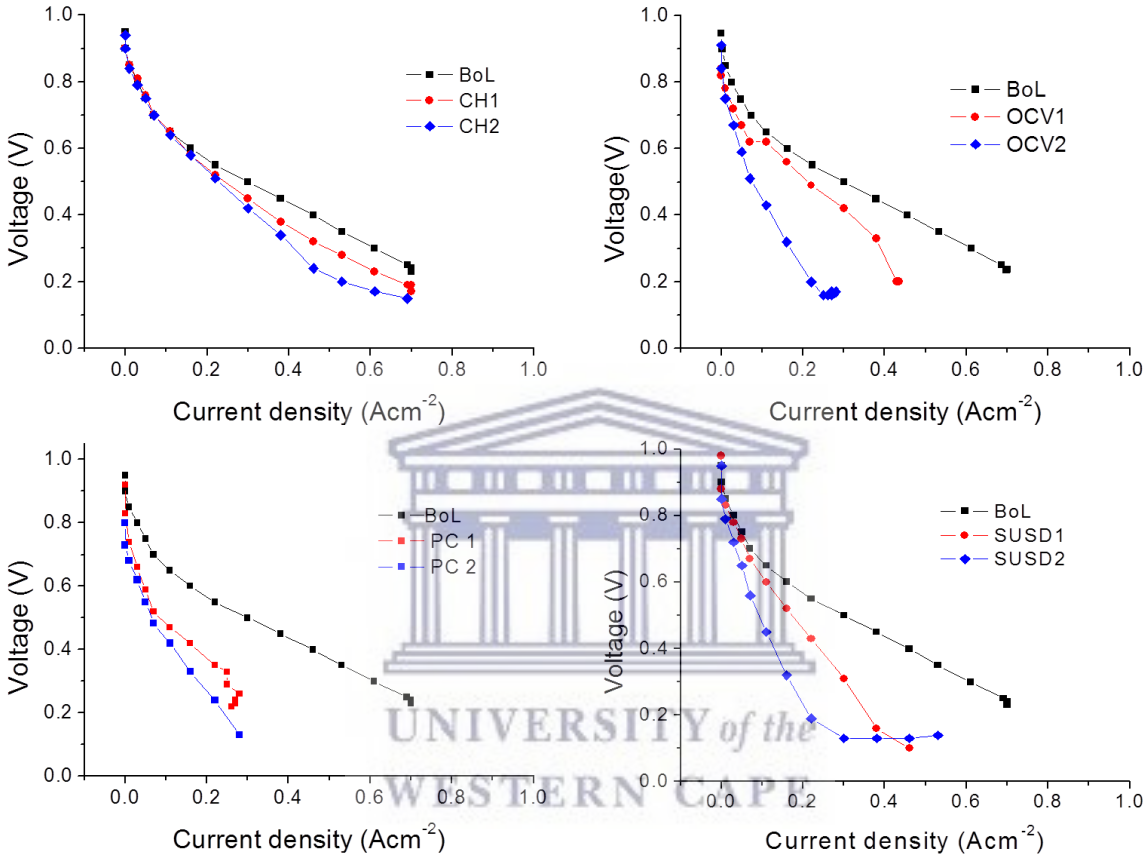

Figure 33: Polarization curves measured at beginning of the tests (BoL) and at the end of cruise mode (CH1 and CH2), variable load demand (PC1 and PC2), idling (OCV1 and OCV2) and start-up/shutdowns (SUSD1 and SUSD2) tests carried out at 60 and 90°C. Measurement conditions: atmospheric pressure, cell temperature 60°C, reactants supplied at 65°C and 100% RH, 1.8/2.5 anode/cathode stoichiometry.

The idling mode (OCV1 and OCV2) experienced significant activation losses at both temperatures. The losses were more severe at the nominal temperature (OCV1) than at the extreme 90°C. The reason for this could be the shorter exposure during the OCV2. On the other hand, the ohmic losses increased with increasing operating temperature. The observations reveal that the activation losses (membrane SoH) are mostly affected by the length of exposure to high voltages whereas the ohmic losses (catalyst SoH) are influenced by the cell temperature.

The variable load demand phases (PC1 and PC2) showed similar overall performance transition from 60 to 90°C with the CH mode but with greater losses. The SUSD stages reveal different behaviours arising from increasing the temperature. The electrical performance demonstrated by the IV curves in Figure 33 shows that PEMFC can withstand the extreme 90°C operating temperature likely to occur in aircrafts. However, whether the PEMFC can generate relative enough power required for each flight stage cannot be deduced from the graphs in Figure 33.

One common trend in all the flight stages is that voltage decay was minimal at the near-OCV region associated with activation losses. Significant voltage decay was apparent as current density increases, thereby revealing that performance loss may be attributed to ohmic losses. The observed fast linear decrease in voltage at high current densities may be caused by mass transport limitations since PEMFC requires larger active surface area to meet the demand from the chemical reactions compared to low current densities [89]. Kim *et al.* also reported that 100% RH may cause excess water that blocks electrode surface area and subsequently result in temporary reactants starvation [88]. Given that the rate of water generation is much faster at high current density compared to low current density, the IV curves results attest that higher humidity introduces additional water into the cell that causes potential flooding and subsequently fosters performance loss. Full humidification conditions were chosen as a worse-case

scenario in this study since PEMFC operated in aeronautic conditions is likely to be periodically flooded due to varying load demands.

5.3 Electrochemical evolution

Voltage loss observed after operating PEMFC at high or variable voltage conditions tends to be attributed to mass transport limitations, increased ionomer resistance and the formation of isolated electrode areas/Pt agglomeration [54, 93, 133]. The latter reflects electrode degradation, which is associated with high voltages and starvation caused by flooding. As a result, the MEAs were characterised for catalyst activity using the CV. Expectedly so, the voltammograms in Figure 34 have peaks showing the different degrees of loss of catalyst activity.

The CV after the SUSD2 test recorded the smallest peak that corresponds to the least performance recorded. The minimal changes in the CH correlates with the least performance loss observed. The significant shrink in the SUSD1 peak could be the cause of 70% voltage decay. The OCV and the PC also show decreasing ability of the catalyst to adsorb hydrogen. The voltammograms reveal that the trend of catalyst activity is relatively similar to the trend of the PEMFC performance. Hence, the performance loss may be attributed to loss of ECSA. Consequently, the catalyst activity was quantified as ECSA to explore the extent of activity lost.

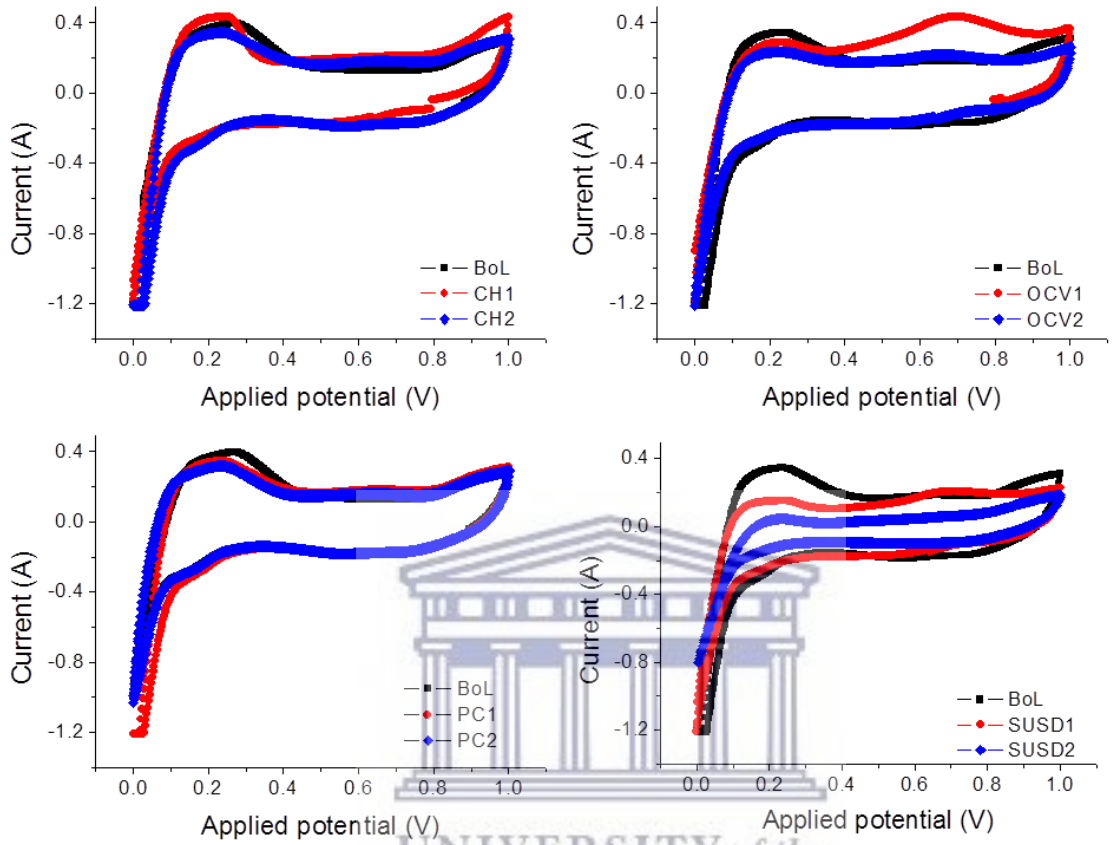

Figure 34: Cyclic voltammetry of fresh and tested MEA measured at 30°C, 100% RH and a voltage range of 0.015 to 1.00 V and a sweep rate of 30 mVs^{-1}. The anode and cathode were supplied with hydrogen and nitrogen gases, respectively.

Table 2 show that the SUSD resulted in the most activity loss followed by the OCV. The high voltages encountered during the OCV and the SUSD promotes electrocatalyst degradation which subsequently results in ECSA loss [56, 89, 134]. The PC stage had second least ECSA loss while the CH resulted in the least loss. Schimittinger *et al*. identified the PC test conditions as one of main causes of loss of ECSA [69]. The

reduced performance observed at higher temperature came through with lower ECSA for all the flight stages carried out at 90°C. Thus reveals that operating PEMFC at higher temperature in aeronautic conditions exerts pressure on the electrocatalyst.

Table 2: Normalized ECSA of pristine and tested MEAs calculated from CV voltammograms using Eq.15.

Flight phase	ECSA at 60°C	ECSA at 90°C
BoL	1.00	
CH	0.95	0.82
OCV	0.73	0.54
SUSD	0.38	0.24
PC	0.77	0.56

More than 40% loss of ECSA reported was potentially due to temperature variation that caused shrinkage and swelling of the cathode Pt surface [48, 90, 116]. A 30% loss of ECSA was probably attributed to load changes posed by start-up/shutdown cycling [88]. Starvation and exposing PEMFC to high voltages result in permanent damages of electrocatalyst that reduces ECSA [32, 44]. The reverse current conditions imposed by start-up/shutdown cycling may have resulted in more than 70% loss of ECSA for temperatures ranging from 40 to 80°C [47]. The SUSD test also resulted in more than

60% loss of ECSA at both operating temperatures. While more than 40% loss was recorded for the OCV and the PC at 90°C. Therefore, the simulated aeronautic conditions cause significant catalyst degradation.

The bottom line from all the research is that the changes in water content of the membrane and the demand for reactant gases stimulated by the load variation damages electrocatalyst, which in turn promotes loss of ECSA. All the studies carried out on influence of operating conditions on Pt catalyst of a PEMFC unanimously report that the weakening of PEMFC electrical performance is associated with degradation of the catalyst layer [53, 70, 104, 127, 135]. Several load profile-related studies showed that both carbon corrosion and platinum loss rates strongly increase with increasing temperature and humidification of the reactant gases [45, 135]. However, the different processes contributing to the ECSA loss and the relationship between operating parameters and catalyst degradation are much more complex.

Both the IV curve and the CV cannot differentiate between flooding, dehydration and starvation. The EIS technique can differentiate between flooding and dehydration by monitoring charge/mass transfer resistance and ohmic resistance. Increasing charge transfer resistance indicates membrane flooding whereas increasing ohmic resistances reflects dehydration [114, 136, 137]. Unfortunately, data gathered from the EIS technique could not be presented due to inaccuracies caused by the complex nature of the Pt/C electrode of the PEMFC studied, uncertainty observed at low frequency range and sensitivity of the EIS technique to operating conditions (e.g. unstable current, gas flow and humidification levels). The challenges encountered with the EIS technique in this study resulted in narrowing the scope to exploring electrical performance and to examine the effects of the imposed simulated flight conditions on the PEMFC components. The necessity to differentiate between these phenomena is well-recognized. Hence, future studies must be conducted in more controlled environment to differentiate between the three phenomena and for database records.

5.4 Ex-situ MEA characterization

In order to examine the cause of fuel cell performance and ECSA losses, MEA components (catalyst and membrane) were characterised ex-situ to assess their evolution with respect to the test conditions imposed by each simulated flight stage. Each flight stage is discussed separately to better understand its effect on fuel cell components.

5.4.1 Idling

Idling represented as OCV, where there is no current drawn or power output required. The OCV flight stage may cause significant performance loss, and as measured during the experiment around 10% loss for both nominal and extreme temperature was obtained. The ECSA results revealed a nearly 30% and 50% loss of catalyst activity at 60 and 90°C, respectively. Both performance and ECSA losses are symptoms of degradation. The data acquired from ex-situ characterization was explored to determine the nature and extent of fuel cell components transformations that resulted in the loss of ECSA.

5.4.1.1 Catalyst layer

HRTEM micrographs in Figure 35 demonstrate increasing PSD after idling at both temperatures. The high voltage during the OCV stage promotes carbon support corrosion, which subsequently results in loss of Pt particles. The Pt particles redeposit and agglomerate in efforts to minimize their specific surface energy [49, 50]. The larger Pt particles in Figure 35 suggest that particle growth/agglomeration is one of the sources for the performance loss and the reduced catalyst activity.

The pristine Pt particles were distributed among the 3 to 4 nm particle diameter while after the OCV1 test shifted towards 4 to 6 nm. The extreme temperature (OCV2) caused more shift towards 5 to 7 nm. There is clearly a consistent increase on Pt particle PSD after the OCV flight stage with increasing operating temperature. The XRD peaks confirm the rise in PSD by the narrower peaks observed in Figure 37.

As shown in Figure 36 the Pt particles of pristine MEA were distributed among the 2 to 4 nm particle diameter while after the OCV1 test shifted towards 4 to 6 nm. The extreme temperature (OCV2) caused more shift towards 5 to 7 nm of particle size. There is clearly a consistent increase of Pt particle PSD after the OCV flight stage with increasing operating temperature. The XRD peaks confirm the rise in PSD by the narrower peaks observed in Figure 37.

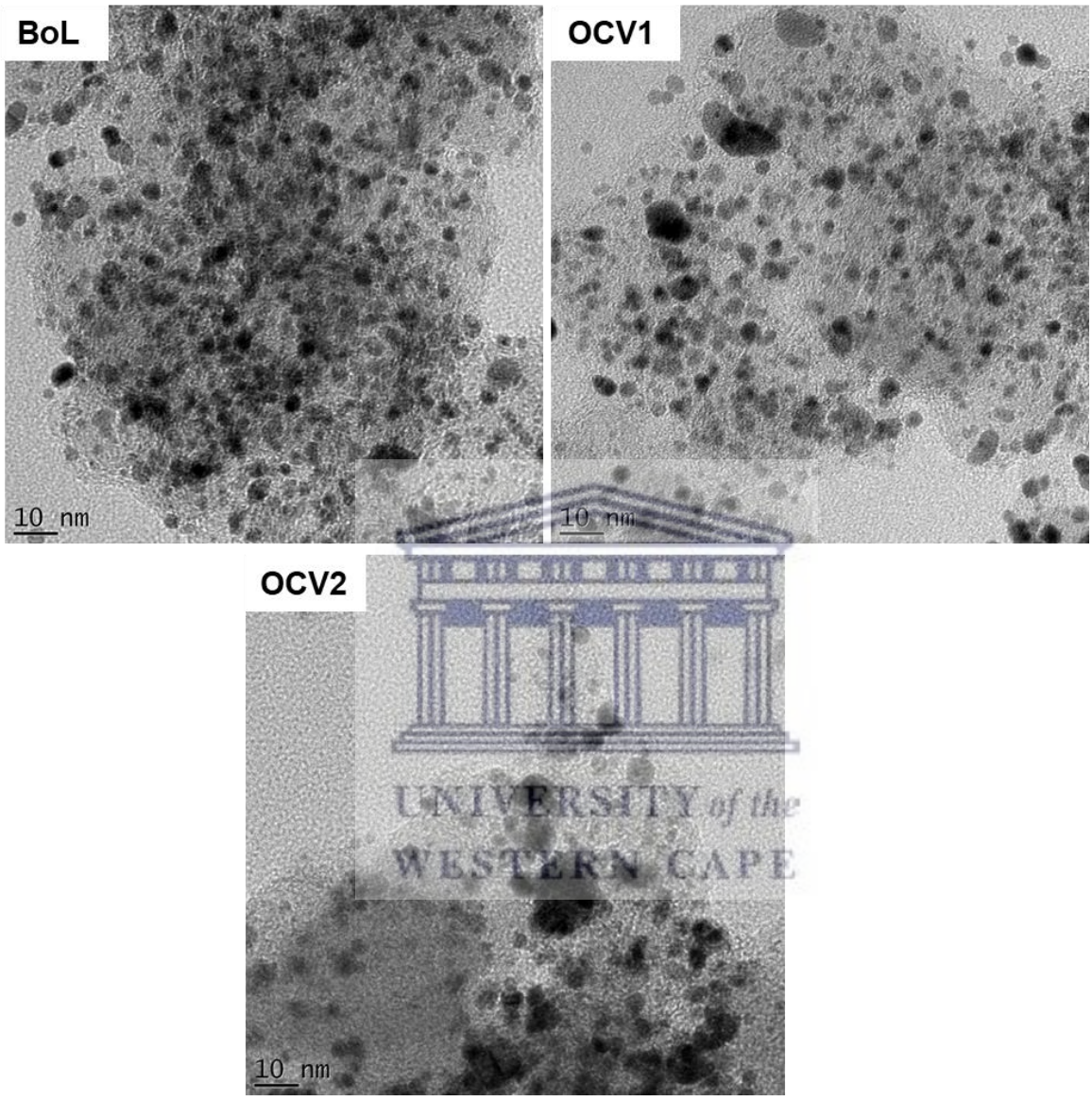

Figure 35: Cathode catalyst's HRTEM micrographs of pristine cathode catalyst (BoL) and tested catalysts after the simulated idling flight phase at 60°C (OCV1) and 90°C (OCV2).

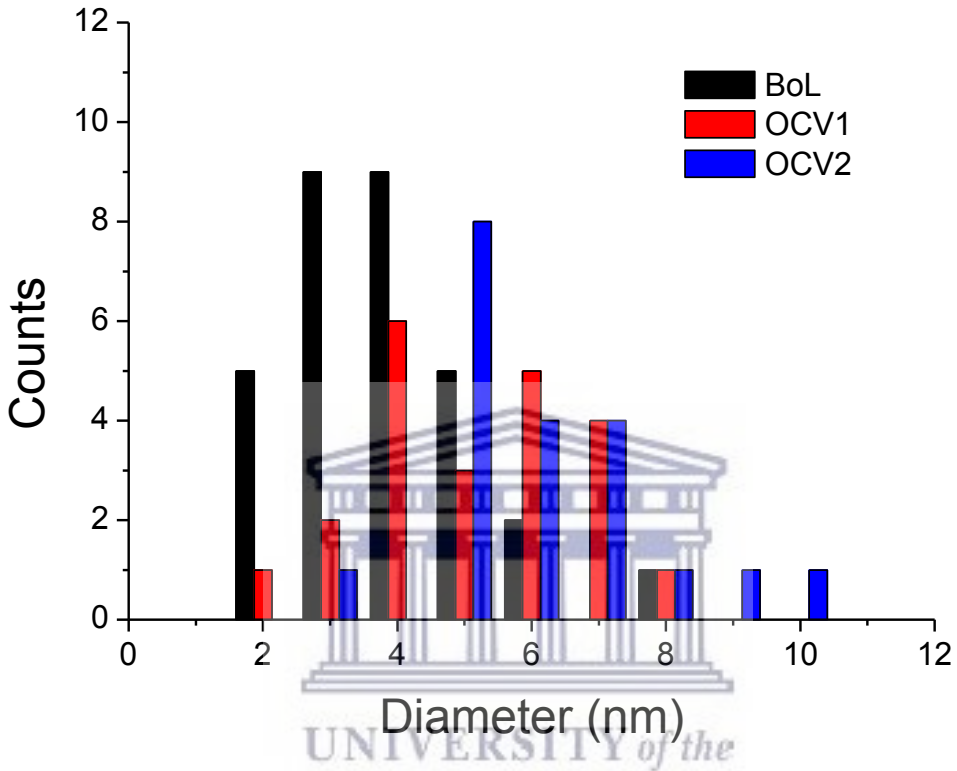

Figure 36: Relative PSD of Pt particles for pristine cathode catalyst (BoL) and tested catalysts after the simulated idling flight phase at 60°C (OCV1) and 90°C (OCV2).

Various mechanisms that lead to particle growth range from collapse of carbon support, oxidation of Pt into PtO and reaction of Pt ions with $–SO_3H$ group of the membrane to form PtS. However, the degradation of catalyst layer due to OCV conditions is believed to be due to faster dissolution of Pt at higher voltage and the subsequent migration/redeposition mechanism [39]. The mechanisms laid out on the review by de Bruijn *et al*. are water oxidation, carbon corrosion and formation of unsupported Pt particles that ultimately lead to loss of catalyst activity [39]. The review by Rodgers *et al*.

on the other hand mentions that catalyst degradation is sometimes accelerated by membrane degradation and vice versa [46]. Hence, the MEAs were further characterized ex-situ to assess membrane degradation or other related mechanisms.

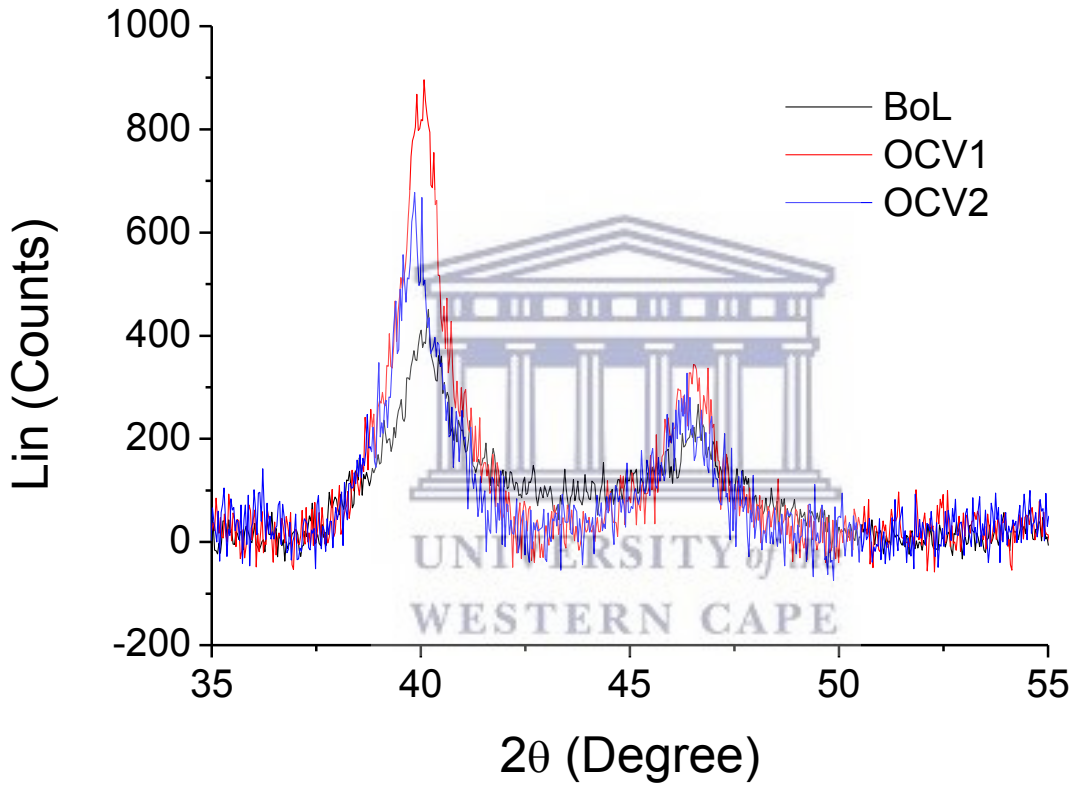

Figure 37: XRD patterns of cathode catalyst for pristine cathode catalyst (BoL) and treated catalyst after the simulated idling flight phase at 60°C (OCV1) and 90°C (OCV2).

5.4.1.2 Membrane

The cross-sections (Figure 38) obtained from HRSEM eloquently illustrate the change in membrane thickness as compared between the BoL and after the OCV1 test. The thickness of the membrane after the OCV1 test is almost half the size at BoL, implying that the membrane underwent chemical or mechanical degradation. The membrane of the OCV2 test is not visible to determine its thickness. Chemical degradation is prevalent at high voltage conditions encountered during the OCV flight stage due to formation of radicals from decomposition of ORR by-product (peroxide). The peroxyl/hydroxyl radicals attack polymer chains of the membrane through the mechanism devised by Curtin *et al*., shown in Eq. 4-7 on Chapter 2 [37]. The radical attack on the membrane results in formation of HF, which is shown by the increasing F composition after the OCV tests (see Table 3). The higher F content after the OCV tests further supports the proposed mechanism of HF formation due to peroxyl radical attack.

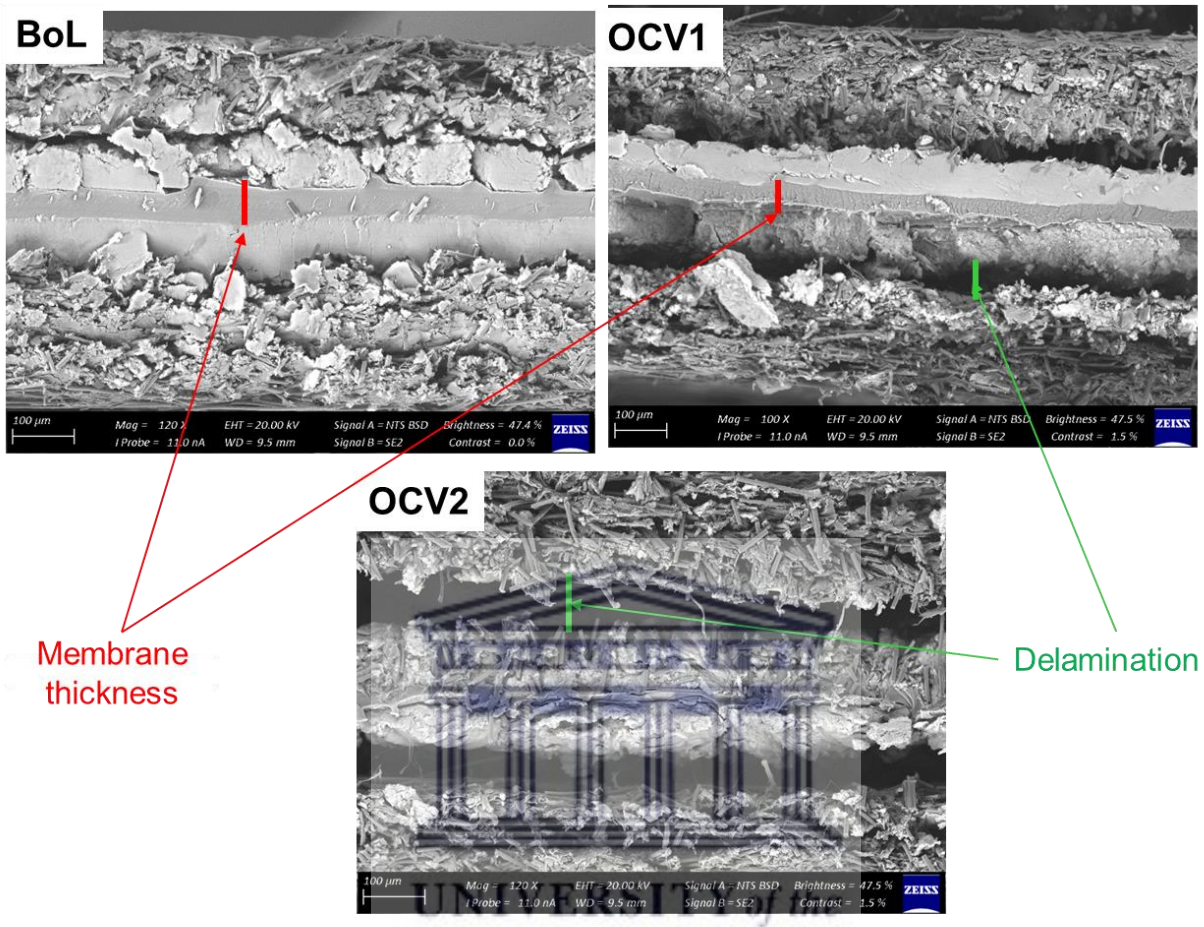

Figure 38: HRSEM back-scattered electron images of fresh (BoL) and tested MEAs after the simulated idling flight phase at 60°C (OCV1) and 90°C (OCV2).

The membrane could not be examined for cracks and pinholes since it is catalyst-coated. The delamination between the MEA and the GDL after OCV1 is a sign of mechanical degradation. Mechanical degradation is normally associated with high temperature and RH cycling. The OCV1 test was carried out at 60°C considered as nominal temperature and thereby ruling out high temperature as cause of the delamination. Periodic dehydration and flooding of the membrane causes shrinking and swelling that results in delamination. Therefore, the delamination can be attributed to

changes in water levels in the MEA. If the delamination is due to periodic flooding and dehydration, thus could be the reason for the observed temporary voltage recovery in Figure 30. The presented results revealed that the OCV test conditions are sensitive to temperature changes induced by unplanned rest periods and characterization intervals. Therefore, performance loss during the OCV flight stage will be minimized in real application during rest periods induced by other flight stages.

It is difficult to distinguish between the catalyst and the membrane layer after the OCV2 test (Figure 38). Loose Pt particles due to collapsed carbon support that migrated from catalyst layer and redeposited on membrane layer tend to react with $–SO_3H$ group to form PtS [49]. The meshed membrane may be reflective of combined catalyst and membrane degradation. Thus is in line with the review by Rodgers *et al*. which stated that both membrane and catalyst degradation affect each other [46]. The delamination between the membrane and the GDL is even more pronounced after the OCV2 test. The delamination may be aggravated by the high operating temperature at the OCV2 test. Table 3 shows no notable changes in carbon and Pt concentrations after the OCV1 test. The minute change in carbon content on fresh and tested MEA suggests that carbon corrosion was not the major cause of the loss of ECSA. The increase in fluoride reveals degradation of the perfluorinated sulfonate polymer membrane. The formation of PtS from membrane degradation is indicated by the consistently decreasing concentration of elemental Pt and S.

Table 3: Elemental composition of a pristine (BoL) and tested MEAs, the simulated idling flight phase at 60°C (OCV1) and 90°C (OCV2), as obtained from HRSEM/EDS.

Test/Element	BoL (wt.%)	OCV1 (wt.%)	OCV2 (wt.%)
Carbon	70.07	70.13	72.04
Fluoride	2.96	3.68	4.15
Sulphur	0.72	0.67	0.59
Platinum	26.26	25.52	23.22

The cross-section of pristine MEA (BoL) shows elemental content of each layer. The Pt are intact in catalyst layer while the sulphur and fluoride in membrane, respectively. There are Pt particles identified in the GDL and in the membrane through the elemental mapping as shown in Figure 39 for the sample after the OCV1 test. The carbon support is not visible on the cross-sections and therefore difficult to assess the extent of its degradation. However, loss of Pt particles redeposited in all the MEA layers is the evidence of collapsed carbon support.

Similarly to the BSE cross-sections, all the elements meshed up and there is no clear definition of each layer after the OCV2 test. All the elements are mixed up on all the layers. Pt and S dominate all the layers; possibly reflective of the formed PtS. The thin line of membrane in OCV2 may not be a true reflection of the thickness since it is covered by the catalyst layers. There are GDL particles (green C) identified in the membrane layer as well.

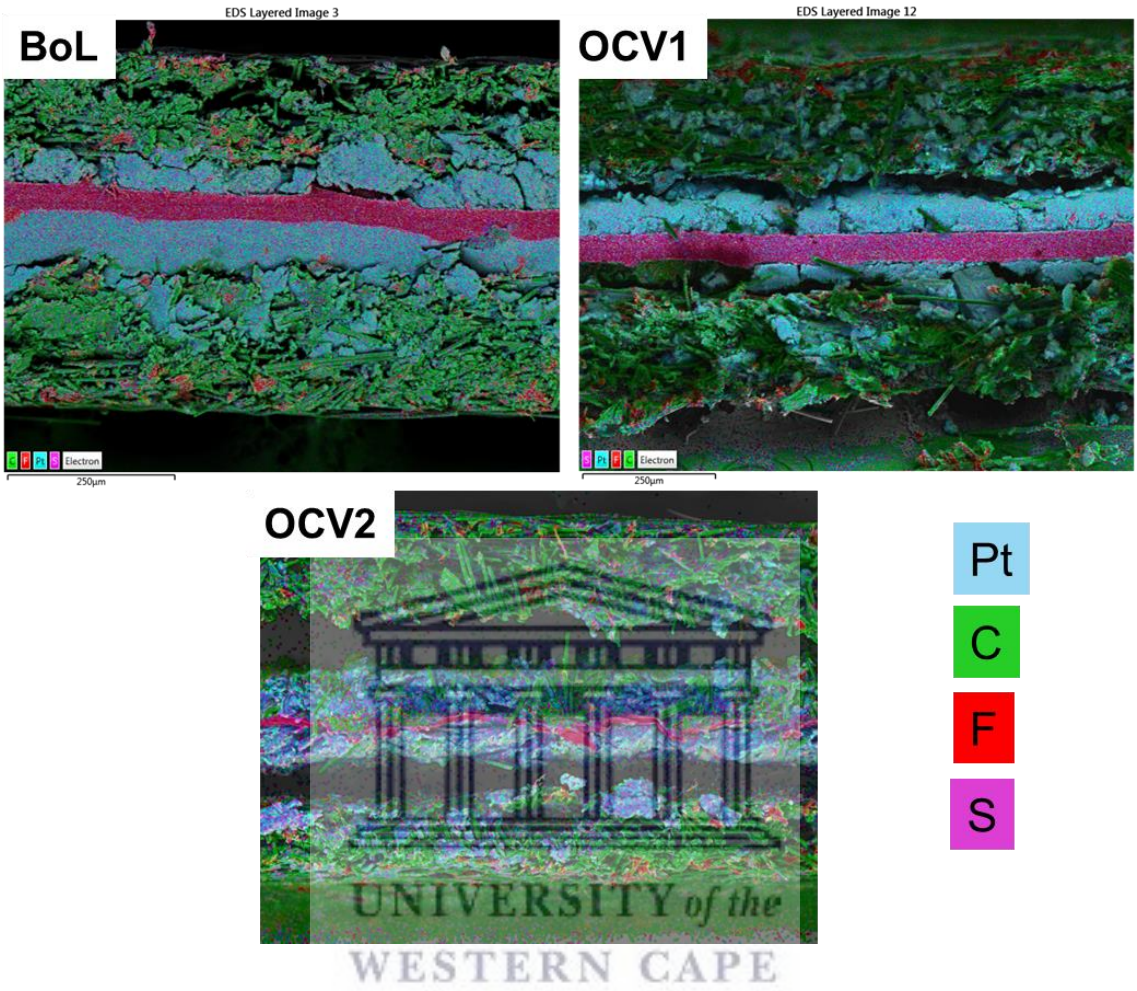

Figure 39: HRSEM/EDS elemental mapping of fresh (BoL) and treated MEAs after the simulated idling flight phase at 60°C (OCV1) and 90°C (OCV2).

The cross-section results of the OCV2 support the hypothesis: carbon support degradation at high voltages promotes catalyst degradation which in turn accelerated membrane degradation. The carbon corrosion reaction is also enhanced by wet conditions through the reaction between water and carbon. The gathered information highlight the need for better management of water content in the MEA and motivates for

future studies on optimization of water control/balance in PEMFC during the operation at aeronautic conditions.

5.4.2 Start-up and shutdown

The SUSD flight stage incorporated temperature variations likely to occur in aeronautic operations. The 70% voltage loss recorded after the SUSD1 test attest the extremity of subjecting PEMFC to simultaneous high voltages and variable load while cycling the operating temperature.

5.4.2.1 Catalyst layer

Both SUSD tests caused more than 60% loss of ECSA. High voltages favour platinum dissolution and carbon corrosion [134, 138]. On the other hand, Pt particles are easily redeposited at reverse current conditions created by SUSD [47, 139]. The loss of ECSA (Figure 34) and particle growth (Figure 41) suggest Pt particle agglomeration. Hence the increased PSD on the HRTEM micrographs (Figure 40) is taken as indication that the Pt particles experienced Ostwald ripening, migration/dissolution and redeposition.

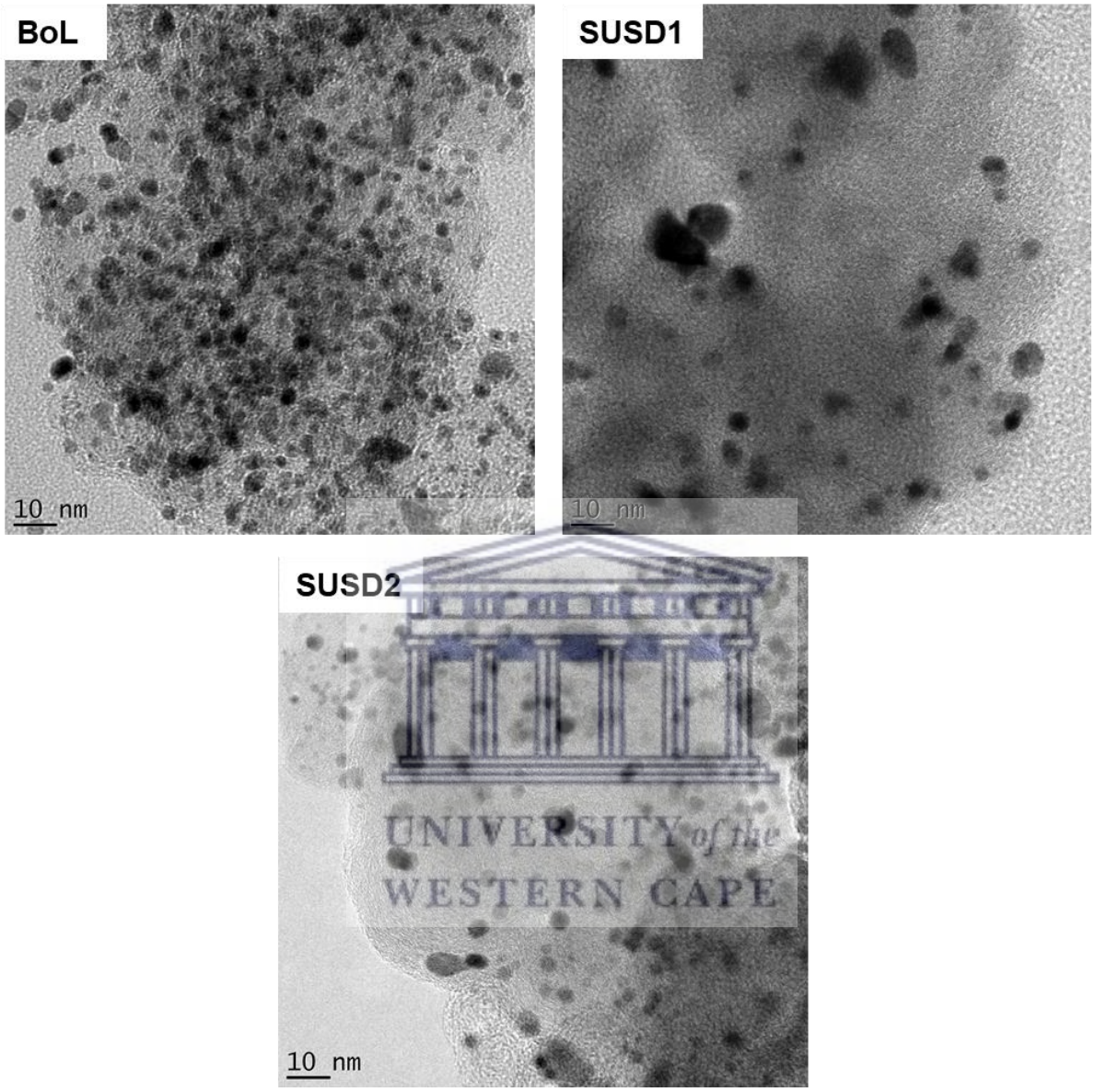

Figure 40: Cathode catalyst's HRTEM micrographs of fresh (BoL) MEA and sample after the simulated start-up and shutdown flight phase at 60°C (SUSD1) and 90°C (SUSD2).

Figure 42 shows the shift in diameter from 3-4 nm at BoL to 5-9 nm after the SUSD1. Worth noting is that particle growth is more apparent at 60°C compared to 90°C. The reason for the behaviour could be the length of exposure to the reverse current conditions since the OCV2 test was terminated quicker than the OCV1.

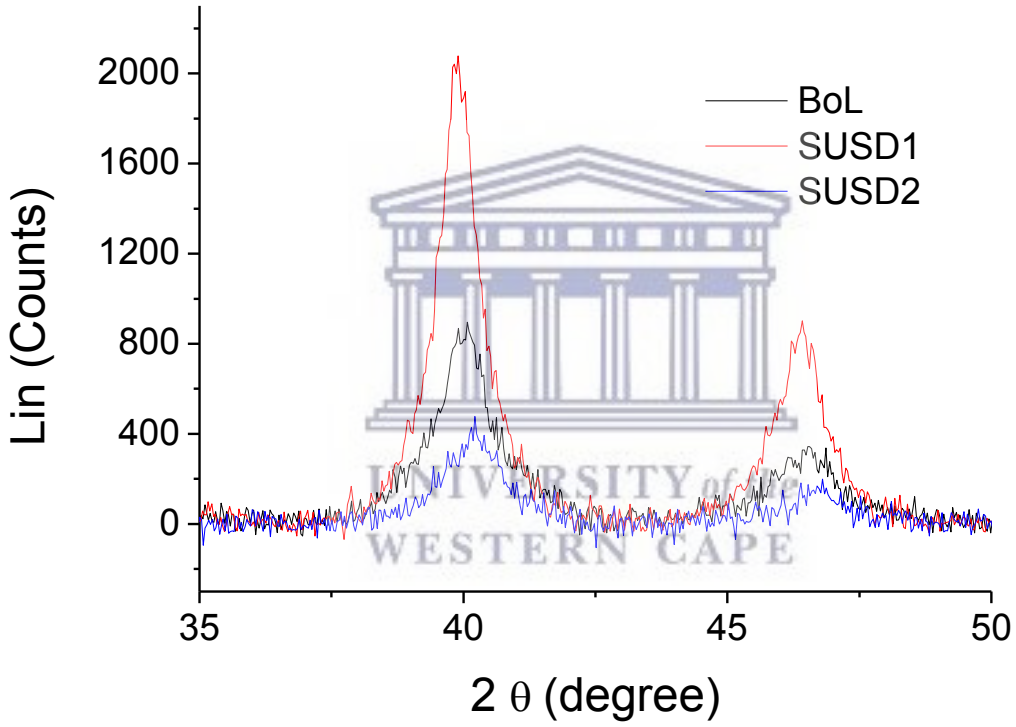

Figure 41: XRD patterns of cathode before (BoL) and after the simulated start-up and shutdown flight phase at 60°C (SUSD1) and 90°C (SUSD2).

Additional reason for the ECSA loss may be adsorption of OH^- on Pt-M surfaces which forms PtO. Pt sintering mostly occurs at cathode due to chemical oxidation of Pt into PtO by residual oxygen present in the cathode layer, following the mechanism outlined by [41]. The hydrogen and oxygen presence may be due to the short time of purging since the IV curves and OCV data hinted no signs of crossover.

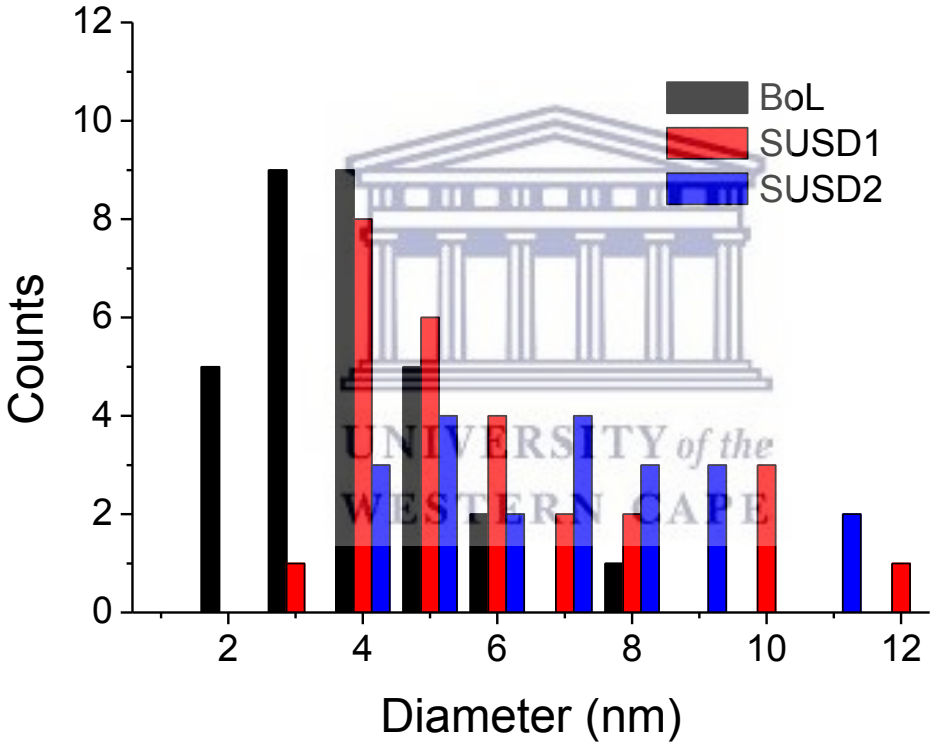

Figure 42: Relative PSD of Pt particles at beginning of life (BoL) and after the simulated start-up and shutdown flight phase at 60°C (SUSD1) and 90°C (SUSD2).

The cathode catalyst layer on the cross-section in Figure 43 is drastically thinner after SUSD1 and SUSD2, insinuating corrosion of carbon support and subsequent catalyst degradation. The presence of oxygen in the tested MEA (Table 4) substantiate occurrence of the PtO reactions. The minute change in concentrations proves that Pt did not leach out but rather migrated and redeposited. The turquoise Pt particles in Figure 44 are visible on all the layers captured after the SUSD1 and the SUSD2 stages, implying migration and redeposition. The leached out carbon indicates corrosion of the catalyst support. Pt agglomeration shown by the particle growth in Figure 40 tends to be aggravated by carbon corrosion. Therefore, the reasons for the loss of ECSA are the carbon support corrosion which caused loose Pt particles that either agglomerated or migrated.

Table 4: Elemental composition of a pristine (BoL) and tested MEAs, the simulated start-up and shutdown flight phase at 60°C (SUSD1) and 90°C (SUSD2), as obtained from HRSEM/EDS.

Test/Element	BoL (wt.%)	SUSD1 (wt.%)	SUSD2 (wt.%)
Carbon	70.07	59.42	70.43
Fluoride	2.96	4.76	2.38
Sulphur	0.72	0.66	0.51
Platinum	26.26	27.21	26.68
Oxygen	0.00	7.95	0.00

5.4.2.2 Membrane

There is significant decrease of thickness of the membrane layer after both the SUSD tests. The near-OCV voltage loss was less than 1.0% after all the SUSD tests despite the magnitude loss of performance and ECSA. The negligible loss of OCV voltage is known to be reflective of no pinholes or membrane perforations. Both Jo *et al*. and Shan *et al*. verified this hypothesis by measuring hydrogen crossover using LSV [32, 47]. Despite the thinner catalyst layer, membrane degradation was minimal. Therefore, one can conclude that the test conditions of the SUSD flight stage did not cause significant chemical degradation of the membrane.

The loose Pt particles underwent oxidation instead of reacting with the sulphonic group. The presence of oxygen after the SUSD1 is evident for PtO formation. The elemental composition after the SUSD2 stage is relatively similar to that of fresh MEA. The trends reveal that there were no major chemical degradations that took place. One of the reasons to the minimal change of elemental composition could be the test duration versus kinetics of the chemical degradation mechanisms. The BSE cross-section also shows no notable changes on the MEA after the SUSD2.

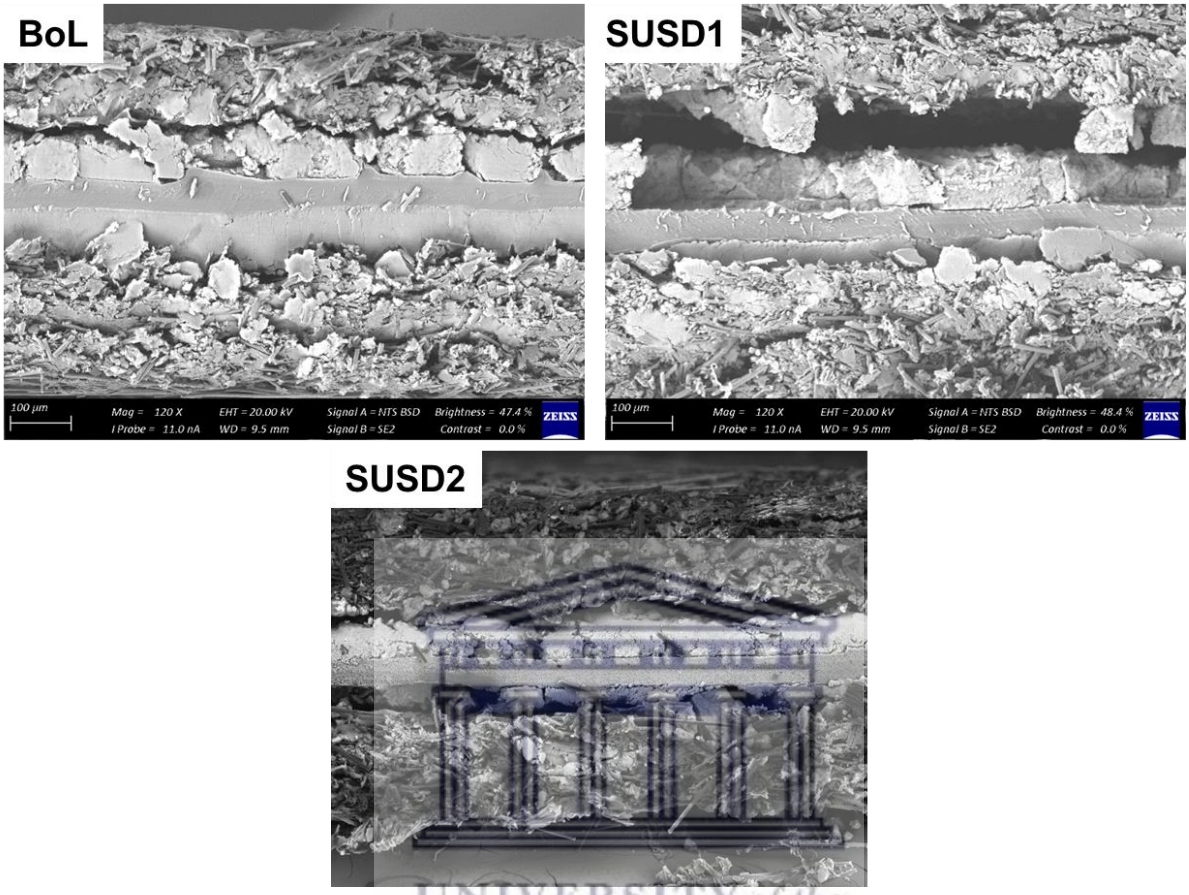

Figure 43: HRSEM back-scattered electron images of cross-sections of fresh (BoL) and treated MEAs after the simulated start-up and shutdown flight phase at 60°C (SUSD1) and 90°C (SUSD2).

The elemental mapping in Figure 44 also confirms that membrane degradation was minimal. The fluoride and sulphur elements are intact on the membrane layer after the SUSD1 test while there is a huge delamination and loss of catalyst layer. The loss of catalyst layer is unanimous with the leached out carbon shown by the EDS results (Table 4). The visible differences in the elemental mapping between BoL and SUSD2 are the thinner cathode catalyst layer and Pt particles scattered all over the MEA

components. Therefore, it can be deduced that high voltages coupled with thermal cycling and extremely high operating temperature caused severe carbon corrosion that resulted in loose Pt particles.

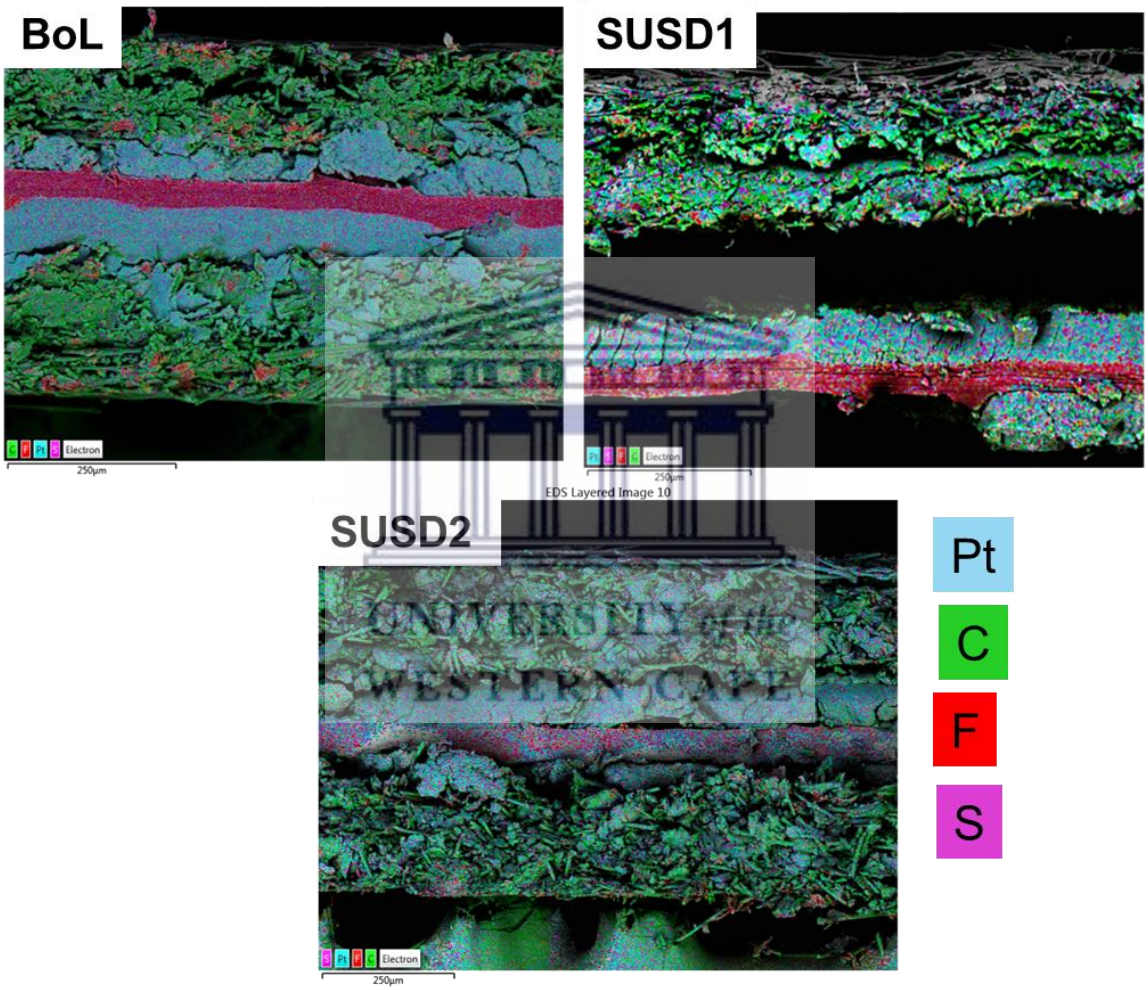

Figure 44: HRSEM/EDS elemental mapping of fresh (BoL) and treated MEAs after the simulated start-up and shutdown flight phase at 60°C (SUSD1) and 90°C (SUSD2).

The recorded performance and ECSA loss during the SUSD stage at higher temperature is due to carbon corrosion and subsequent catalyst degradation. This is in line with the observations by Kim *et al*. and Linse *et al*., Pt particles migration is more pronounced at higher temperatures and full humidification [88, 140]. Jo *et al*. also confirmed that the SUSD conditions have negligible effect on membrane through LSV studies that showed no notable hydrogen crossover and the fact that less than a percent of voltage was lost (symptom of membrane perforation) [47]. The SUSD operating conditions cause carbon support corrosion which in turn results in catalyst degradation rather than membrane degradation. The recommendations by Yu *et al*. to minimize the carbon corrosion are operating at low humidification, low temperature and shutting off oxygen supply prior to supplying hydrogen to the fuel cell [141]. However, implementing the recommendations is not yet practical in the real aeronautic applications.

5.4.3 Cruise mode

The cruise mode caused the least recorded electrical performance loss and less than 20% ECSA loss at both temperatures. The cruise mode stage might be the longest exposure of PEMFC depending on the route of flight. It is a good thing for PEMFC reliability to observe the least degradation at this flight phase. The MEA components are examined ex-situ and the obtained data is analysed as a measure of the effect of aeronautic conditions on potential PEMFC degradation.

5.4.3.1 Catalyst layer

The particle size increase is visible but not severe for both the CH1 and the CH2 stages (Figure 45). The PSD is much larger for the CH2 compared to the CH1. The larger PSD indicates the accelerated particle growth by the higher operating temperature. The XRD

patterns (Figure 46) almost overlap each other. The particle diameters are mostly distributed within 2 to 5 nm region. All the characterization techniques suggest that Pt particle growth was very little.

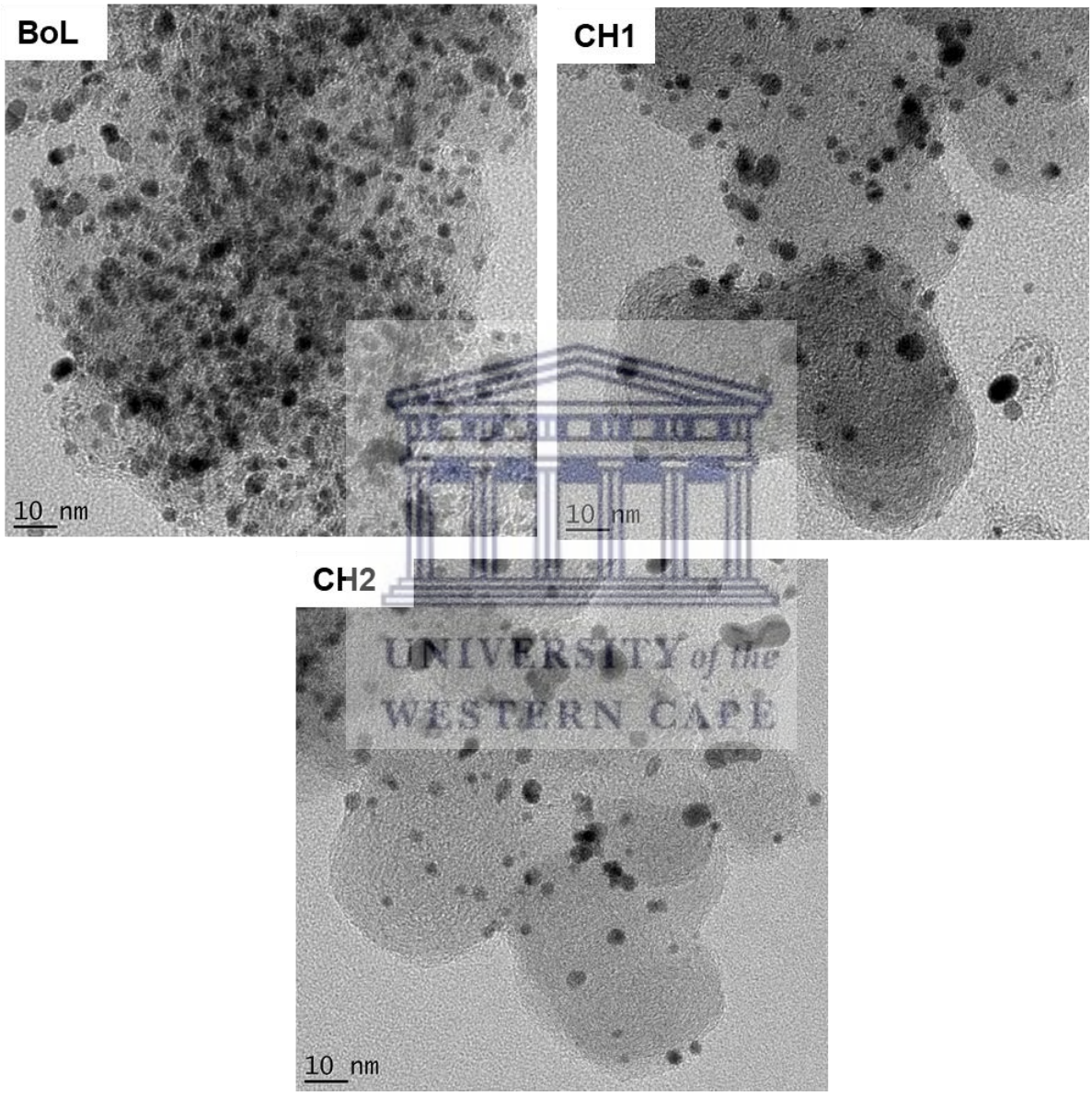

Figure 45: Cathode catalyst's HRTEM micrographs of fresh (BoL) MEA and sample after the cruise flight phase at 60°C (CH1) and 90°C (CH2).

The minute increase in PSD and loss of ECSA reveals that there was little degradation that took place during the cruise mode. The mild voltage conditions do not create conditions that are aggressive enough to facilitate carbon corrosion. Franck-Lacaze *et al*. also reported that current density of 0.12 Acm^{-2} did not cause any severe damage to fuel cell components [91]. The current density of 0.2 Acm^{-2} also did not cause any notable damage to the catalyst layer. The lower performance at higher temperature (CH2) can be attributed to the slight increase in PSD and the almost 20% loss of catalyst activity.

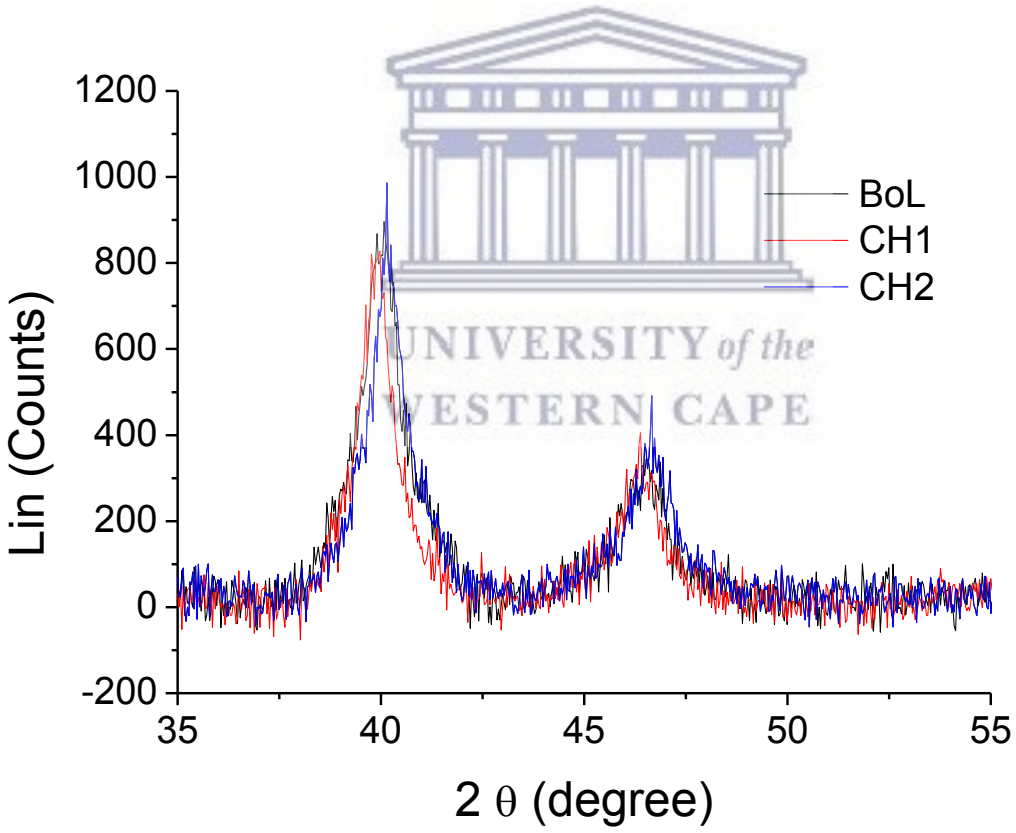

Figure 46: XRD patterns of cathode before (BoL) and after the simulated cruise flight phase at 60°C (CH1) and 90°C (CH2).

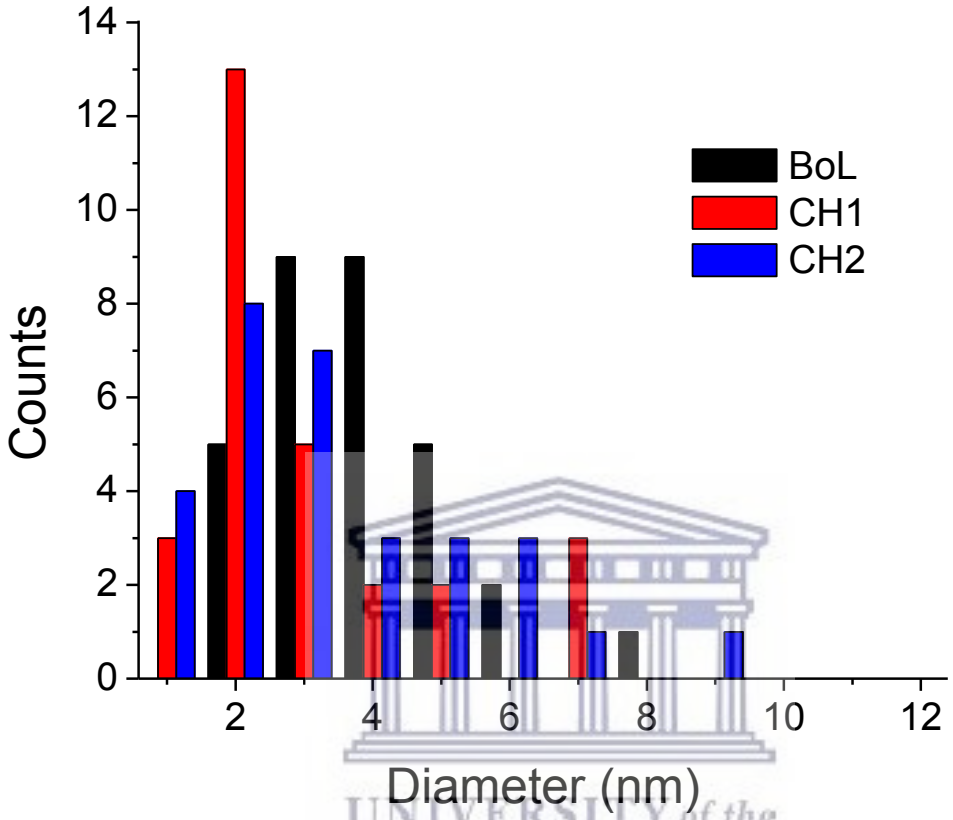

Figure 47: Relative PSD of Pt particles at beginning of life (BoL) and after the simulated cruise mode at 60°C (CH1) and 90°C (CH2).

The operating current density applied during the CH tests facilitated adequate water generation and the constant load nature of the test conditions allowed for relatively stable water levels in the MEA. It can be speculated that increasing temperature to 90°C exerted enough heat to cause drying but not enough to cause hotspots. One can draw a conclusion that the operating temperature of PEMFC can be stretched to 90°C during cruise mode. The PEMFC can generate adequate and stable power but much lesser

than at 60°C. Periodic exposures of PEMFC to higher temperature during cruise mode will not cause severe damages to the MEA components.

5.4.3.2 Membrane

There are no significant changes on thickness of all the MEA components (Figure 48). There is neither change in membrane thickness nor visible delamination. Thus reveals that there are no membrane mechanical degradations. The occurrence of chemical degradation is further studied through the HRSEM elemental mapping (Figure 49) and the EDS elemental composition quantification (Table 5).

Table 5: Elemental composition of a pristine (BoL) and tested MEAs, the simulated cruise flight mode at 60°C (CH1) and 90°C (CH2), as obtained from HRSEM/EDS.

Test/Element	BoL (wt.%)	CH1 (wt.%)	CH2 (wt.%)
Carbon	70.07	69.18	70.31
Fluoride	2.96	3.39	4.04
Sulphur	0.72	0.56	0.45
Platinum	26.26	26.87	25.20

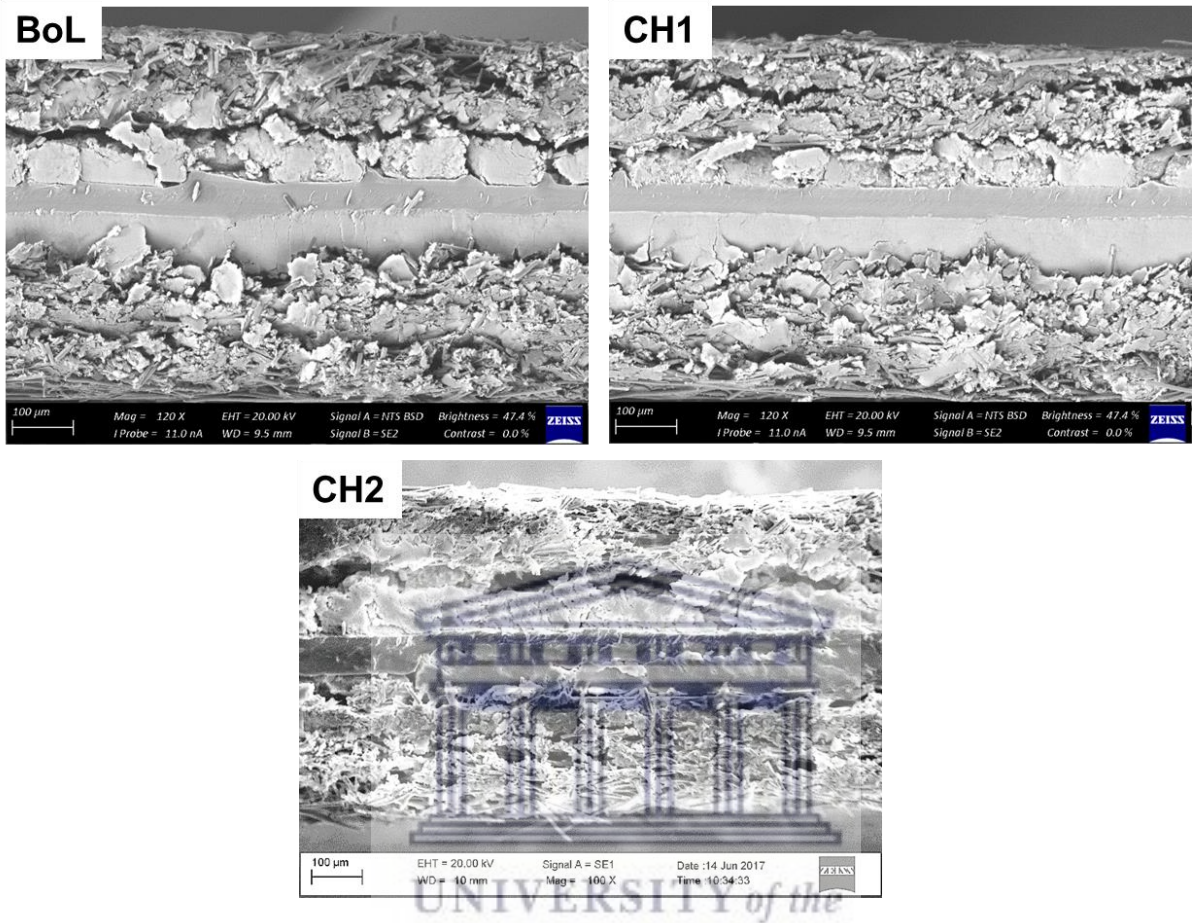

Figure 48: HRSEM back-scattered electron images of MEA cross-sections presented for fresh (BoL) and treated MEAs after the simulated cruise mode at 60°C (CH1) and 90°C (CH2).

The minor changes in concentration of the elements contained in Table 5 implies that neither notable Pt migration nor leaching out occurred. Therefore, revealing that there was no significant membrane degradation or carbon corrosion occurred. The elemental mapping in Figure 49 also confirms that all elements are still intact in their layers.

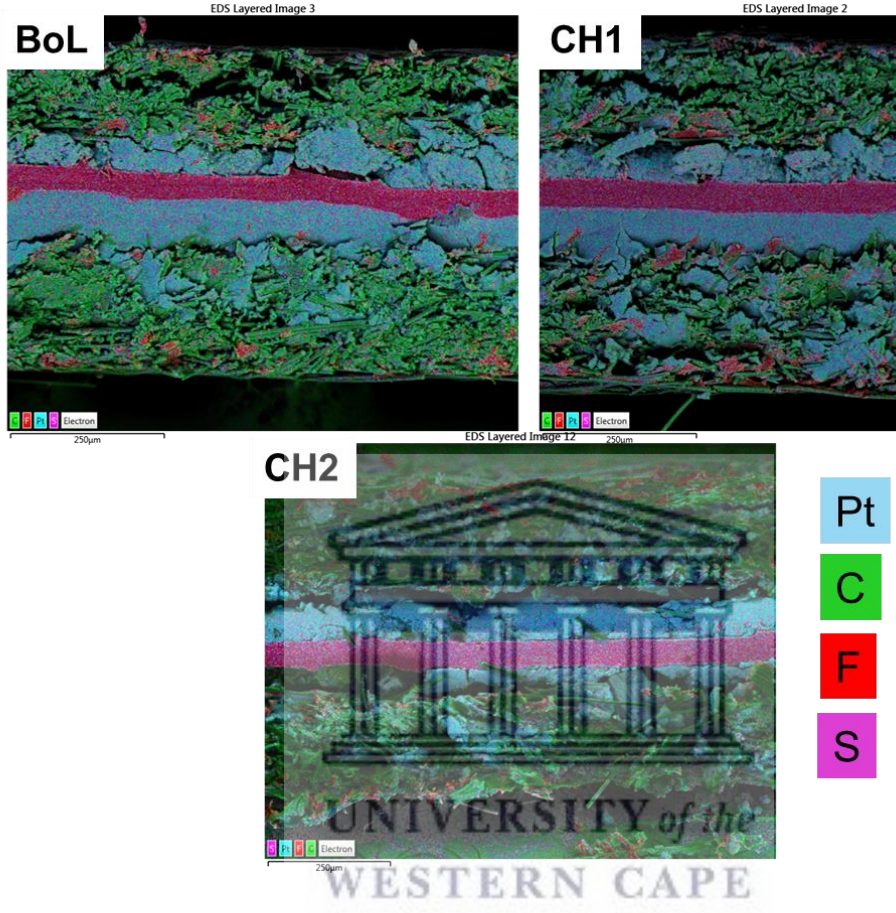

Figure 49: HRSEM elemental mapping of cross-sections of fresh (BoL) and treated MEAs after the simulated cruise at 60°C (CH1) and 90°C (CH2).

All the data gathered from the analytical techniques employed in this study unanimously show that current drawn during cruise mode caused minute performance loss. The ECSA results also showed only slight decline after the exposure to the extreme temperature of 90°C. Both the catalyst and the membrane characterization show no significant degradation symptoms. The presented information in this section is evident of cruise mode being the nominal operating conditions for aeronautic applications.

5.4.4 Variable load demand

The variable load demand (PC) mode characterized by the fast changing load is the major cause of performance deterioration in vehicular application [74]. The PC stages resulted in 30 and 40% performance losses from the PC1 and the PC2, respectively. The performance decline was associated with ohmic losses and loss of catalyst activity. The operating conditions of the PC2 caused more than 40% loss of ECSA. Hence, the following sections investigate the causes of the performance and the ECSA losses.

5.4.4.1 Catalyst layer

The changes in water levels and reactants demand due to variable load are known to cause catalyst degradation [54, 74, 142]. The Pt particle growth is visible in Figure 50 for sample after the PC1 test and particle size continue to increase for the sample after the PC2 test. The PSD was quantified using the ImageJ software and plotted in Figure 51. The average PSD for pristine Pt particles (BoL) was 4.7 nm with particles distributed in the 2 to 5 nm diameter. The particles after the PC1 tests grew to 5.28 nm average diameter with particles distributed between 3 and 7 nm with few larger particles at more than 7 nm. Once again, the effect of higher temperature was apparent. The PSD after the PC2 was 5.79 nm, covering the 3 to 6 nm diameter with larger particles that have more than 9 nm.

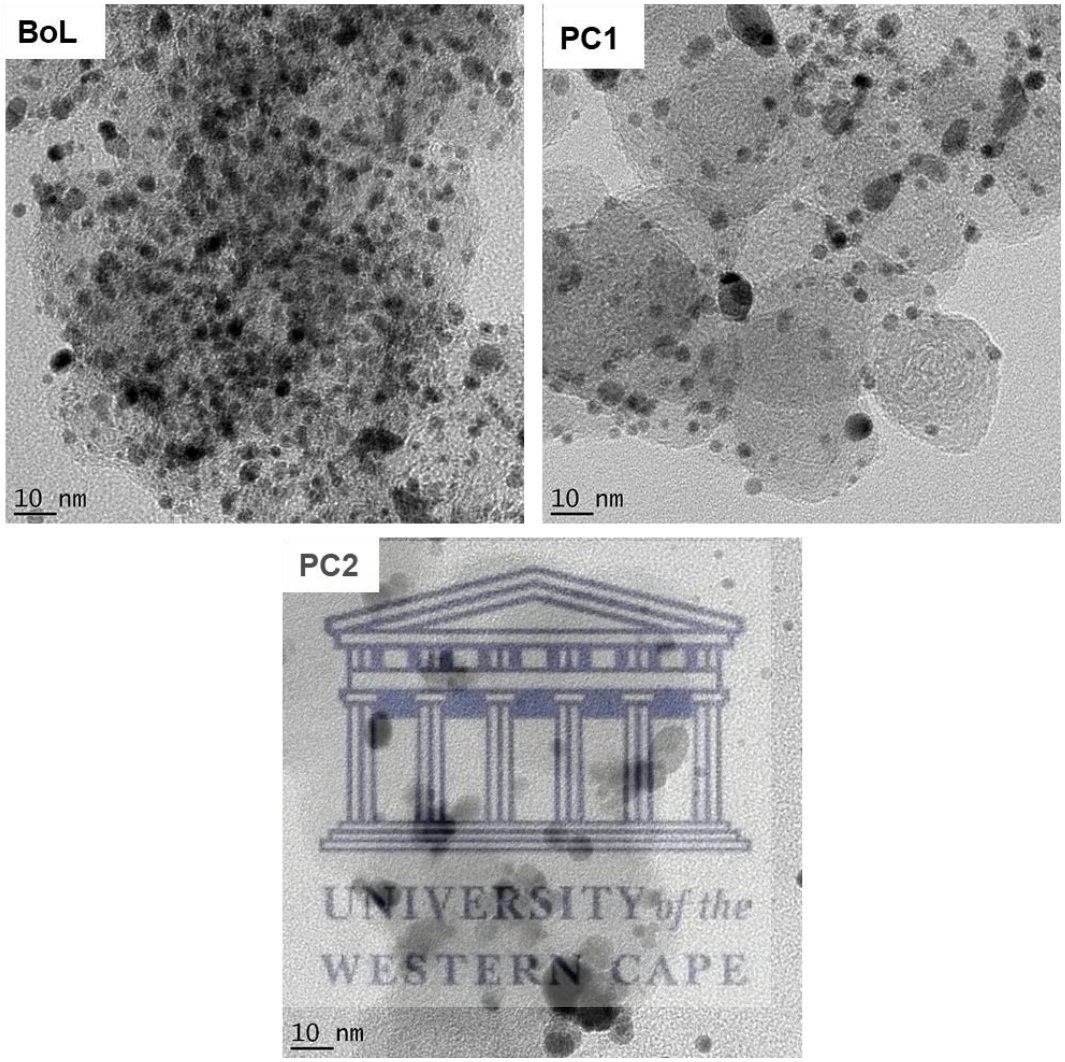

Figure 50: Cathode catalyst's HRTEM micrographs of fresh (BoL) MEA and sample after the simulated variable load demand flight phase at 60°C (SUSD1) and 90°C (SUSD2).

The variable load demand conditions encountered during the PC stage are part of the operating terms at SUSD stage. The catalyst degradation mechanism discussed in the SUSD flight stages (5.4.2.1) are expected to be relatively similar. The difference is

thermal cycling and periodic near-OCV conditions that makes the SUSD stage more aggressive. For instance, the ECSA loss after the PC stage (20% for PC1) is almost half of the SUSD stage (60% for SUSD1). The common cause of the loss of catalyst activity is carbon corrosion aggravated by high voltages. The fast changing voltage during the PC stage causes unstable water levels that affect catalyst activity and also promote carbon corrosion in cases where wet conditions prevail.

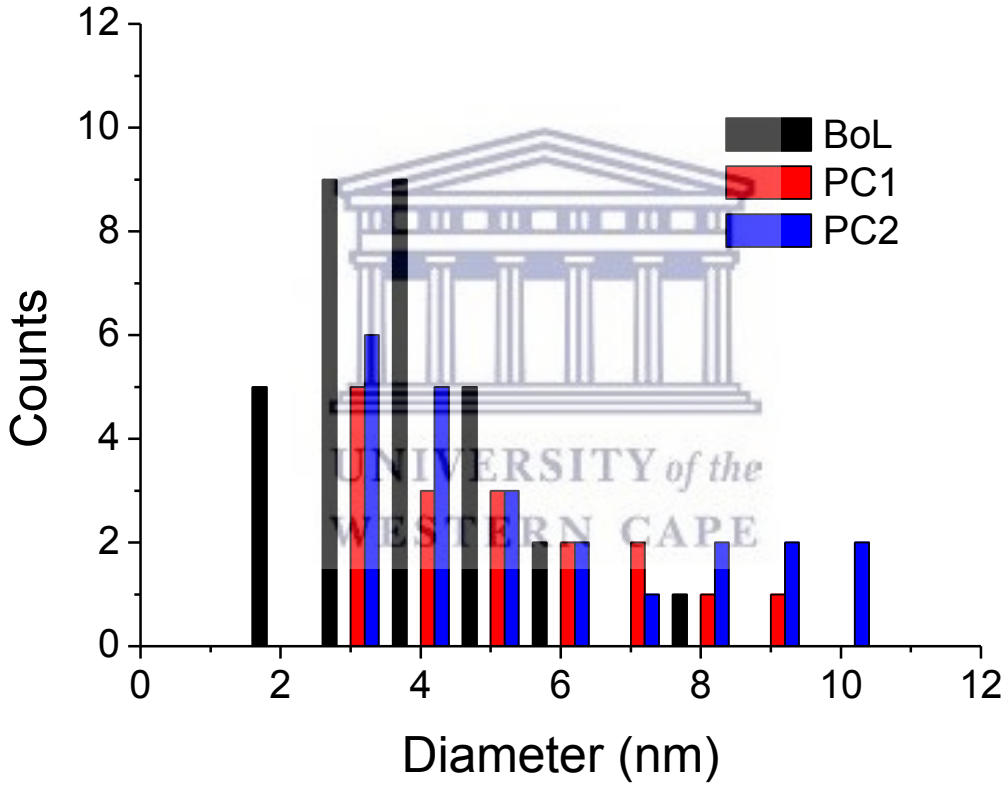

Figure 51: Relative PSD of Pt particles at beginning of life (BoL) and after variable load demand flight stage 60°C (PC1) and 90°C (PC2).

The XRD peaks in Figure 52 were consistently narrowing with increasing PSD. The loss of ECSA can be attributed to particle growth and agglomeration of loose Pt particles due to collapse of carbon support. The larger particles have smaller surface area that reduces reactive sites and ultimately cause performance deterioration of the PEMFC. The XRD peaks for Pt shifted from 40° after both the PC1 and the PC2 tests. The shift may be indicative of damaged crystallinity or compromised phase purity due to change in Pt particles encountered during migration/redeposition.

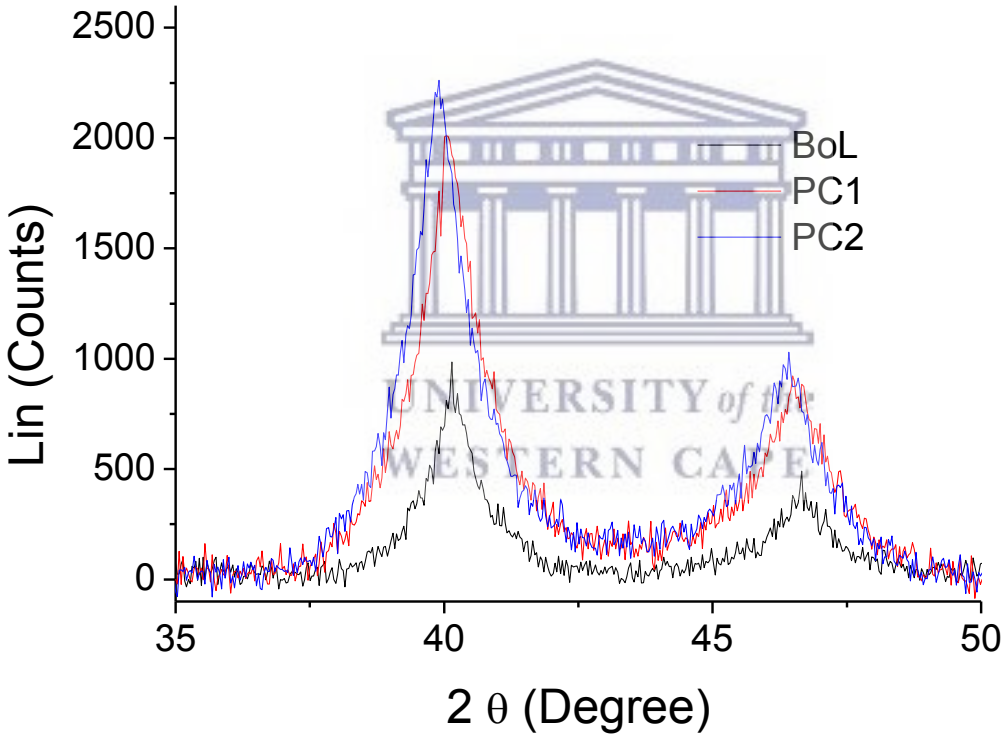

Figure 52: XRD patterns of cathode before (BoL) and after variable load demand flight stage at 60°C (PC1) and 90°C (PC2).

The loose Pt particles also redeposit on the catalyst layer and agglomerate or migrate to the membrane layer where they react with its functional groups. The Pt particles supposed to be in the catalyst layer are visible in the other layers after the PC1 test (Figure 53). The elemental mapping in Figure 53 reveals that one of the mechanisms for catalyst degradation due to the PC operating conditions is particle migration and redeposition. The Pt particles are in all the layers and almost cover the membrane layer after the PC2 test. The observations may reflect severe carbon corrosion exacerbated by high temperatures during the PC2 test.

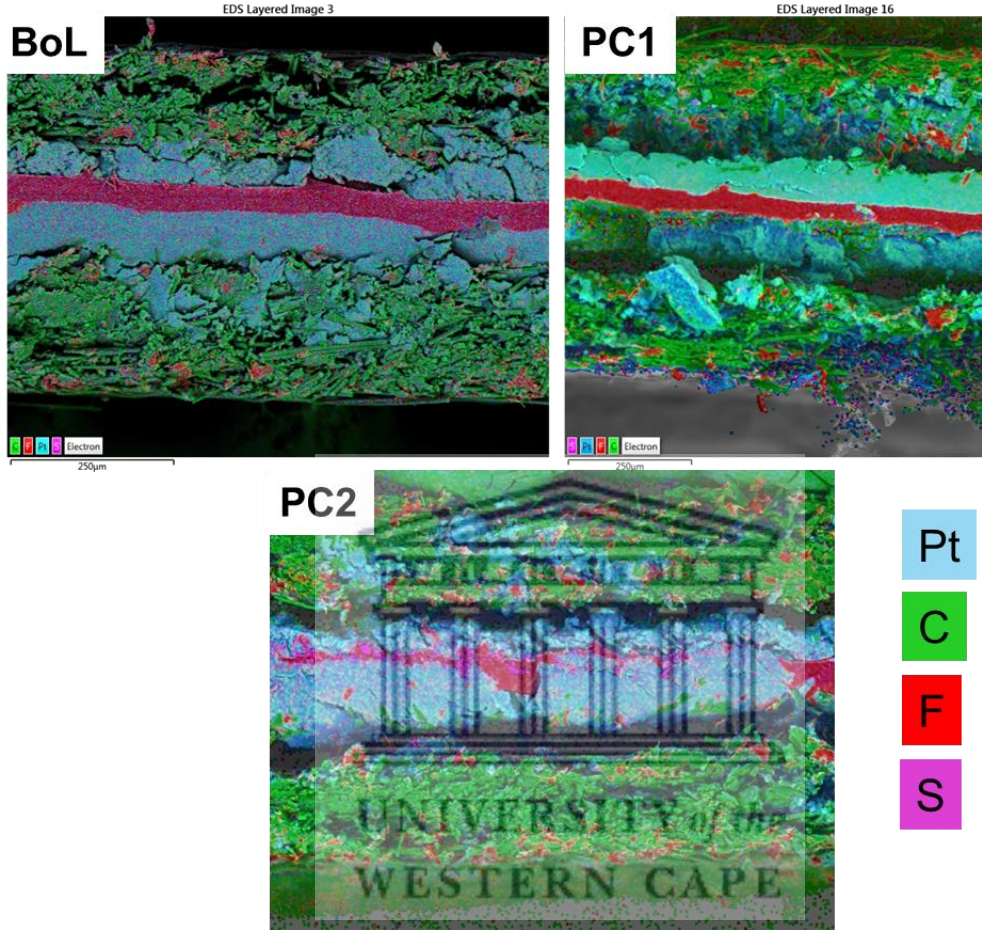

Figure 53: HRSEM/EDS elemental mapping of fresh (BoL) and treated MEA cross-sections after the variable load demand flight phase at 60°C (PC1) and 90°C (PC2).

The PC test conditions are known for creating conducive environment for carbon corrosion and the subsequent catalyst degradation. Hence, the PC was classified as the AST method to study electrocatalyst degradation [30]. The ex-situ results revealed that the performance deterioration witnessed during the PC flight stage is due to catalyst degradation. The identified mechanisms are loose Pt particles due collapse of the

carbon support, agglomeration, migration and redeposition to all the MEA layers. The observed catalyst degradation mechanisms attest that the PC stage results in catalyst degradation.

5.4.4.2 Membrane

The F is more visible in the membrane layer after the PC1 whereas the S is the most visible in the membrane layer of the pristine MEA (BoL). The cross-sections of the PC2 (Figure 54) demonstrate the similar observation of meshed MEA after operating the PEMFC at 90°C for the SUSD2 test (Figure 43). The membrane thickness is relatively the same for the pristine and tested MEAs after the PC1 stage. The delamination is not so significant after the PC1 test compared to the PC2 test. Once again, the mechanical degradation of the MEA may be attributed to intermittent dehydration and flooding imposed by after-effects of fast changing operating load and the extreme temperature applied at the PC2 test. The delamination is between the GDL and the catalyst layer, not necessarily representative of membrane degradation. The only visible sign of mechanical membrane degradation is reduced thickness, which is not apparent in the case of the PC1 test results.

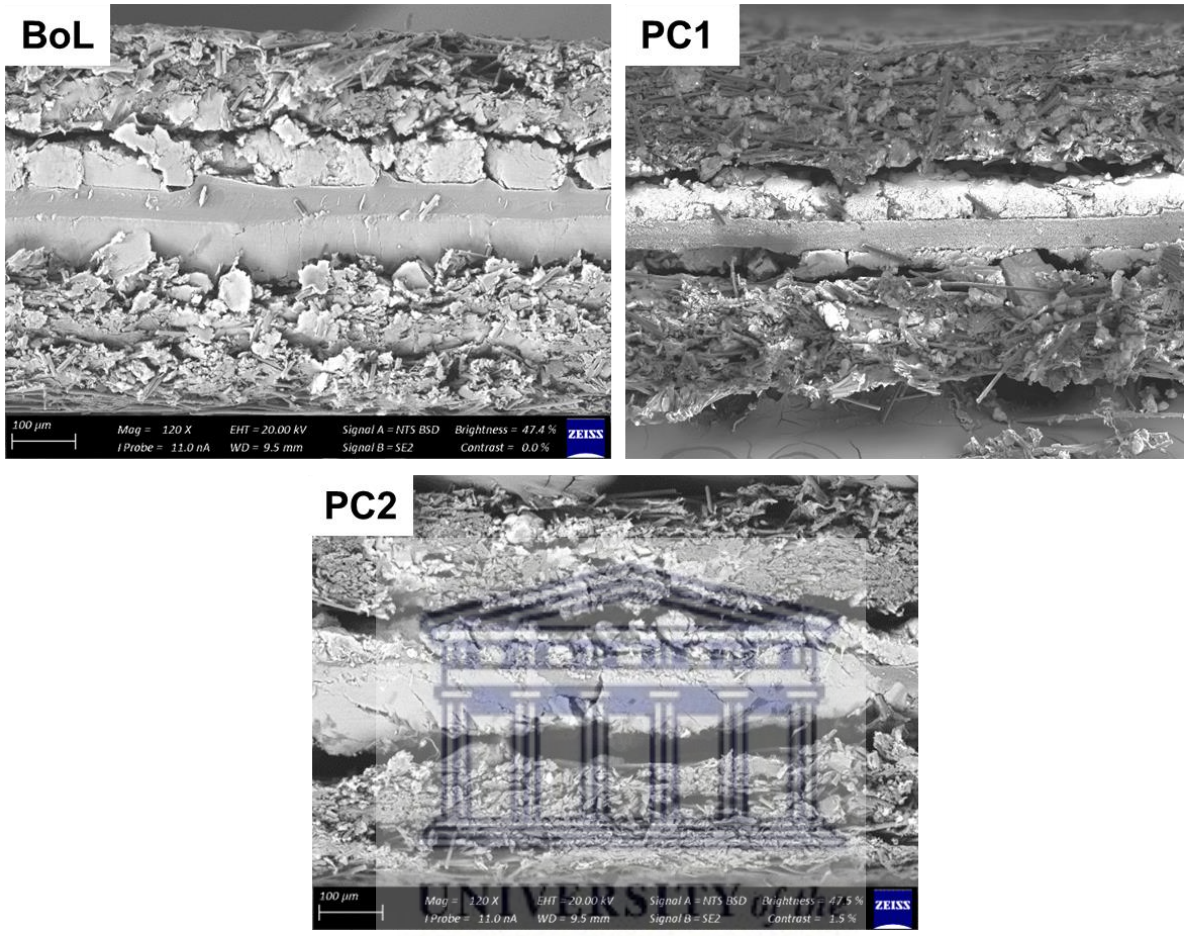

Figure 54: HRSEM back-scattered electron images of fresh (BoL) and treated MEA cross-sections after the variable load demand flight phase at 60°C (PC1) and 90°C (PC2).

The elemental composition (Table 6) shows no notable changes in elements associated with membrane chemical degradation, except for F after the PC1 test. The elemental mapping also shows F scattered in all the layers in Figure 53. The lower carbon content after the PC1 test suggests that the corroded carbon leached out of the MEA. While increased carbon concentration after the PC2 test confirms the meshed up MEA, which indicates chemical reactions within the MEA. The very low concentrations of S and Pt

after the PC2 test are taken as reflective of the loose Pt particles with the sulphonic group of the polymer membrane. The higher temperature applied during the PC stage resulted in membrane degradation, which is deduced to be accelerated by catalyst degradation.

Table 6: Elemental composition of a pristine (BoL) and tested MEAs, the simulated variable load demand flight phase at 60°C (PC1) and 90°C (PC2), as obtained from HRSEM/EDS.

Test/Element	BoL (wt.%)	PC1 (wt.%)	PC2 (wt.%)
Carbon	70.07	66.23	76.78
Fluoride	2.96	8.76	2.81
Sulphur	0.72	0.77	0.43
Platinum	26.26	22.32	19.98

The fast changing operating load imposed by the PC stage causes carbon corrosion due to changes in water levels on the MEA. The collapsed carbon support resulted in loose Pt particles that either agglomerate in efforts to minimize their surface energy or react with available elements. The extreme temperature of 90°C promoted degradation of the membrane layer which subsequently contributed to catalyst degradation through the reaction between Pt and $–SO_3H$ groups. Therefore, temperature must be carefully controlled during the variable load demand flight stage to minimize performance loss and degradation. The variable load demand is likely to occur during take-off, landing and occasionally when cruising. It can be deduced that PEMFC can withstand the

aeronautic conditions since acceptable performance levels were achieved even in extreme conditions such as the variable load and high temperatures.

5.5 Summary

The results of electrical performance obtained for all the tests are promising from the point of view of PEMFC application in aeronautics. The achieved power density output is acceptable, with the lowest power density of 0.06 Wcm^{-2} recorded from the PC stage at 90°C. In general, one can state that this confirms that PEMFC can be a reliable supply electrical energy for aeronautic applications. The power output decreased with increasing the operating temperature from 60 to 90°C. The study of performance loss and degradation rate revealed that the cruise mode caused the least voltage decay, probably due to the steady-state nature of its operating conditions.

The SUSD phase recorded the highest performance loss, thereby revealing that it is the most aggressive flight phase for PEMFC life. The IV curves further revealed that the performance loss is mainly due to ohmic losses that are reflective of mass transfer and catalyst activity. The reasons for this encounter are the combination of variable load changes that result in unstable water levels in the MEA, rapid changes in demand for reactant gases, thermal cycling and periodic exposures to near-OCV voltages.

The high voltage operating conditions during the idling stage also resulted in significant performance loss followed by the variable load demand. The performance deterioration was not only due to ohmic but to activation losses as well for the idling, take-off and landing flight phases. The common factor of these stages is that they occur on ground rather than at the high altitudes associated with aeronautic applications. Another realization is that performance loss at the stages is due to load induced stress than

changes in available oxygen content. Therefore, PEMFC operation at these stages must be revised to improve its performance.

The study showed that only the idling stage recovers temporary voltage decay. The performance loss is recovered during rest period or purging that either stabilizes water content in the MEA. The pulsing of voltage is also used as a measure to recover decayed voltage. Interestingly, there were no voltage recoveries witnessed during the PC flight stage. Instead, slight fluctuations were observed at higher current densities for the PC and the SUSD flight stages. The phenomena were postulated to be associated with excess water derived from the increased rate of water generation at high current densities coupled with fully humidified both reactant gases. The findings of this thesis highlighted the necessity of better understanding the effects of the load on water content in the MEA.

The 0.2 Acm^{-2} applied current density during the cruise mode revealed that it is the near-ideal operating condition for aeronautic applications. The flight stage recorded the least performance and ECSA losses. The changes in the MEA components were also minimal compared to changes obtained for the other flight stages. The SUSD flight stage recorded the most catalyst degradation which also caused membrane degradation, particularly at higher temperature. The PC stage also caused significant catalyst degradation but there was no severe chemical membrane degradation witnessed.

The major cause of the catalyst degradation after the idling, SUSD, take-off and landing flight phases was collapse of carbon support due to the high voltages. The resulted loose Pt particles migrated and redeposited on the MEA layers. The Pt particles agglomerated resulting in particle growth while others reacted with the membrane sulphonic group. The membrane degradation was more apparent after the idling stage. The membrane degradation could be promoted by the catalyst degradation since the high voltages create conducive conditions for chemical attack and reaction of Pt and the

–SO_3H group. Contrarily, the SUSD mode showed no notable signs of membrane degradation irrespective of the severe catalyst degradation. The delamination was presumed to be due to changes in water content in the MEA that caused swelling and shrinking.

CHAPTER 6

CONCLUSION AND RECOMMENDATIONS

The deployment of PEMFC for aeronautic applications is a value-added alternative that not only generates useful by-products (oxygen depleted air, water and heat) but addresses sensitive issues such as improving health conditions of airport personnel (silent operation minimizes noise) and decreasing greenhouse gases emission (in-situ zero emissions). However, the PEMFC is yet to be industrialized due to its fast degrading components. There are several factors that contributes to the degradation such as surrounding environment, operating system and operating conditions. There is limited information on the effects of operating conditions encountered in aeronautic environment. Hence, this study seeks to better understand behaviour of PEMFC under the simulated aeronautic operating conditions. The information gathered is essential in devising a method of assessment to monitor the PEMFC SoH. The objectives were achieved by answering the following research questions:

I. What are factors that influence fuel cell life in aeronautic environment?
    a. Which of the factors are influenced by aeronautic environment?
    b. Which of the factors have reversible effects?

II. What are measurable parameters associated with the factors?
    a. Is the signal/symptom dependent of time or operating conditions?

III. Which non-intrusive test methods are capable of evaluating the measurable parameters on-board?

IV. What does the information obtained tell about the fuel cell State of Health?

The key questions were answered through experimental work conducted on a low temperature single cell PEMFC. The PEMFC was subjected to the simulated aeronautic operating conditions and characterized for electrochemical, physical and chemical properties. The details of the experimental work carried out are presented in Chapter 4. The results obtained from the experimental work are presented and further discussed in Chapter 5. The outcomes of the study will be subsequently presented based on the key questions which had been set out.

6.1 Research outcomes

The research outcomes are discussed by reviewing the hypotheses and the key questions:

Hypothesis I: Start-ups and shutdowns cause more degradation than cruise mode.

Hypothesis I proved true: The start-up and shutdowns flight stages resulted in the highest degradation while the cruise mode caused the least. The steady-state operating conditions and the 0.2 Acm^{-2} current density during the cruise mode were taken as near-ideal operating conditions for the aeronautic applications since there was minimal degradation witnessed. On the other hand, the thermal cycling, high voltages and rapid fluctuating load encountered during the SUSD caused severe damage to the catalyst and membrane layer.

Hypothesis II: Variable load demand (take-off and landing) and idling partially recovers temporary degradation.

Hypothesis II proved false. The variable load demand did not show any signs of recovering voltage. The rapid change in voltage that disrupts water levels and movement of reactants to the reactive sites caused by the variable load demand instead caused significant performance loss. The idling mode partially recovers voltage but the recovery is temporary. The idling also caused notable performance loss, even with the partial recoveries.

Hypothesis III: Operating PEMFC at 90°C for a short period lowers performance but does not cause significant damage to fuel cell components.

Hypothesis III proved false: The performance achieved at 90°C was less than at 60°C but the degradation was also more pronounced at high temperature.

Key questions:

I. The identified main factors that have significant influence on fuel cell life are cathode stoichiometry, operating temperature and load profile.

   a. All the factors are interlinked. It is difficult to isolate each factor and its effect in aeronautic environment. The witnessed performance loss and degradation of components revealed that the factors are influenced by the aeronautic environment. Hence, it is deduced that all the factors are affected by the aeronautic environment.

   b. None of the identified factors have reversible effects. The ex-situ characterization of the MEA showed permanent damages to the fuel cell components. The catalyst layer degraded mostly due to collapse of carbon support. The loose Pt particles due to the collapsed support migrated, redeposited in the MEA layers, agglomerated and reacted with the sulphonic group of the membrane. The membrane thinned, delaminated

and smashed with the catalyst layers. The PEMFC performance continued to deteriorate in all the tests irrespective of the factors.

II. The degradation mechanisms established in this study revealed that the PEMFC operation in aeronautic conditions is mostly governed by water management in the MEA and available reactants on the reactive sites of the catalyst. The measurable parameters identified are voltage, current, power output, relative humidity, ohmic resistance and charge/mass transfer resistance.

   a. All the identified measurable parameters are time dependent and the signal is influenced by the operating conditions, including temperature. The signal output depends on the time it is detected since fuel cell operation is dynamic and its conditions changes over time. For instance, localized starvation signal output is fluctuating cell voltages when detected early while the signal changes to negative cell voltage over time.

III. The available methods of assessing the PEMFC SoH are still in development stages. Each method has advantages and drawbacks. So far, the methods need to be validated separately prior to devising a consolidated technique. Nonetheless, the defined non-intrusive method of assessment proposed in this study is an electrochemical scanning device equipped with nanosensors. The nanosensors will emulate the concept of the existing sensors (namely 5-in-1, fibre Bragg grating sensor) but using nanomaterials to improve compactness.

IV. The nanosensor electrochemical scanner will provide real time information on current, reactants and water distribution in the fuel cell (mapping), cell voltages, resistance and average RH. The acquired data will inform operators whether there are underperforming cells, spatial dehydration or flooding, localized starvation.

6.2 Concluding remarks

The overarching aim of this thesis was to define a non-intrusive diagnostic tool capable of providing real time information on fuel cell SoH used in aeronautic applications. The aim was broken down into attainable objectives which showed that the first step towards establishing a reliable non-intrusive diagnostic technique for the PEMFC SoH is to better understand factors that have direct influence on fuel cell life in aeronautic environment. The factors identified were cathode stoichiometry, operating/cell temperature and load profile of an aircraft. The effects of the factors on fuel cell life in aeronautic environment were explored through studying the PEMFC behaviour under simulated aeronautic conditions.

The factors influencing fuel cell life in aeronautic environment were identified through literature survey. The cathode stoichiometry of 2.5 minimizes performance loss at high altitudes caused by low ambient pressure (0.7 bar at 2200 m) and low oxygen content (16.0% at 2200 m). As such, a cathode stoichiometry of 2.5 was used. However, different cathode stoichiometries were not experimental examined and therefore there were no conclusions drawn. Additionally, the findings of the study were that the performance losses experienced during aeronautic applications are mostly due to the impact of aircraft load profile.

The operating temperature directly affects the fuel cell since it influences water levels in the MEA and reaction kinetics. Operating temperature must be high enough to facilitate the ORR reaction and reduce membrane resistance. However, extremely high temperature causes dehydration that promotes membrane degradation and performance loss. The operating temperatures of 60 and 90°C were selected as nominal and extreme conditions. The nominal temperature yielded better performance and the degradation of fuel cell components was minimal (for the control cruise mode

test). The performance was consistently lower at the extreme temperature for all the flight stages. On the other hand, the ADR was varied with flight stage rather than with operating temperature. Overall, the study revealed that the PEMFC can reliable generate electricity even at extreme temperature likely to be encountered in aeronautic environment.

The load profile of aircraft entails idling (taxiing), take-off, cruise mode (steady and dynamic state) and landing. The effects of load on the PEMFC life in aeronautic environment was studied by means of load-related AST. The AST were OCV, current hold, variable load demand and start-up/shutdown cycling. The novelty of this research was that all the AST were conducted with fully humidified reactants to examine worse-case scenario and the use of 2.5 cathode stoichiometry suitable for optimizing performance at high altitudes and maximizing efficiency of multifunctional fuel cell. The SUSD flight stages were incorporated with thermal cycling to simulate heating and cooling occurring in real aeronautic applications. The dataset generated in this study is essential in developing benchmark-quality database for modelling purposes.

Unlike in vehicular applications where the load changing is the highest contributor to PEMFC degradation, the SUSD caused the most degradation in aeronautic applications. The cruise mode resulted in the least degradation and was consequently regarded as the nominal load operating condition for aircraft. The idling, take-off and landing also caused significant degradation that was attributed to the high voltage conditions.

The mostly affected fuel cell components were the catalyst and the membrane. The high voltages experienced in all the stages except for the cruise mode caused severe carbon support collapse reflected by the loose Pt particles observed through the employed analytical techniques. The major causes of performance losses were loose Pt particles migrating, redepositing and agglomerating. The membrane showed thinning, delamination and symptoms of reacting with the Pt particles. The cause of the identified

degradation mechanism was speculated to be uneven water distribution in the MEA and the lagged response time for reactants supplied to the rapid changing rate of demand imposed by the dynamic load profile.

Therefore, measurable parameters related to water management and reactants supply are voltage, current, power output, RH and resistances (ohmic, charge and mass transfer). The parameters can be effectively monitored online by using nanosensor electrochemical scanner that will provide real time diagnosis of water content in the MEA and available reactants on reactive sites. Currently, available sensors only generate information on certain parameters without providing comprehensive diagnostics. Therefore, the scanner will generate map of water, reactants and cell voltage distribution while producing signal output of current and power. The maps and signals in combination with the known performance loss/degradation mechanisms revealed through this study will be processed (using models and algorithms) within the sensor to produce real-time diagnostics of the fuel cell SoH.

6.3 Outlook for future work

The outlook for future work was informed based on the literature survey and the findings of this research:

- Monitoring water and reactants distribution during testing – the degradation mechanisms observed in this study through the electrochemical and ex-situ characterization of the fuel cell revealed that the techniques do not provide any information on water content and starvation. Monitoring the water levels and available reactants would assist in discovering which and when operating conditions trigger dehydration, flooding or localized starvation.

- Behavioural study of PEMFC under a complete aircraft load profile – the results acquired in this study showed that the idling stage partially recovers performance and that the voltage decay is slower at the upper limit of variable load demand (during take-off and landing). Studying the complete profile would demonstrate whether relaxation imposed by the different flight stages recovers significant lost performance, if any.

- Development of nanosensor electrochemical scanner – the available methods of assessing the PEMFC SoH are capable of proving real time diagnosis. However, they each have complex electrical connections and need to cover portion of reactive sites in order to function. The covered reactive sites reduce overall PEMFC performance and the area can be too large to be negligible for bigger stacks. The available sensors presented by Mao *et al.* and David *et al.* can only detect a certain parameter [122, 124]. For instance, using fibre Bragg grating sensor and micro current sensor to monitor relative humidity and current

respectively [123, 124]. Hence, the proposal for a nanosensor scanner that would have all the sensor for the measurable parameters incorporated in one small device that will scan through the fuel cell without physical contact.

REFERENCES

[1] Larminie J, Dicks A. Fuel Cell Systems Explained. 2nd ed. England: John Wiley & Sons Ltd; 2003.

(2) Hydrogenics. Fuel Cell Megawatt power generation platform. 2018:1-2.

[3] Pollet BG, Pasupathi S, Swart G, Mouton K, Lototskyy M, Williams M, *et al*. Hydrogen South Africa (HySA) Systems Competence Centre: Mission, objectives, technological achievements and breakthroughs. Int J Hydrogen Energy 2014 3/6;39[8]:3577-3596.

(4) Fuel Cells Bulletin. SA government, HySA launch prototype fuel cell generator solution. Fuel Cells Bulletin 2014 12;2014[12]:5-6.

(5) Reuters. South African village becomes first to be powered by fuel cells. 2014; Available at: http://www.reuters.com/article/safrica-anglo-platinum-fuelcells-idUSL6N0QB4YD20140805.

(6) Fuel Cells Bulletin. HySA Systems unveils first hydrogen forklift, refueling station in SA. Fuel Cells Bulletin 2016 4;2016(4):4.

(7) Lototskyy MV, Tolj I, Parsons A, Smith F, Sita C, Linkov V. Performance of electric forklift with low-temperature polymer exchange membrane fuel cell power module and metal hydride hydrogen storage extension tank. J Power Sources 2016 6/1;316:239-250.

[8] Airbus International Press Release. Emission Free Power for Civil Aircraft successfully Demonstrates Fuel Cell in Flight. 2008; Available at: http://www.airbus.com/presscentre/pressreleases/press-release-detail/detail/emission-

free-power-for-civil-aircraft-airbus-successfully-demonstrates-fuel-cells-in-flight. Accessed 04/30, 2015.

[9] Friedrich KA, Kallo J, Schirmer J, Schimitthals G. Fuel Cell Systems for Aircraft Application. ECS Transitions 2009;25[1]:193-202.

[10] Lapeña-Rey N, Mosquera J, Bataller E, Ortí F, Dudfield C, Orsillo A. Environmentally friendly power sources for aerospace applications. J Power Sources 2008 7/1;181(2):353-362.

[11] Tibaquirá JE, Hristovski KD, Westerhoff P, Posner JD. Recovery and quality of water produced by commercial fuel cells. Int J Hydrogen Energy 2011 3;36(6):4022-4028.

[12] Renouard-Vallet G, Saballus M, Schmithals G, Schirmer J, Kallo J, Friedrich KA, *et al*. Improving the environmental impact of civil aircraft by fuel cell technology: concepts and technological progress. - Energy Environ Sci 2010[10]:1458-1468.

[13] Eelman S, Pozo y de Poza I, Krieg T. Fuel Cell APU's in Commercial Aircraft - An Assessment of SOFC and PEMFC Concepts. 24th international Congress of the Aeronautical Sciences, 29 Aug - 3 Sept; 2004.

[14] Seidel A, Jonathan, Sehra K, Arun, Colantonio O, Renato. NASA Aeropropulsion Research: Looking forward. 2001:1-11.

[15] Daggett DL, Eelman S, Kristiansson G. Fuel Cell APU for Commercial Aircraft. AIAA/ICAS International Air and Space Symposium and Exposition: The Next 100 Years, 14 - 17 July; 2003.

[16] DLR International Press Release. Fuel cells power first takeoff for DLR's Antares aircraft. Fuel Cells Bulletin 2009 9;2009[9]:3.

(17) Renouard-Vallet G, Saballus M, Schumann P, Kallo J, Friedrich KA, Müller-Steinhagen H. Fuel cells for civil aircraft application: On-board production of power, water and inert gas. Chem Eng Res Design 2012 1;90[1]:3-10.

(18) Romeo G, Borello F, Correa G, Cestino E. ENFICA-FC: Design of transport aircraft powered by fuel cell & flight test of zero emission 2-seater aircraft powered by fuel cells fueled by hydrogen. Int J Hydrogen Energy 2013 1/11;38[1]:469-479.

(19) Werner C, Busemeyer L, Kallo J. The impact of operating parameters and system architecture on the water management of a multifunctional PEMFC system. Int J Hydrogen Energy 2015 9/21;40(35):11595-11603.

[20] European Commission, Directorate-General for Research and Innovation, Directorate-General for Mobility and Transport. Flightpath 2050 Europe's vision for Aviation. Maintaining Global Leadership & Serving Society's Needs. 2011:1-28.

[21] Borup R, Meyers J, Pivovar B, Kim YS, Mukundan R, Garlland N, *et al*. Scientific Aspects of Polymer Electrolyte Fuel Cell Durability and Degradation. Chemical Reviews 2007;107:3904-3951.

(22) Spendelow J, Papageorgopoulos D, Garbak J, Satyapal S. Fuel Cell Technologies Program Record - Fuel Cell Stack Durability. US Energy Department Report #11003. 2012.

(23) Han I, Park S, Chung C. Modeling and operation optimization of a proton exchange membrane fuel cell system for maximum efficiency. Energy Conversion and Management 2016 4/1;113:52-65.

[24] Jouin M, Gouriveau R, Hissel D, Péra M, Zerhouni N. Degradations analysis and aging modeling for health assessment and prognostics of PEMFC. Reliab Eng Syst Saf 2016 4;148:78-95.

[25] Barbir F. PEM Fuel Cells: Theory and Practice. 2nd ed.: Elsevier; 2012.

[26] Li H, Tang Y, Wang Z, Shi Z, Wu S, Song D, *et al*. A review of water flooding issues in the proton exchange membrane fuel cell. J Power Sources 2008 3/15;178[1]:103-117.

[27] Collier A, Wang H, Zi Yuan X, Zhang J, Wilkinson DP. Degradation of polymer electrolyte membranes. Int J Hydrogen Energy 2006 10;31[13]:1838-1854.

(28) Tolj I, Bezmalinovic D, Barbir F. Maintaining desired level of relative humidity throughout a fuel cell with spatially variable heat removal rates. Int J Hydrogen Energy 2011 10;36[20]:13105-13113.

[29] Holmstrom N, Wiezell K, Lindbergh G. Studying Low-Humidity Effects in PEFCs using EIS I. Experimental. J Electrochem Soc. 2012;159[8]:F369-F378.

[30] US DOE. Fuel Cell Technologies Program Multi-Year Research, Development and Demonstration Plan. 2011:1-49.

[31] Lim C, Ghassemzadeh L, Van Hove F, Lauritzen M, Kolodziej J, Wang GG, *et al*. Membrane degradation during combined chemical and mechanical accelerated stress testing of polymer electrolyte fuel cells. J Power Sources 2014 7/1;257:102-110.

[32] Shan J, Lin R, Xia S, Liu D, Zhang Q. Local resolved investigation of PEMFC performance degradation mechanism during dynamic driving cycle. Int J Hydrogen Energy 2016 2/23;41(7):4239-4250.

[33] Banan R, Bazylak A, Zu J. Combined effects of environmental vibrations and hygrothermal fatigue on mechanical damage in PEM fuel cells. Int J Hydrogen Energy 2015 1/30;40(4):1911-1922.

(34) Inaba M, Kinumoto T, Kiriake M, Umebayashi R, Tasaka A, Ogumi Z. Gas crossover and membrane degradation in polymer electrolyte fuel cells. Electrochim Acta 2006 8/15;51[26]:5746-5753.

(35) Ramaswamy N, Hakim N, Mukerjee S. Degradation mechanism study of perfluorinated proton exchange membrane under fuel cell operating conditions. Electrochim Acta 2008 3/10;53[8]:3279-3295.

[36] Healy J, Hayden C, Xie T, Olson K, Waldo R, Brundage M, *et al*. Aspects of the Chemical Degradation of PFSA Ionomers used in PEM Fuel Cells. Fuel Cells 2005;5(2):302-308.

[37] Curtin DE, Lousenberg RD, Henry TJ, Tangeman PC, Tisack ME. Advanced materials for improved PEMFC performance and life. J Power Sources 2004 14 May 2004;131[1]:41-48.

[38] Liang H, Su H, Pollet BG, Linkov V, Pasupathi S. Membrane electrode assembly with enhanced platinum utilization for high temperature proton exchange membrane fuel cell prepared by catalyst coating membrane method. J Power Sources 2014 11/15;266:107-113.

[39] de Bruijn FA, Dam VAT, Janssen GJM. Review: Durability and Degradation Issues of PEM Fuel Cell Components. Fuel Cells 2008;8[1]:3-22.

[40] Uribe FA, Zawodzinski Jr. TA. A study of polymer electrolyte fuel cell performance at high voltages. Dependence on cathode catalyst layer composition and on voltage conditioning. Electrochim Acta 2002 8/30;47(22–23):3799-3806.

[41] Chung CG, Kim L, Sung YW, Lee J, Chung JS. Degradation mechanism of electrocatalyst during long-term operation of PEMFC. Int J Hydrogen Energy 2009 11;34[21]:8974-8981.

[42] Pei P, Yuan X, Chao P, Wang X. Analysis on the PEM fuel cells after accelerated life experiment. Int J Hydrogen Energy 2010 4;35(7):3147-3151.

[43] Taniguchi A, Akita T, Yasuda K, Miyazaki Y. Analysis of electrocatalyst degradation in PEMFC caused by cell reversal during fuel starvation. J Power Sources 2004 5/3;130(1–2):42-49.

[44] Taniguchi A, Akita T, Yasuda K, Miyazaki Y. Analysis of degradation in PEMFC caused by cell reversal during air starvation. Int J Hydrogen Energy 2008 5;33[9]:2323-2329.

[45] Oyarce A. Electrode degradation in proton exchange membrane fuel cells. 2013:1-87.

[46] Rodgers MP, Bonville LJ, Kunz HR, Slattery DK, Fenton JM. Fuel Cell Perfluorinated Sulfonic Acid Membrane Degradation Correlating Accelerated Stress Testing and Lifetime. Chem Rev 2012 11/14;112[11]:6075-6103.

[47] Jo YY, Cho E, Kim JH, Lim T, Oh I, Kim S, *et al*. Degradation of polymer electrolyte membrane fuel cells repetitively exposed to reverse current condition under different temperature. J Power Sources 2011 1 December 2011;196(23):9906-9915.

[48] Zhao M, Shi W, Wu B, Liu W, Liu J, Xing D, *et al*. Influence of Membrane Thickness on Membrane Degradation and Platinum Agglomeration under Long-term Open Circuit Voltage Conditions. Electrochim Acta 2015 20 January 2015;153:254-262.

[49] Rohendi D, Majlan EH, Mohamad AB, Daud WRW, Kadhum AAH, Shyuan LK. Effects of temperature and backpressure on the performance degradation of MEA in PEMFC. Int J Hydrogen Energy 2015 9/14;40(34):10960-10968.

(50) Mamat MS, Grigoriev SA, Dzhus KA, Grant DM, Walker GS. The performance and degradation of Pt electrocatalysts on novel carbon carriers for PEMFC applications. Int J Hydrogen Energy 2010 7;35[14]:7580-7587.

(51) Wang Z, Zuo P, Chu Y, Shao Y, Yin G. Durability studies on performance degradation of Pt/C catalysts of proton exchange membrane fuel cell. Int J Hydrogen Energy 2009 5;34[10]:4387-4394.

[52] Dubau L, Castanheira L, Chatenet M, Maillard F, Dillet J, Maranzana G, *et al*. Carbon corrosion induced by membrane failure: The weak link of PEMFC long-term performance. Int J Hydrogen Energy 2014;39[36]:21902-21914.

[53] Maass S, Finsterwalder F, Frank G, Hartmann R, Merten C. Carbon support oxidation in PEM fuel cell cathodes. J Power Sources 2008 2/1;176(2):444-451.

[54] Linse N, Gubler L, Scherer GG, Wokaun A. The effect of platinum on carbon corrosion behavior in polymer electrolyte fuel cells. Electrochim Acta 2011 9/1;56(22):7541-7549.

[55 Knights SD, Colbow KM, St-Pierre J, Wilkinson DP. Aging mechanisms and lifetime of PEFC and DMFC. J Power Sources 2004 3/10;127(1–2):127-134.

(56) Young AP, Stumper J, Gyenge E. Characterizing the Structural Degradation in a PEMFC Cathode Catalyst Layer: Carbon Corrosion. J Electrochem Soc 2009;156[8]:B913-B922.

(57) Seo D, Lee J, Park S, Rhee J, Choi SW, Shul Y. Investigation of MEA degradation in PEM fuel cell by on/off cyclic operation under different humid conditions. Int J Hydrogen Energy 2011 1;36(2):1828-1836.

[58] Romeo G. The First European Commission Funded Aircraft Powered by a Hydrogen Fuel Cell took its First Flight. 2010:1-5.

[59] DLR International Press Release. DLR Airbus A320 ATRA taxis uses fuel cell-powered nose wheel for the first time. 2011; Available at: http://www.dlr.de/dlr/presse/en/desktopdefault.aspx/tabid-10307/470_read-931/year-2011/#/gallery/2079. Accessed 04/30, 2015.

[60] Rouss V, Lesage P, Bégot S, Candusso D, Charon W, Harel F, *et al*. Mechanical behaviour of a fuel cell stack under vibrating conditions linked to aircraft applications part I: Experimental. Int J Hydrogen Energy 2008 11;33(22):6755-6765.

[61] Rouss V, Candusso D, Charon W. Mechanical behaviour of a fuel cell stack under vibrating conditions linked to aircraft applications part II: Three-dimensional modelling. Int J Hydrogen Energy 2008 11;33[21]:6281-6288.

[62] Bégot S, Harel F, Candusso D, François X, Péra M, Yde-Andersen S. Fuel cell climatic tests designed for new configured aircraft application. Energy Convers and Manag 2010 7;51(7):1522-1535.

(63) Uno M, Shimada T, Ariyama Y, Fukuzawa N, Noguchi D, Ogawa K, *et al*. Development and demonstration flight of a fuel cell system for high-altitude balloons. J Power Sources 2009 9/5;193(2):788-796.

[64] Hordé T, Achard P, Metkemeijer R. PEMFC application for aviation: Experimental and numerical study of sensitivity to altitude. Int J Hydrogen Energy 2012 7;37[14]:10818-10829.

(65) Werner C, Gores F, Busemeyer L, Kallo J, Heitmann S, Griebenow M. Characteristics of PEMFC operation in ambient- and low-pressure environment considering the fuel cell humidification. CEAS Aeronautical Journal 2014:1-15.

(66) Stolten D, Grube T, editors. Fuel Cell System Development and Testing for Aircraft Applications. 18th World Hydrogen Energy Conference, 16 - 21 May; 2010.

(67) Keim M, Kallo J, Friedrich KA, Werner C, Saballus M, Gores F. Multifunctional fuel cell system in an aircraft environment: An investigation focusing on fuel tank inerting and water generation. Aerosp Sci and Technol 2013 8;29[1]:330-338.

[68] Amirinejad M, Rowshanzamir S, Eikani MH. Effects of operating parameters on performance of a proton exchange membrane fuel cell. J Power Sources 2006 161(2):872-875.

[69] Schmittinger W, Vahidi A. A review of the main parameters influencing long-term performance and durability of PEM fuel cells. J Power Sources 2008 180[1]:1-14.

[70] Wasterlain S, Candusso D, Hissel D, Harel F, Bergman P, Menard P, *et al*. Study of temperature, air dew point temperature and reactant flow effects on proton exchange membrane fuel cell performances using electrochemical spectroscopy and voltammetry techniques. J Power Sources 2010 195(4):984-993.

(71) Pei P, Chen H. Main factors affecting the lifetime of Proton Exchange Membrane fuel cells in vehicle applications: A review. Appl Energy 2014 125(0):60-75.

[72] Harms C, Köhrmann F, Dyck A. Study of the influence of key test parameters on the performance of a PEMFC stack. Solid State Ionics 2015 275(0):75-79.

(73) Qiu Y, Zhong H, Wang M, Zhang H. Effect of relative humidity cycles accompanied by intermittent start/stop switches on performance degradation of membrane electrode assembly components in proton exchange membrane fuel cells. J Power Sources 2015 283(0):171-180.

[74] Pei P, Chang Q, Tang T. A quick evaluating method for automotive fuel cell lifetime. Int J Hydrogen Energy 2008 33[14]:3829-3836.

(75) Candusso D, Harel F, De Bernardinis A, François X, Péra MC, Hissel D, *et al*. Characterisation and modelling of a 5 kW PEMFC for transportation applications. Int J Hydrogen Energy 2006 31[8]:1019-1030.

(76) Urbani F, Barbera O, Giacoppo G, Squadrito G, Passalacqua E. Effect of operative conditions on a PEFC stack performance. Int J Hydrogen Energy 2008 33[12]:3137-3141.

[77] Kim B, Cha D, Kim Y. The effects of air stoichiometry and air excess ratio on the transient response of a PEMFC under load change conditions. Appl Energy 2015 138:143-149.

[78] Yan X, Hou M, Sun L, Liang D, Shen Q, Xu H, *et al*. AC impedance characteristics of a 2 kW PEM fuel cell stack under different operating conditions and load changes. Int J Hydrogen Energy 2007 32(17):4358-4364.

[79] Pratt JW, Klebanoff LE, Munoz-Ramos K, Akhil AA, Curgus DB, Schenkman BL. Proton exchange membrane fuel cells for electrical power generation on-board commercial airplanes. Appl Energy 2013 101(0):776-796.

(80) Klebanoff LE, Cornelius CJ. Analysis of hydrogen storage for a fuel cell emergency power system (FCEPS) for commercial aircraft. Journal of The Electrochemical Society 2007 152[11]:1-10.

(81) Makharia R, Kocha S, Yu P, Sweikart MA, Gu W, Wagner F, *et al*. Durabile PEM Fuel Cell Electrode Materials: Requirements and Benchmarking Methodologies. ECS Trans 2006 [8]:3-18.

(82) Tang H, Peikang S, Jiang SP, Wang F, Pan M. A degradation study of Nafion proton exchange membrane of PEM fuel cells. J Power Sources 2007 170[1]:85-92.

[83] Zhang S, Yuan X, Hin JNC, Wang H, Wu J, Friedrich KA, *et al*. Effects of open-circuit operation on membrane and catalyst layer degradation in proton exchange membrane fuel cells. J Power Sources 2010 195(4):1142-1148.

[84] Kundu S, Fowler M, Simon LC, Abouatallah R. Reversible and irreversible degradation in fuel cells during Open Circuit Voltage durability testing. J Power Sources 2008 182[1]:254-258.

[85] Wu J, Yuan X, Martin JJ, Wang H, Yang D, Qiao J, *et al*. Proton exchange membrane fuel cell degradation under close to open-circuit conditions. J Power Sources 2010 195(4):1171-1176.

[86] Jouin M, Bressel M, Morando S, Gouriveau R, Hissel D, Péra M, *et al*. Estimating the end-of-life of PEM fuel cells: Guidelines and metrics. Appl Energy 2016 177:87-97.

(87) Sugawara S, Maruyama T, Nagahara Y, Kocha SS, Shinohra K, Tsujita K, *et al*. Performance decay of proton-exchange membrane fuel cells under open circuit conditions induced by membrane decomposition. J Power Sources 2009 187(2):324-331.

[88] Kim JH, Cho EA, Jang JH, Kim H, Lim T, Oh I, *et al*. Effects of Cathode Inlet Relative Humidity on PEMFC Durability during Startup-Shutdown Cycling. J Electrochem Soc 2010 157[1]:B104-B112.

[89] Lin R, Cui X, Shan J, Técher L, Xiong F, Zhang Q. Investigating the effect of start-up and shut-down cycles on the performance of the proton exchange membrane fuel cell by segmented cell technology. Int J Hydrogen Energy 2015 40[43]:14952-14962.

[90] Liu D, Case S. Durability study of proton exchange membrane fuel cells under dynamic testing conditions with cyclic current profile. J Power Sources 2006 162[1]:521-531.

[91] Franck-Lacaze L, Bonnet C, Choi E, Moss J, Pontvianne S, Poirot H, *et al*. Ageing of PEMFC's due to operation at low current density: Investigation of oxidative degradation. Int J Hydrogen Energy 2010 10;35(19):10472-10481.

(92) Yan Q, Toghiani H, Causey H. Steady state and dynamic performance of proton exchange membrane fuel cells (PEMFCs) under various operating conditions and load changes. J Power Sources 2006 161[1]:492-502.

[93] Bose A, Babburi P, Kumar R, Myers D, Mawdsley J, Milhuff J. Performance of individual cells in polymer electrolyte membrane fuel cell stack under-load cycling conditions. J Power Sources 2013 243:964-972.

(94) Shao Y, Wang J, Kou R, Engelhard M, Liu J, Wang Y, *et al*. The corrosion of PEM fuel cell catalyst supports and its implications for developing durable catalysts. Electrochim Acta 2009 54[11]:3109-3114.

(95) Enz S, Dao TA, Messerschmidt M, Scholta J. Investigation of degradation effects in polymer electrolyte fuel cells under automotive-related operating conditions. J Power Sources 2015 274(0):521-535.

(96) Shao Y, Yin G, Gao Y. Understanding and approaches for the durability issues of Pt-based catalysts for PEM fuel cell. J Power Sources 2007 171(2):558-566.

(97) Yousfi-Steiner N, Moçotéguy P, Candusso D, Hissel D. A review on polymer electrolyte membrane fuel cell catalyst degradation and starvation issues: Causes, consequences and diagnostic for mitigation. J Power Sources 2009 194[1]:130-145.

[98] Liu M, Wang C, Zhang J, Wang J, Hou Z, Mao Z. Diagnosis of membrane electrode assembly degradation with drive cycle test technique. Int J Hydrogen Energy 2014 39[26]:14370-14375.

(99) Tian G, Wasterlain S, Candusso D, Harel F, Hissel D, François X. Identification of failed cells inside PEMFC stacks in two cases: Anode/cathode crossover and anode/cooling compartment leak. Int J Hydrogen Energy 2010 35(7):2772-2776.

[100] Rubio MA, Urquia A, Dormido S. Diagnosis of performance degradation phenomena in PEM fuel cells. Int J Hydrogen Energy 2010 35(7):2586-2590.

(101) Miller M, Bazylak A. A review of polymer electrolyte membrane fuel cell stack testing. J Power Sources 2011 196(2):601-613.

(102) Wasterlain S, Candusso D, Harel F, Hissel D, François X. Development of new test instruments and protocols for the diagnostic of fuel cell stacks. J Power Sources 2011 196[12]:5325-5333.

(103) Yuan X, Li H, Zhang S, Martin J, Wang H. A review of polymer electrolyte membrane fuel cell durability test protocols. J Power Sources 2011 196(22):9107-9116.

(104) Bezmalinovic D, Simic B, Barbir F. Characterization of PEM fuel cell degradation by polarization change curves. J Power Sources 2015 294(0):82-87.

(105) Jouin M, Gouriveau R, Hissel D, Péra M, Zerhouni N. Prognostics and Health Management of PEMFC – State of the art and remaining challenges. Int J Hydrogen Energy 2013 38(35):15307-15317.

[106] Petrone R, Zheng Z, Hissel D, Péra MC, Pianese C, Sorrentino M, *et al*. A review on model-based diagnosis methodologies for PEMFCs. Int J Hydrogen Energy 2013 38(17):7077-7091.

[107] Zheng Z, Petrone R, Péra MC, Hissel D, Becherif M, Pianese C, *et al*. A review on non-model based diagnosis methodologies for PEM fuel cell stacks and systems. Int J Hydrogen Energy 2013 38[21]:8914-8926.

(108) Chevalier S, Trichet D, Auvity B, Olivier JC, Josset C, Machmoum M. Multiphysics DC and AC models of a PEMFC for the detection of degraded cell parameters. Int J Hydrogen Energy 2013 38[26]:11609-11618.

(109) Chevalier S, Auvity B, Olivier JC, Josset C, Trichet D, Machmoum M. Detection of Cells State-of-Health in PEM Fuel Cell Stack Using EIS Measurements Coupled with Physics Modelling. Fuel Cells 2014 14[3]:416-429.

[110] Cadet C, Jemeï S, Druart F, Hissel D. Diagnostic tools for PEMFCs: from conception to implementation. Int J Hydrogen Energy 2014 39[20]:10613-10626.

[110] Wu J, Yuan XZ, Wang H, Blanco M, Martin JJ, Zhang J. Diagnostic tools in PEM fuel cell research: Part I Electrochemical techniques. Int J Hydrogen Energy 2008 33(6):1735-1746.

(112) Lee K, Lee B, Yoo SJ, Kim S, Hwang SJ, Kim H, *et al*. Development of a galvanostatic analysis technique as an in-situ diagnostic tool for PEMFC single cells and stacks. Int J Hydrogen Energy 2012 37(7):5891-5900.

(113) Brightman E, Hinds G, O'Malley R. In-situ measurement of active catalyst surface area in fuel cell stacks. J Power Sources 2013 11/15;242(0):244-254.

[114] Fouquet N, Doulet C, Nouillant C, Dauphin-Tanguy G, Ould-Bouamama B. Model based PEM fuel cell state-of-health monitoring via ac impedance measurements. J Power Sources 2006 159(2):905-913.

(115) Cleghorn SJC, Mayfield DK, Moore DA, Moore JC, Rusch G, Sherman TW, *et al*. A polymer electrolyte fuel cell life test: 3 years of continuous operation. J Power Sources 2006 158[1]:446-454.

(116) Migliardini F, Corbo P. CV and EIS Study of Hydrogen Fuel Cell Durability in Automotive Applications. Int J Electrochem Sc 2013;8:11033-11047.

(117) Paganin VA, Oliveira CLF, Ticianelli EA, Springer TE, Gonzalez ER. Modelistic interpretation of the impedance response of a polymer electrolyte fuel cell1. Electrochim Acta 1998 8/21;43[24]:3761-3766.

(118) Gomodam P, M., Weidner J, W. Analysis of Electrochemical Impedance Spectroscopy in Proton Exchange Membrane Fuel Cells. Int J Energ Res 2005 29:1131-1151.

(119) Yuan X, Wang H, Colin Sun J, Zhang J. AC impedance technique in PEM fuel cell diagnosis—A review. Int J Hydrogen Energy 2007 32(17):4365-4380.

(120) Rezaei Niya SM, Hoorfar M. Study of proton exchange membrane fuel cells using electrochemical impedance spectroscopy technique – A review. J Power Sources 2013 240:281-293.

[121] Chevalier S, Josset C, Olivier J, Auvity B, Trichet D, Machmoum M. Experimental Validation of an Identification Procedure of PEMFC Stack State of Health Using EIS Combined with a Physical Impedance Modelling. Chem Eng Trans 2013 1015-1020.

[122] Lee C, Weng F, Chuang S, Lee S, Huang Y, Cheng Y, *et al*. Flexible five-in-one micro sensor for in-situ diagnosis of high-temperature proton exchange membrane fuel cell stack. Int J Hydrogen Energy 2015 40[45]:15679-15689.

[123] Mao L, Davies B, Jackson L. Application of the sensor selection approach in the polymer electrolyte membrane fuel cell prognostics and health management. Energies 2017 (1511):1-13.

[124] David N, Von Schilling K, Wild PM, Djilali N. In-situ measurement of relative humidity in a PEM fuel cell using fibre Bragg grating sensors. Int J Hydrogen Energy 2014 39[31]:17638-17644.

(125) Dyantyi N, Parsons A, Sita C, Pasupathi S. PEMFC for aeronautic applications: A review on durability aspects. Open Engineering 2017 7[1]:287-302.

(126) Kim S, Shimpalee S, Van Zee JW. The effect of stoichiometry on dynamic behavior of a proton exchange membrane fuel cell (PEMFC) during load change. J Power Sources 2004 135(1–2):110-121.

[127] Kang J, Jung DW, Park S, Lee J, Ko J, Kim J. Accelerated test analysis of reversal potential caused by fuel starvation during PEMFCs operation. Int JHydrogen Energy 2010 35[8]:3727-3735.

(128) Zhang S, Yuan X, Wang H, Mérida W, Zhu H, Shen J, *et al*. A review of accelerated stress tests of MEA durability in PEM fuel cells. Int J Hydrogen Energy 2009 34[1]:388-404.

(129) Liu M, Wang C, Zhang J, Wang J, Hou Z, Mao Z. Diagnosis of membrane electrode assembly degradation with drive cycle test technique. Int J Hydrogen Energy 2014 39[26]:14370-14375.

[130] Yan Q, Toghiani H, Wu J. Investigation of water transport through membrane in a PEM fuel cell by water balance experiments. J Power Sources 2006 158[1]:316-325.

[131] Kundu S, Fowler MW, Simon LC, Grot S. Morphological features (defects) in fuel cell membrane electrode assemblies. J Power Sources 2006 157(2):650-656.

[132] Le Canut J, Abouatallah R, M., Harrington D, A. Detection of Membrane Drying, Fuel Cell Flooding, and Anode Catalyst Poisoning on PEMFC Stacks by Electrochemical Impedance Spectroscopy. J Electrochem Soc 2006 153(5):A857-A864.

(133) Weng F, Hsu C, Li C. Experimental investigation of PEM fuel cell aging under current cycling using segmented fuel cell. Int J Hydrogen Energy 2010 4;35[8]:3664-3675.

(134) Zhao M, Shi W, Wu B, Liu W, Liu J, Xing D, *et al*. Analysis of carbon-supported platinum through potential cycling and potential-static holding. Int J of Hydrogen Energy 2014 39[25]:13725-13737.

(135) Ball SC, Hudson SL, Thompsett D, Theobald B. An investigation into factors affecting the stability of carbons and carbon supported platinum and platinum/cobalt alloy catalysts during 1.2V potentiostatic hold regimes at a range of temperatures. J Power Sources 2007 171[1]:18-25.

(136) Freire TJP, Gonzalez ER. Effect of membrane characteristics and humidification conditions on the impedance response of polymer electrolyte fuel cells. J Electroanal Chem 2001 503(1–2):57-68.

(137) Rodat S, Sailler S, Druart F, Thivel PX, Bultel Y, Ozil P. EIS measurements in the diagnosis of the environment within a PEMFC stack. J Appl Electrochem 2010 40(5):911-920.

(138) Wang X, Kumar R, Myers D. Effect of voltage on platinum dissolution relevance to polymer electrolyte fuel cells. Electrochem and Solid State Lett 2006 9(5):A225-A227.

(139) Ferreira PJ, Ia O' GJ, Shao-Horn Y, Morgan D, Makharia R, Kocha S, *et al*. Instability of Pt/C Electrocatalysts in Proton Exchange Membrane Fuel Cells. A Mechanistic Fuel Cells. J Electrochem Soc 2005 152[11]:A2256-A2271.

(140) Linse N. Start/stop phenomena in polymer electrolyte fuel cells. PhD thesis 2012:1-221.

[141] Yu Y, Li H, Wang H, Yuan X, Wang G, Pan M. A review on performance degradation of proton exchange membrane fuel cells during startup and shutdown processes: Causes, consequences, and mitigation strategies. J Power Sources 2012 205(0):10-23.

(142) Lin R, Li B, Hou YP, Ma JM. Investigation of dynamic driving cycle effect on performance degradation and micro-structure change of PEM fuel cell. Int J Hydrogen Energy 2009 34(5):2369-2376.